National Library of Canada
Acquisitions and Bibliographic Services Branch
395 Wellington Street
Ottawa, Ontario
K1A 0N4

Bibliothèque nationale du Canada
Direction des acquisitions et des services bibliographiques
395, rue Wellington
Ottawa (Ontario)
K1A 0N4

Your file Votre référence

Our file Notre référence

NOTICE

The quality of this microform is heavily dependent upon the quality of the original thesis submitted for microfilming. Every effort has been made to ensure the highest quality of reproduction possible.

If pages are missing, contact the university which granted the degree.

Some pages may have indistinct print especially if the original pages were typed with a poor typewriter ribbon or if the university sent us an inferior photocopy.

Reproduction in full or in part of this microform is governed by the Canadian Copyright Act, R.S.C. 1970, c. C-30, and subsequent amendments.

AVIS

La qualité de cette microforme dépend grandement de la qualité de la thèse soumise au microfilmage. Nous avons tout fait pour assurer une qualité supérieure de reproduction.

S'il manque des pages, veuillez communiquer avec l'université qui a conféré le grade.

La qualité d'impression de certaines pages peut laisser à désirer, surtout si les pages originales ont été dactylographiées à l'aide d'un ruban usé ou si l'université nous a fait parvenir une photocopie de qualité inférieure.

La reproduction, même partielle, de cette microforme est soumise à la Loi canadienne sur le droit d'auteur, SRC 1970, c. C-30, et ses amendements subséquents.

Canada

Kinetic Study of Cobalt Extraction From Bis(2,2,4-trimethylpentyl) Phosphinic Acid

By

Changmin Yan

A Thesis submitted to
the School of Graduate Studies
in partial fulfilment of the requirements for the
degree of Master of Applied Science
in
Chemical Engineering

DEPARTMENT OF CHEMICAL ENGINEERING
UNIVERSITY OF OTTAWA
OTTAWA, ONTARIO

© CHANGMIN YAN, OTTAWA, CANADA 1994

National Library of Canada

Acquisitions and Bibliographic Services Branch

395 Wellington Street
Ottawa, Ontario
K1A 0N4

Bibliothèque nationale du Canada

Direction des acquisitions et des services bibliographiques

395, rue Wellington
Ottawa (Ontario)
K1A 0N4

Your file Votre référence

Our file Notre référence

THE AUTHOR HAS GRANTED AN IRREVOCABLE NON-EXCLUSIVE LICENCE ALLOWING THE NATIONAL LIBRARY OF CANADA TO REPRODUCE, LOAN, DISTRIBUTE OR SELL COPIES OF HIS/HER THESIS BY ANY MEANS AND IN ANY FORM OR FORMAT, MAKING THIS THESIS AVAILABLE TO INTERESTED PERSONS.

L'AUTEUR A ACCORDE UNE LICENCE IRREVOCABLE ET NON EXCLUSIVE PERMETTANT A LA BIBLIOTHEQUE NATIONALE DU CANADA DE REPRODUIRE, PRETER, DISTRIBUER OU VENDRE DES COPIES DE SA THESE DE QUELQUE MANIERE ET SOUS QUELQUE FORME QUE CE SOIT POUR METTRE DES EXEMPLAIRES DE CETTE THESE A LA DISPOSITION DES PERSONNE INTERESSEES.

THE AUTHOR RETAINS OWNERSHIP OF THE COPYRIGHT IN HIS/HER THESIS. NEITHER THE THESIS NOR SUBSTANTIAL EXTRACTS FROM IT MAY BE PRINTED OR OTHERWISE REPRODUCED WITHOUT HIS/HER PERMISSION.

L'AUTEUR CONSERVE LA PROPRIETE DU DROIT D'AUTEUR QUI PROTEGE SA THESE. NI LA THESE NI DES EXTRAITS SUBSTANTIELS DE CELLE-CI NE DOIVENT ETRE IMPRIMES OU AUTREMENT REPRODUITS SANS SON AUTORISATION.

ISBN 0-612-00626-3

Canada

UNIVERSITÉ D'OTTAWA
UNIVERSITY OF OTTAWA

Abstract

A modified Lewis cell was used to study the kinetics of the extraction of cobalt from sulfate solution into bis (2,4,4-trimethylpentyl) phosphinic acid (HDTMPP), commercially known as Cyanex 272. The pH was controlled with an auto-titration technique instead of using the traditional buffer solution which could affect or change the extraction mechanism. A "gravity leg" was used to control the position of the liquid-liquid interface level in the cell. A study of the extraction of cobalt into HDTMPP was carried out to determine the effect of the following variables on the extraction, namely: (i) aqueous phase cobalt concentration, (ii) aqueous phase ionic strength, (iii) interfacial area, (iv) extractant concentration, (v) modifier concentration in the organic phase, (vi) pH, (vii) hydrodynamic conditions in both phases and (viii) temperature.

It was found that the mechanism of the extraction process was more accurately described using activities rather than concentrations. Both the aqueous phase cobalt activities and concentrations were calculated at high concentrations, up to 0.50 kmol m^{-3}. The extraction resistance was found to arise from 1) the aqueous phase boundary layer,

2) the interface and 3) the organic phase boundary layer. These three resistances were observed to be independent of each other. The interfacial resistance was dependent on pH. The boundary layer resistances were dependent on the hydrodynamic conditions of the aqueous and the organic phases. The thickness of the aqueous phase boundary layer was estimated. The apparent activation energy of this extraction process was found to be 39.4 kJ mol^{-1}.

The extraction rate was found to be a function of the pH and depended on: the aqueous phase cobalt concentration, the extractant concentration and the hydrodynamic conditions in both the aqueous and the organic phases. A model describing the extraction process was found to be:

$$J = \frac{A \times a_{Co} \times a_{H_2A_2}}{3.69 \times 10^{6} Re_{aq}^{-1/2} + 4.89 \times 10^{5} Re_{org}^{-1/2} + 1.52 \times 10^{9} a_{H}} .$$

Acknowledgement

I would like to express my sincere gratitude and appreciation to Dr. J.A. Golding for his supervision and financial support throughout my research.

I would like to thank Mr. Louis Tremblay and his colleagues of the machine shop of the Department of Chemical Engineering for their assistance through the experiments associated with this research.

I also would like to express my appreciation to the faculty and the staff in the Department of Chemical Engineering for their advice and companionship.

Contents

List of Tables

List of Figures

Nomenclature

A = Interfacial area, m^2

a = Activity, kmol m^{-3}

Ab = Absorbance

b_A = Ratio of organic phase cobalt concentration to its absorbance, kmol m^{-3}

b_L = Slope of the linear relationship of absorption with times

C = Concentration, kmol m^{-3}

C* = Equilibrium Concentration, kmol m^{-3}

D = Extraction distribution constant

$\mathcal{D}$ = Diffusion coefficient, $m^2 s^{-1}$

d = Stirrer diameter, m

E = Apparent activation energy, kJ mol^{-1}

I = Ionic strength, kmol m^{-3}

J = Extraction rate, mol s^{-1}

K = Overall extraction rate coefficient, m s^{-1}

k = Individual phase extraction rate coefficient, m s^{-1}

M = Extracted metal ion

m = Molar concentration, kmol m^{-3}

N = Extraction rate per unit area, mol m^{-2} s^{-1}

n = Stirrer speed, s^{-1}

Q = Flow rate, m^3 s^{-1}

R = Extraction resistance, s m^{-1}

r = Correlation coefficient

Re = Stirrer Reynolds number, $Re = nd^2\rho\mu^{-1}$

T = Temperature, ^oC or K

t = Time, s

Z = Chemical valency of ions

$\bar{}$ = Over bar; indicates organic phase concentration or activity

Greek Symbols

α = Parameter in Pitzer's equation

β = Parameter in Pitzer's equation

γ = Activity coefficient

δ = Thickness of the boundary layer, m

μ = Viscosity, Pa s

ρ = Density, kg m^{-3}

ν = Valency number of the positive or negative ions

e = Error or difference in Equation 3-4, 5-18 and Table 2-1.

Subscripts

ad = Adsorption

aq = Aqueous phase

d = Diffusion

i = Interface

org = Organic phase

r = Chemical reaction

Abbreviations

HA = Molecule of extractant

HC = Citric acid

HD = Dithizone

HDEHP = bis (2-ethylhexyl) phosphoric acid

HDTMPP = bis (2,4,4-trimethylpentyl) phosphinic acid

HEHEHP = 2-ethylhexyl phosphonic acid, 2-ethylhexyl ester

HMHHP = mono-methylheptyl hexyl-phosphonic acid

MTWCR = mass transfer with chemical reaction mechanism model

TBP = tributyl phosphate

CHAPTER 1

Introduction

Solvent extraction is widely used in hydrometallurgy for the recovery of metals from aqueous solutions. In particular, most of the cobalt produced at present is a by-product of nickel manufacture using solvent extraction technology.

The actual solvent extraction process can take place in two or more steps. Considering, for example, the recovery and separation of cobalt and nickel from aqueous solutions [Ritcey et al., 1975]. First step is extraction of cobalt from the aqueous phase into the organic phase at a pH value greater than 5.0. An optional step can be included next which removes the co-extracted nickel by scrubbing. This is done by contacting the organic phase with a concentrated aqueous solution of cobalt. The last step is the recovery of the extracted metal from the organic phase by contacting with an acidic aqueous phase, called stripping. It is this reversibility

of the process that makes liquid-liquid extraction a viable process.

The development of an industrial process requires an understanding of the extraction mechanism. Extraction kinetics can be affected by diffusion mass transfer or chemical reaction which can take place in the aqueous phase, in the organic phase or at the interface. The extraction rate is determined by the rate-controlling step, that is, the slowest one of the several elementary steps in the extraction process. In general, metal extraction can be considered to be controlled by diffusion or chemical reaction, depending on the actual extraction conditions. As a result, it is important to know the extraction mechanism for the solvent extraction.

It is difficult to study the kinetics of extraction because of the complexity of the extraction process and the experimental techniques involved. The aim of this work was to establish and improve the experimental method for the study of the cobalt extraction kinetics and to determine the mechanism controlling the extraction. The system, studied in this investigation, was the bis (2,4,4-trimethyl pentyl) phosphinic acid (HDTMPP) - $CoSO_4$ system in sulfate solution. The variables considered to affect the extraction rate were (1) the aqueous phase cobalt concentration; (2) the aqueous phase ionic strength; (3) the pH; (4) the aqueous phase hydrodynamic conditions; (5) the interfacial area; (6) the extractant

concentration; (7) the organic phase modifier concentration; (8) the organic phase hydrodynamic conditions; and (9) the temperature. All of the above variables were studied in detail. The controlling steps were determined by analyzing every possible essential step for the extraction process.

In addition, investigators have suggested that extraction kinetics should be represented using activities rather than concentrations [Li et al., 1985]. Analysis of the kinetic data would therefore be made on the basis of both concentration and activity to test this suggestion.

CHAPTER 2

Literature Survey

Cobalt is an important metal resource. The major use of cobalt is in superalloys where it improves the strength, wear and the corrosion-resistance characteristics of alloys at elevated temperatures. Cobalt-based alloys are widely used in turbine blades for aircraft jet engines, in gas turbines, for pipeline compressors and in production of magnets. Cobalt metal powder has an important application as a binder in the production of cemented tungsten carbides for heavy-duty and high-speed cutting tools. Cobalt oxide is an important additive in paint, glass and ceramics. Cobalt is also used to promote the adherence of enamel to steel for applications such as appliances, and steel to rubber for the construction of steel-belted tires [Perron, 1994].

Natural cobalt coexists with other metals such as nickel, copper, iron and calcium. These ores are usually low grade. Similar chemical and physical

properties of these metals make it difficult to separate and refine them from each other by using chemical separation processes other than extraction [Blumberg, 1988].

One hundred years ago, Berthelot and Jungfleisch [Berthelot and Jungfleisch, 1872] discovered a law which governed the distribution of metal species between two immiscible phases. This law is thought to be the beginning of the study of extraction. Since then, the technology and theory of solvent extraction have advanced, as the theories and knowledge of solution systems and metal complexes have progressed.

In the 1940's the need for the separation and recovery of radioactive materials saw the introduction of solvent extraction to large scale operations. The extraction has been applied to metallurgical processing from that time largely as a result of the interest shown in hydrometallurgical routes for the treatment of complex ore bodies [Ritcey and Ashbrook, 1984]. Based on extraction technology, the processes have been developed successfully for over two decades for the recovery of metals such as uranium, fission products, copper and cobalt.

Extraction has the advantage of high selectivity, high separation factors and high recovery for treatment of the substances which possess similar properties.

These advantages make the extraction process unique and superior over other separation processes [Lo et al., 1983].

The kinetics of solvent extraction involves mass transfer with chemical reaction in a heterogeneous system. If the extraction rate is diffusion controlled, it would depend on the interfacial area and the concentrations of the diffusing species. When the extraction rate is chemically controlled, it is important to ascertain the location of the rate-controlling chemical reaction or reactions; that is, whether they exist within a bulk phase, at the interface or in a thin zone adjacent to the interface. For a bulk phase rate controlling chemical reaction, the important parameters will be the solubility of reactants, their distribution coefficients (which will vary with diluent choice and the aqueous phase ionic strength), ionization constants if appropriate, and the phase volumes. For an interfacial chemical reaction, the composition of the interface will correspond to the concentrations of species as given by the equilibrium expression for the interfacial reaction. When interfacial chemical reactions are rate controlling, the important parameters are the interfacial area, the interfacial activity of the reacting species, and the molecular geometry with respect to the preferential molecular orientation at the interface.

Figure 2-1 shows the concentration profiles at the interface on the basis of the two-film theory for the extraction process. The two-film theory proposed by

Whitman [Whitman, 1923] involves two postulates: (1) the resistance to transfer resides in two stagnant films, one on each side of the interface, through which transfer of solute occurs by molecular diffusion; and (2) the phases are in equilibrium or there is a slow heterogeneous reaction at the interface.

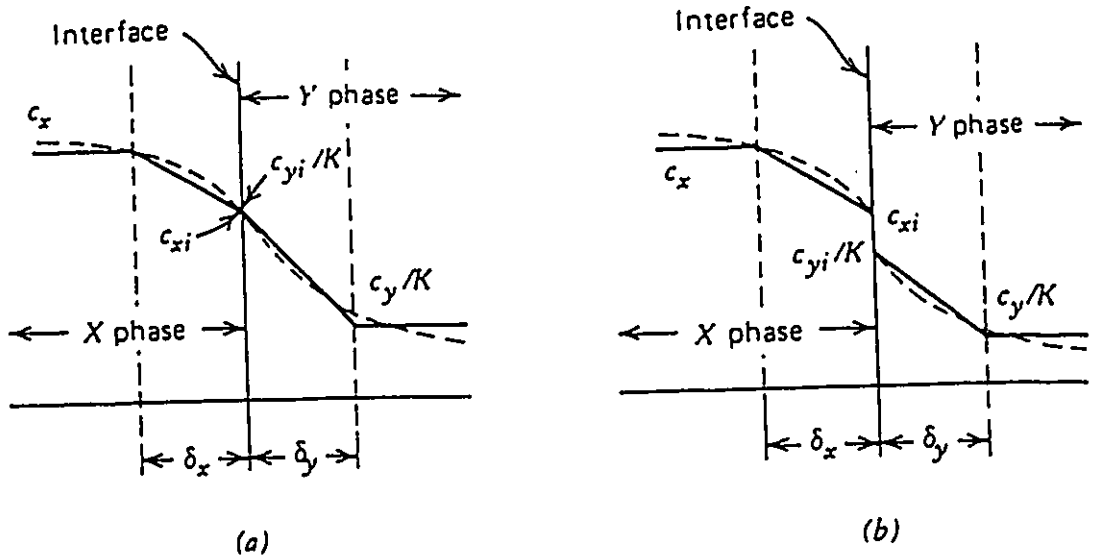

Figure 2-1: Concentration profiles at interface on basis of the two-film theory (the dashed lines show more realistic forms of the profiles): a. with equilibrium at the interface; and b. with slow heterogeneous reaction at the interface.

2.1 Extraction System

As early as 1949, the extractant for cobalt and nickel extraction, bis(2-ethylhexyl) phosphoric acid, was developed [Ritcey and Ashbrook, 1984]. The organic derivatives of phosphoric acids play an important role in the cobalt extraction industry, which include phosphoric esters, phosphonic acids, phosphoric

acids and phosphinic acids. Commercial extractants used to recover cobalt are bis (2-ethylhexyl) phosphoric acid (HDEHP), 2-ethylhexyl phosphonic 2-ethylhexyl ester (HEHEHP), mono-methylheptyl hexyl-phosphonic acid (HMHHP) and bis (2,4,4-trimethyl pentyl) phosphinic acid (HDTMPP). The structures of these extractants are shown in Figure 2-2.

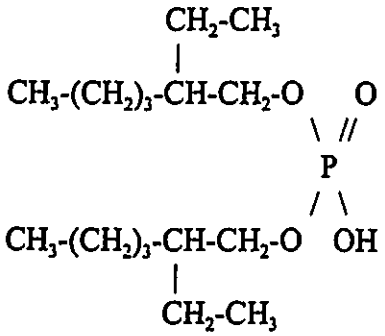

HDEHP

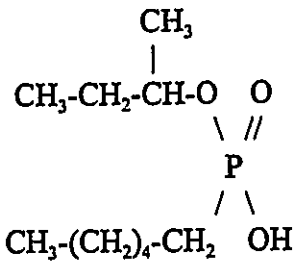

HMHHP

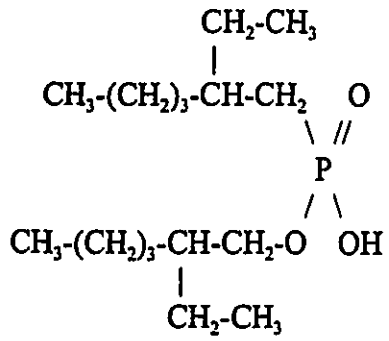

HEHEHP

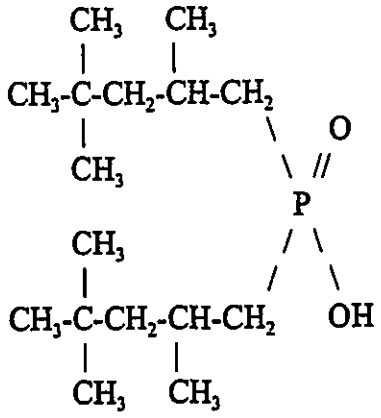

HDTMPP

Figure 2-2: Structure of various phosphoric acid extractants: HMHHP: mono-methylheptyl hexyl-phosphonic acid; HEHEHP: 2-ethylhexyl phosphonic acid, 2-ethylhexyl ester; HDEHP: bis (2-ethylhexyl) phosphoric acid; and HDTMPP: bis (2,4,4-trimethylpentyl) phosphinic acid.

It has been found that the extractants exist as dimers in the organic phase [Komasawa, 1983]. The particular extraction reaction equation can be written as [Komasawa, 1981]:

$$Co^{2+} + 2\overline{(HA)_2} = \overline{CoA_2(HA)_2} + 2H^+$$

When the cobalt ion is chelated by the extractant, the structure of the resulting organic cobalt compound is shown in Figure 2-3 [Albery and Fick, 1981].

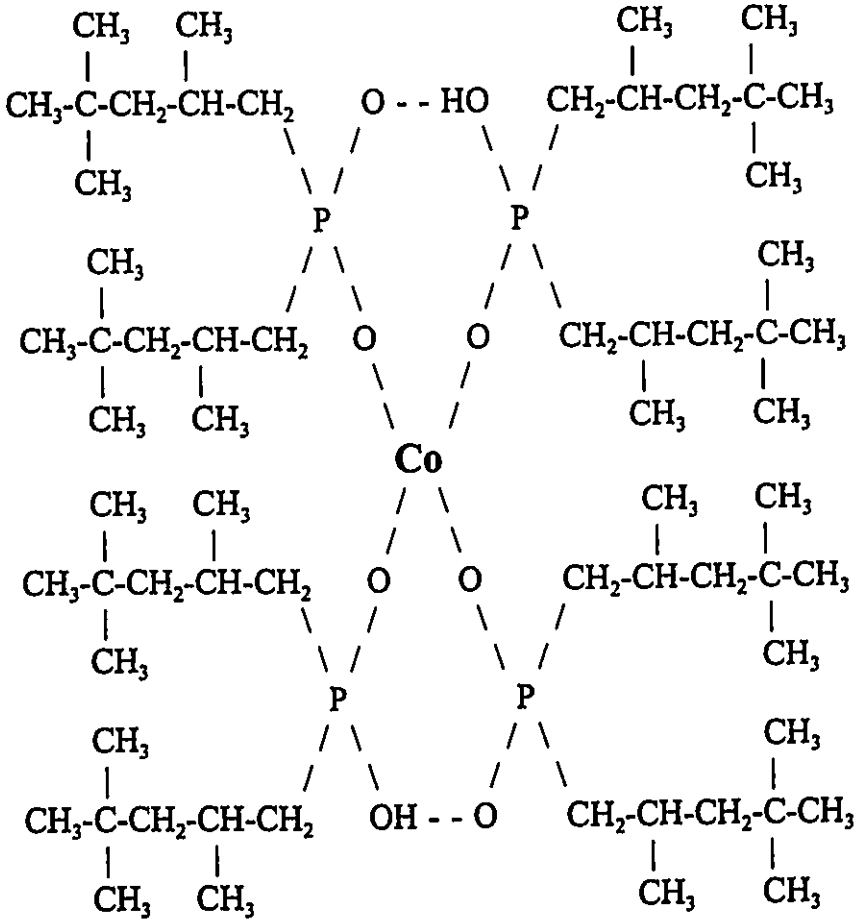

Figure 2-3: Organic cobalt compound with HDTMPP.

2.2 Experimental Techniques for Extraction Kinetics Studies

The ideal apparatus for the study of extraction kinetics should have the following characteristics [Li, 1987]: 1) ease of operation, 2) capability of studying the effect of individual variables, 3) possibility of determining the interfacial areas accurately, 4) constant hydrodynamic conditions, 5) possibility of continuous measurement of the variables, 6) simple calculation and evaluation of the extraction rate constants and 7) good reproducibility. Several types of the traditional techniques for kinetic studies of liquid-liquid extraction are discussed in the following paragraphs.

2.2.1 Single-drop Technique [Shen et al., 1984]

In the single-drop technique, drops of known size and hence interfacial area are passed through the continuous phase in a vertical column, as in Figure 2-4. Mass transfer and diffusion are strongly enhanced when there is internal circulation within the drops. However, this is difficult to control in this type of apparatus.

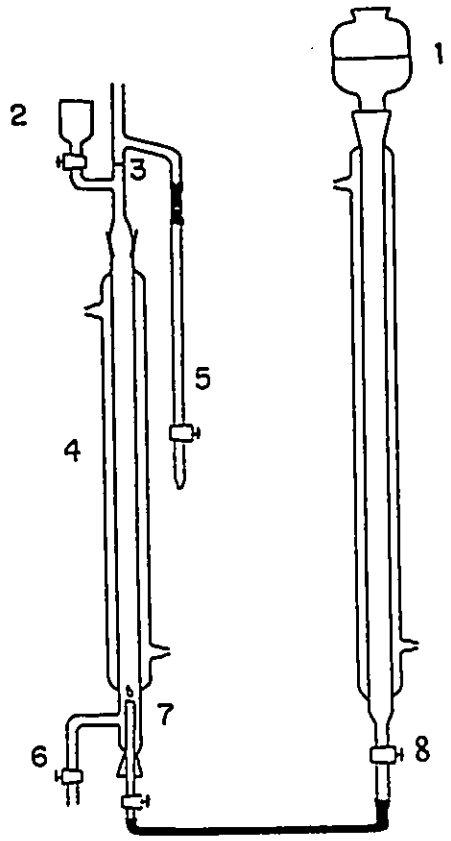

Figure 2-4: Single drop method [Shen et al., 1984]: 1. organic extractant reservoir; 2. aqueous phase reservoir; 3. interface; 4. jacketed extraction column; 5. organic phase collector; 6. aqueous phase outlet; 7. organic phase inlet; and 8. jacketed column for temperature equilibration.

2.2.2 Lewis Cell

The original Lewis cell, as seen in Figure 2-5, was first used by Lewis in 1954 [Lewis, 1954] when he studied the individual mass transfer coefficients for

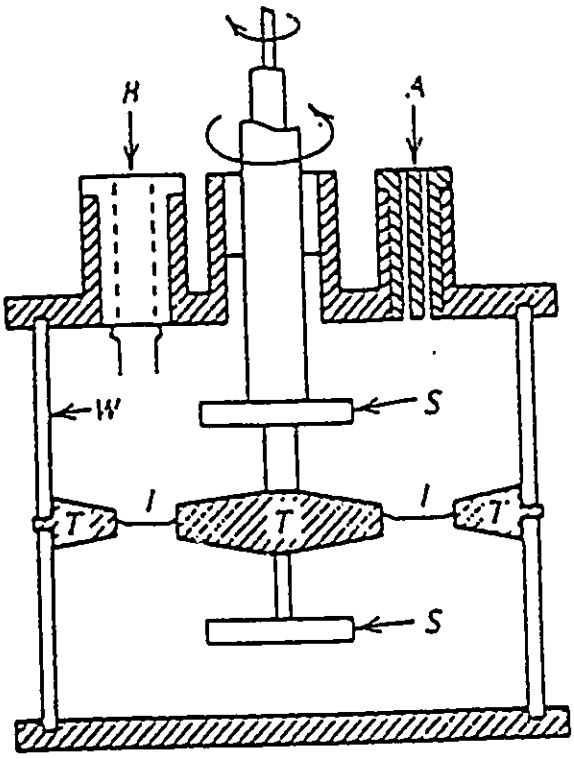

Figure 2-5: The original Lewis cell [Lewis, 1954]: A. sampling plug; B. polythene plug with electrodes; S. impellers; T. stator baffles; I. interface; and W. cylindrical glass wall.

eight partially miscible binary systems. This apparatus consists of a vessel containing the phases that are stirred simultaneously to achieve mixing within each phase without causing interfacial rippling. Interfacial area is controlled by the vessel geometry and can be measured accurately.

The different models of the Lewis cell for the study of liquid-liquid extraction and their characteristics were discussed by Li [Li, 1987]. These cells are mainly classified into two distinct types. The Type I cell refers to the Kamen type [Kamen, 1983], and is shown in Figure 2-6. The Type II cell is an interfacial contactor with a diverging cylindrical baffle, as shown in Figure 2-7 [Reinhardt et al., 1972].

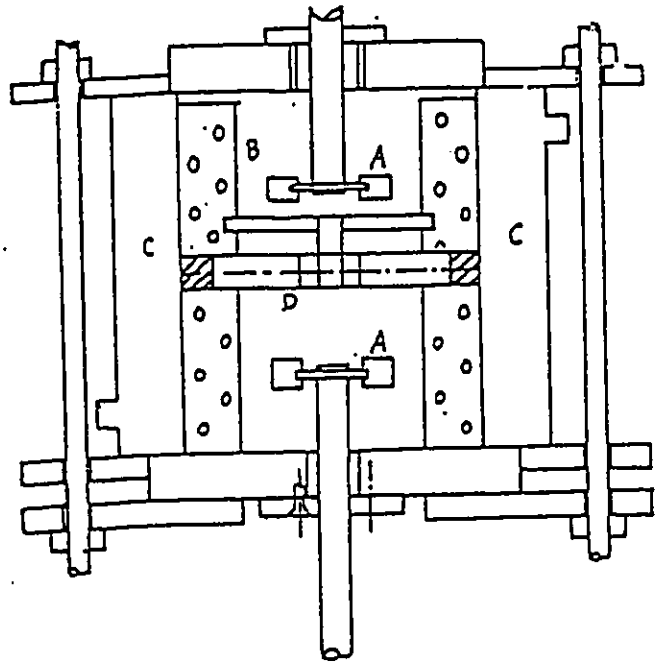

Figure 2-6: Type I version of the Lewis cell [Kamen, 1983]: A. stirrers; B. wall baffles; C. jacket; and D. interfacial ring.

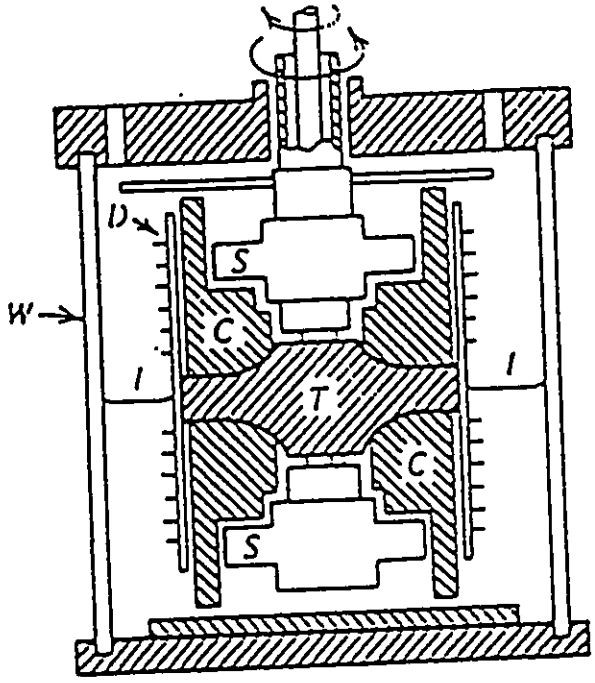

Figure 2-7: Type II version of the modified Lewis cell [Reinhardt et al., 1972]: C. vertical baffles; D. cylindrical grid; S. impellers; T. stator ring; I. interface; and W. cylindrical glass wall.

The hydrodynamic conditions in the two modified types of Lewis cell are very different. In the Type I cell the paddle stirrers are close to the interface. The boundary layers in the two phases at the interface are sensitive to the hydrodynamic conditions in the two phases respectively. By varying the two individual stirrer speeds, the relationship between the boundary layers and the hydrodynamic

conditions can be observed clearly. It is convenient in this type of cell to study the mass transfer diffusion from the two individual bulk phases to the interface. However, this type of Lewis cell can not be used at high impeller speeds because of the interfacial area fluctuations caused by rippling. The cylindrical baffle in the Type II cell makes it possible to change the hydrodynamic conditions without affecting the interface. As a result, the Type II cell is only suitable for studying the chemical reaction mechanism in the two bulk phases, i.e., the aqueous phase or the organic phase.

2.2.3 Stirred Contactor

Complete dispersion of the phases can be achieved with either shaking flasks or stirred contactors. A contactor that has been extremely useful in studying metal extraction is the AKUFVE equipment, which essentially consists of a mixer and a centrifuge for rapid and complete phase separation and recycle [Reinhardt and Rydbery, 1983], as seen in Figure 2-8. This is a totally enclosed system. On-line sensing can be used in the recycle loops to yield kinetic data, which provides an advantage over a simple stirred mixer or a shaken flask. However, the AKUFVE technique cannot be used to study the effect of interface-related rate-controlling processes because it is not possible to control and measure the interfacial area when using this method.

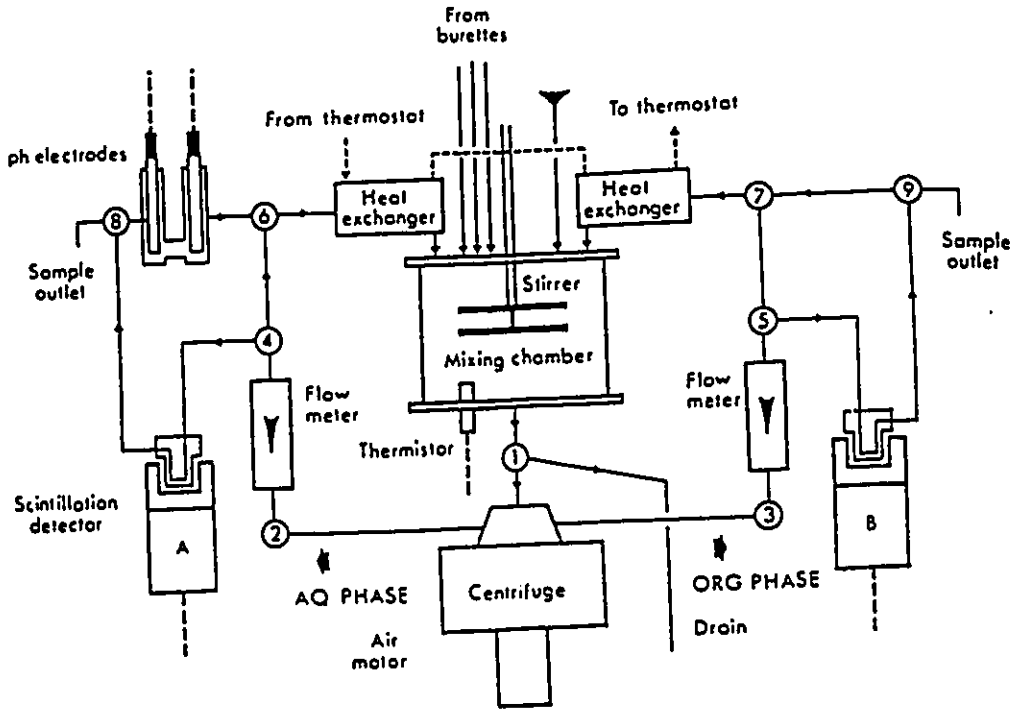

Figure 2-8: AKUFVE liquid flow system [Reinhardt and Rydbery, 1983].

The hydrodynamic conditions are of major importance in the study of the rate processes in solvent extraction. Each of these three methods employs quite different hydrodynamic conditions and this must be considered when comparison is made between the kinetic data obtained by these types of contactors.

2.3 Mechanism Models

Various models of extraction mechanisms have been proposed for solvent extraction systems [Coleman and Roddy, 1971; Danesi and Chiavizia, 1980 and Zhu, 1993]. The models are usually classified in terms of their rate controlling steps. These include:

(1) aqueous bulk phase reaction,

(2) interfacial film diffusion,

(3) interfacial diffusion with aqueous phase chemical reaction,

(4) interfacial chemical reaction and

(5) organic bulk phase reaction.

Model 1 predicts that the extraction rate should be independent of the interfacial area. Model 2 predicts that purely physical processes control the kinetics. Model 3 is the combination of Model 1 and Model 2. Model 4 predicts that the extraction rate should be independent of the hydrodynamic conditions in both aqueous phase and organic phase. Model 5 assumes that the extraction rate is controlled by the chemical reaction in the organic phase.

The mechanisms developed by several investigators are discussed in the following paragraphs.

Albery and Fick [Albery and Fick, 1981] proposed that the following series of reactions describe an interfacial extraction mechanism for cobalt extraction into HEHEHP:

Step 1 $$\overline{(HA)_2} \rightleftharpoons \overline{(HA)_{2,i}}$$

Step 2 $$\overline{(HA)_{2,i}} + M^{2+} \rightleftharpoons \overline{MA_2H^+}_i + H^+$$

Step 3(i) $$\overline{(HA)_{2,i}} + \overline{MA_2H^+_i} \rightleftharpoons \overline{MA_2(HA)_{2,i}} + H^+$$

Step 3(ii) $$\overline{(HA)_2} + \overline{MA_2H^+_i} \rightleftharpoons \overline{MA_2(HA)_{2,i}} + H^+$$

Step 4 $$\overline{MA_2(HA)_{2,i}} \rightleftharpoons \overline{MA_2(HA)_2}$$

Step 1 involves the interfacial adsorption of an HEHEHP dimer. Step 2

involves the reaction between the adsorbed dimer and a metal ion in close proximity to the interface. Step 3 has two possibilities, reaction between the interfacially adsorbed species and another HEHEHP dimer either at the interface or dimer diffusing from the bulk organic phase. Step 4 involves the desorption of the reaction product from the interface. A basic reaction scheme has been chosen which treats Step 1 as a rapid equilibrium, and Step 3(ii) as the rate controlling step. Note the over bars indicate an organic phase concentration.

The mass transfer with chemical reaction mechanism model (MTWCR) proposed by Dreisinger and Cooper [Dreisinger and Cooper, 1986] involves both interfacial film diffusion of the reactant and product species and aqueous phase chemical reactions. For solvent extraction systems, only the aqueous side boundary film was considered in the development of the model. Ionic reaction intermediates were not thought to be able to form in the organic phase.

The authors applied this model to the Cobalt-HEHEHP system and assumed that there was a fast reaction occurring close to the interface. In addition, they considered that the extractant was dimerized in the organic phase and two dimers were associated with the extracted cobalt extracted complex. The extractant molecule is usually considered to exist as a dimer in the organic phase and as a monomer in the aqueous phase [Danesi, 1984]. The reaction scheme was suggested

as follows:

Step 1 $$\overline{HA_2} \rightleftharpoons HA_2$$

Step 2 $$(HA)_2 \rightleftharpoons HA_2^- + H^+$$

Step 3 $$Co^{2+} + HA_2^- \rightleftharpoons CoHA_2^+$$

Step 4 $$CoHA_2^+ + HA_2^- \rightleftharpoons CoA_2(HA)_2$$

Step 5 $$CoA_2(HA)_2 \rightleftharpoons \overline{CoA_2(HA)_2}$$

They found that the extraction rate was controlled by the aqueous phase boundary layer reaction involving the addition of the first extractant ligand to the metal ion.

Hughes and Rod [Hughes and Rod, 1984] developed a simplified mass transfer with chemical reaction mechanism model (MTWCR) for the general case of divalent metal extraction with an acidic extractant.

Step 1 $\overline{HA} \rightleftharpoons HA$

Step 2 $HA \rightleftharpoons H^{+} + A^{-}$

Step 3 $M^{2+} + A^{-} \rightleftharpoons MA^{+}$

Step 4 $MA^{+} + A^{-} \rightleftharpoons MA_2$

Step 5 $MA_2 \rightleftharpoons \overline{MA_2}$

Step 1 involves the fast partitioning of the extractant in the aqueous phase followed by the fast dissociation of the extractant, Step 2. Step 3 and Step 4 involve the addition of the first and second ligands to the metal ion. Step 5 involves the rapid partitioning of the metal complex into the organic phase. The first ligand addition is considered to be the rate controlling step.

Cianetti and Danesi [Cianetti and Danesi, 1983] considered that there were two limiting and alternative possibilities: that is, the mass transfer rate was controlled by either interfacial chemical reactions or by interfacial film diffusion. The following equations described the extraction mechanism for the Cobalt-HDEHP system, where Step 1 was considered to be the rate controlling step under the experimental conditions used:

Step 1 $$M^{2+}+2(HA)_i \rightleftharpoons (MA_2)_i+2H^+$$

Step 2 $$(MA_2)_i+v\overline{(HA)_2} \rightleftharpoons \overline{MA_2(HA)_{2v-2}}+2(HA)_i$$

Yang et al. [Yang et al., 1993] proposed a consecutive reaction scheme for the extraction of cobalt ions with dithizone (HD_Z) in a buffer-free system:

Step 1 $$HD_Z \rightleftharpoons H^+ + D_Z^-$$

Step 2 $$Co^{2+}+D_z^- \rightarrow CoD_Z^+$$

Step 3 $$CoD_Z^+ + D_Z^- \rightarrow CoD_{Z2}$$

Step 1 was considered to be the rate controlling step while Step 2 and Step 3 were fast reactions. All the reactions were assumed to take place in the aqueous phase. The diffusion processes in the aqueous phase, in the organic phase, and between the interface and either of the bulk phases were not considered. They found that the kinetic mechanism of the interfacial reaction was changed when citric acid was introduced into the aqueous phase. The following two parallel steps were suggested as the rate-limiting-steps by comparing the mechanism model with the experimental data:

Step 1 $CoC^{-}+HD_z \rightarrow CoD_z^{\cdot}+HC^{2-}$

Step 2 $CoHC+HD_z \rightarrow CoD_z^{\cdot}+H_2C^{-}$

It was concluded that the mass transfer regime could be changed from diffusion-controlled to chemical-reaction-controlled by decreasing the concentration of metal ions or by adding an auxiliary complexing agent in the aqueous phase.

Fu and Golding [Fu and Golding, 1988] carried out an investigation of cobalt extraction into mono-acid neutralized extractant HDTMPP. After neutralization, some of the hydrogen ions in the extractant were exchanged with sodium ions. The changes in the organic phase viscosity were also observed, which were a function of the organic phase loading. Mass transfer rates found in the investigation were the same order of magnitude as the results from cobalt extraction into HDEHP [Golding and Pushparajah, 1985]. They observed that the mass transfer coefficient values were a function of the sodium salt concentration in the organic phase. Once the sodium had been replaced by the cobalt, the overall mass transfer coefficient values were lowered substantially, even though the aqueous phase pH was maintained at 5.5. They concluded that the pre-equilibration of the extractant with sodium hydroxide, as carried out in industry, was essential for the maintenance of high extraction rates. They proposed that the extraction kinetics of all the organic

phosphorus extractants would be similar. The following scheme was assumed:

Step 1 $$\overline{NaA.HA} \rightleftharpoons NaA.HA$$

Step 2 $$Co^{2+} + 2NaA.HA \rightleftharpoons CoA_2.(HA)_2 + 2Na^+$$

Step 3 $$CoA_2.(HA)_2 \rightleftharpoons \overline{CoA_2.(HA)_2}$$

Zhou and Li [Zhou and Li, 1986] investigated the cobalt extraction with neutralized mono-methyhhepty1 hexyl phosphonic acid (HMHHP). The following mechanism was suggested:

Step 1 $$\overline{HA} \rightleftharpoons HA$$

Step 2 $$HA \rightleftharpoons H^+ + A^-$$

Step 3 $$Co^{2+} + A^- \rightleftharpoons CoA^+$$

Step 4 $$CoA^+ + A^- \rightleftharpoons CoA_2$$

Step 5 $$CoA_2 \rightleftharpoons \overline{CoA_2}$$

Step 5 was considered to be the rate controlling step under the experimental conditions. It meant that the diffusion from the interface to the organic bulk phase dominated the extraction process. These results were not in agreement with the work of other authors who developed the MTWCR model, in which the diffusion from the interface to the organic bulk phase was not considered.

Using the buffer solution of sodium acetate-acetic acid system, which was proposed to maintain the pH during the cobalt extraction, Chen [Chen, 1986] studied cobalt extraction with the HEHEHP system. The controlling mechanism was considered at low extraction rates. The controlling steps were the diffusion of the reactants and the product species across the interface. Chen assumed that the adsorbed extractant concentration at the interface was different from the boundary film extractant concentration. The following mechanism was suggested:

Step 1 $$\overline{HA} \rightleftharpoons HA_{ad}$$

Step 2 $$HA_{ad} + M_i^{2+} \rightleftharpoons MA_i^{+} + H_i^{+}$$

Step 3 $$MA_i^{\cdot}+HA_i=MA_{2i}+H_i^{\cdot}$$

Chen suggested that the controlling step was Step 2 when the pH was lower than 4, but Step 3 would control the extraction rate when the pH was greater than 4.

Shen et al. [Shen et al., 1985 and Shen, 1984] investigated the cobalt extraction with HDEHP by using the single drop method. The process was considered to be a two-step interfacial chemical reaction:

Step 1 $$Co^{2+}+2\overline{HA_i}=\overline{CoA_{2i}}+2H^{+}$$

Step 2 $$\overline{CoA_{2i}}+2\overline{H_2A_2}=\overline{CoA_2.2HA}+2\overline{HA_i}$$

At high extractant concentrations, Step 1 was the controlling step, while at lower extractant concentrations, Step 2 was the controlling step.

Yan [Yan, 1989] improved the Lewis cell by using the auto-titration technique. The effects of different variables on cobalt extraction rate with the HMHHP extractant were investigated. By controlling the pH, the variables could be changed independently. Using a buffer-free system and utilising the activity coefficients, a mechanism of the extraction was suggested for the kinetics of cobalt extraction with HMHHP:

Step 1 $$Co^{2+} \rightarrow Co_i^{2+}$$

Step 2 $$CoA_{ad}^{+} + \overline{HA_i} \rightleftharpoons CoA_{2ad} + H_i^{+}$$

For pH values > 4.0, the extraction rate was controlled by Step 1, which is the diffusion of the cobalt ions; for pH < 4.0, the chemical reaction controls the extraction rate, as in Step 2.

From the literature survey, it can be seen that several kinetic mechanisms for cobalt extraction have been suggested. In addition, there is some uncertainty as to whether the extraction should be considered diffusion controlled or chemical reaction controlled or a combination of both (see for example the work of Abbery and Fick, Dreisinger and Cooper, and Zhou and Li). It was decided therefore, that further work was required to determine the extraction mechanism and to investigate what factors affect the extraction rate.

2.4 Calculation of Aqueous Phase Cobalt Activities

It has been suggested that kinetic mechanism of extraction can be explained better by using activities rather than concentrations [Li, 1985]. For simple aqueous systems with low ionic strength, the Debye-Hückel and Pitzer equations can be

used to calculate the activity coefficient of the ions in the aqueous phase.

2.4.1 Debye-Hückel Equation

At 25 °C for the ions in the aqueous phase, we have [Fu, 1979]

$$\log\gamma_{\pm}=-AZ_{+}Z_{-}\frac{\sqrt{I}}{1+\sqrt{I}} \qquad 2\text{-}1$$

where,

$$I=\frac{1}{2}\sum m_i Z_i^2 \qquad 2\text{-}2$$

I= ionic strength of the aqueous solution, kmol m^{-3};

Z_+, Z_- = the valencies of the positive or negative ions respectively;

A = 0.509 (at 25 °C);

$\gamma_{\pm}$ = activity coefficient; and

m = molar concentration, kmol m^{-3}.

This equation can be applied at the low ion strength (I is lower than 0.5 kmol m^{-3}). At high acid concentrations, the bisulfate sulfate equilibrium must be considered:

$$HSO_4^- \rightleftharpoons H^+ + SO_4^{2-} \qquad 2\text{-}3$$

$$D = \frac{[H^+]m_{SO_4^{2-}}}{m_{HSO_4^-}} \qquad 2\text{-}4$$

where D is the distribution constant. $D = 1.0\times10^{-2}$ kmol m^{-3} [Wang, 1987]. Considering the ion balance in the aqueous phase, there is

$$2[Co]^{2+}+[H^+] = [CoSO_4^-]+2[CoSO_4^{2-}] \qquad 2\text{-}5$$

Using Equations 2-4 and 2-5, the activities and the coefficients for different cobalt concentrations at pH = 5 are given in Figure 2-9(a) and Figure 2-9(b).

In Figure 2-9, It is seen that when the aqueous phase cobalt concentrations are in the range of 0 - 0.30 kmol m^{-3}, the activity coefficients vary from 1 - 0.0862 (Figure 2-9 (a)), while the activities vary from 0 - 0.0259 kmol m^{-3} (Figure 2-9 (b)).

It was found that pH had little effect on the aqueous phase cobalt activities, as seen in Figure 2-10.

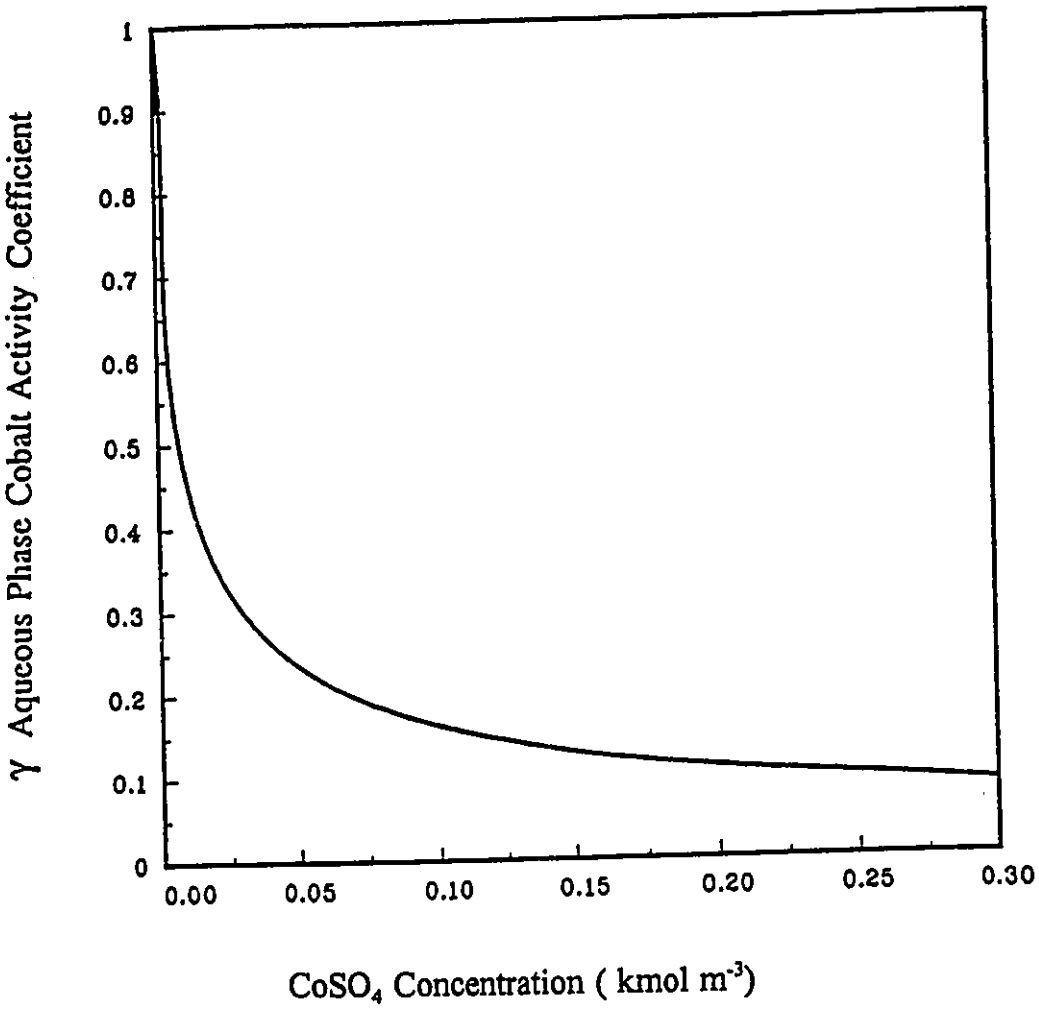

Figure 2-9(a): The activity coefficients of the different aqueous phase cobalt concentrations.

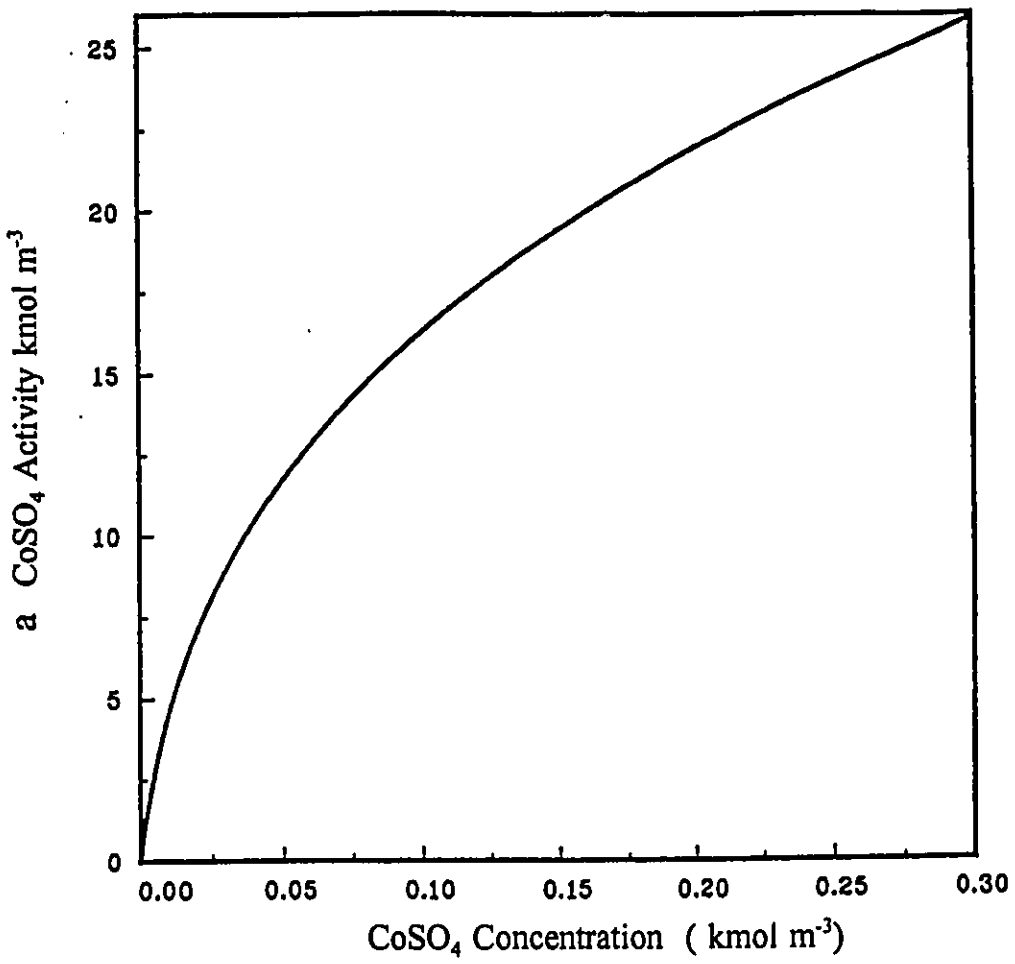

Figure 2-9(b): The activities of the different aqueous phase cobalt concentrations.

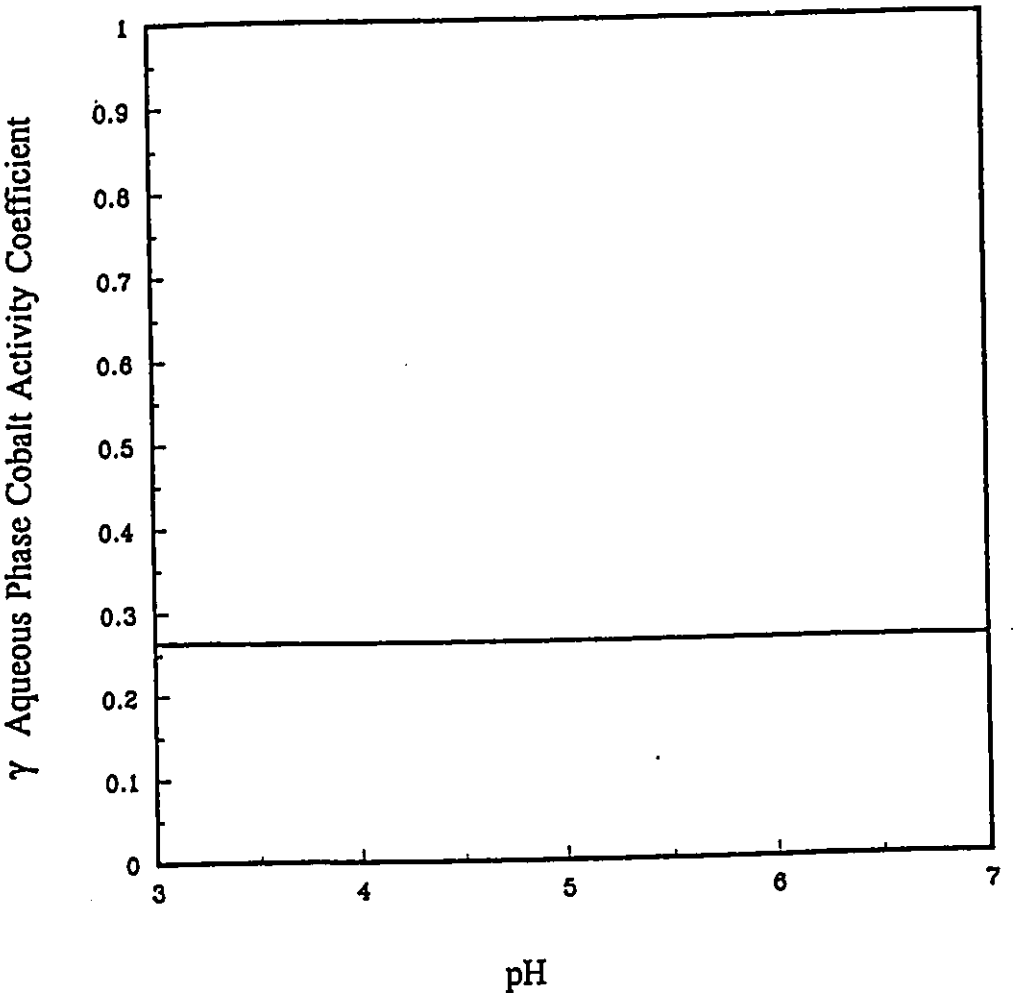

Figure 2-10: Effect of pH on the aqueous phase cobalt activity.

2.4.2 Pitzer Activity Coefficient Equation for Single Electrolyte Solutions

Pitzer deduced the equation for the average activity coefficient based on the ultra free energy theory in 1973 [Pitzer, 1973]. Today, the Pitzer equation is widely used for aqueous phase solutions because of the recent advances in computer technology [Li, 1985]. For a single electrolyte solution:

$$\gamma_{MX} = -|Z_M \times Z_X| f^{\gamma} + m\frac{\nu_m \nu_x}{\nu} B_{MX}^{\gamma} + \frac{m^2 2(\nu_m \nu_x)^{3/2}}{\nu} C_{MX} \qquad 2\text{-}6$$

where,

$$f^{\gamma} = -A_{\phi}\left[\frac{I^{1/2}}{1+bI^{1/2}} + \frac{2}{b}\ln(1+bI^{1/2})\right] \qquad 2\text{-}7$$

For the 2-2 valency electrolyte:

$$B_{MX}^{\gamma} = 2\beta_{MX}^{(0)} + \frac{2\beta_{MX}^{(1)}}{\alpha_1^2 I}\left[1-(1+\alpha_1 I^{1/2} - \frac{1}{2}\alpha_1^2 I)e^{-\alpha_1 I^{1/2}}\right] \qquad 2\text{-}8$$

$$+\frac{2\beta_{MX}^{(2)}}{\alpha_2^2 I}\left[1-(1+\alpha_2 I^{1/2} - \frac{1}{2}\alpha_2^2 I)e^{-\alpha_2 I^{1/2}}\right]$$

where,

ν_M, ν_X = the values of positive and negative ions of molecule MX;

$\nu = \nu_M + \nu_X$; $A\phi = 0.391$, $b = 1.2$, $\alpha_1 = 1.40$, $\alpha_2 = 12.0$;

and for $CoSO_4$ at 25 °C [Li, 1985]: $\beta^{(0)} = 0.20$, $\beta^{(1)} = 2.70$, $\beta^{(2)} = -30.7$ and $C^{\phi} = 0.0$.

The results obtained from the Pitzer equation and the Debye-Hückel equation are compared in Table 2-1.

Table 2-1: Comparison of activities from Pitzer and Debye-Hückel equations.

m_{CoSO4}	0.01	0.02	0.04	0.06	0.12	0.20	0.30
a^P	4.473	6.874	9.960	12.04	16.80	21.67	27.17
a^D	4.578	7.135	10.49	12.84	17.63	21.88	28.88
e, %	2.29	3.66	5.05	5.12	4.71	0.96	4.98

Here, a^P and a^D are the activities obtained by using the Pitzer and Debye-Hückel equations, mol m^{-3}. e is the difference between a^P and a^D.

$e = |a^P - a^d| / a^d \times 100\%$ and $e_{average} = 3.88$ %.

From Table 2-1 it can be observed that there was a small difference between the activities calculated from the Pitzer and the Debyl-Hückel equations for this

system. It has been widely accepted that both are useful for calculating the activities of the aqueous phase ions. However, as the Debye-Hückel equation is easier to use for calculating activities and has been found to be applicable for many systems it was used in this investigation.

2.5 Objectives

As noted previously, the mechanism of the cobalt extraction into phosphorous extractants is uncertain. The $CoSO_4$-HDTMPP system was studied and the main objectives in this study were:

1. the improvement of the experimental method for the study of kinetics of liquid liquid extraction with auto-titration and "gravity leg" techniques, and investigation of the extraction kinetics for the system without using a buffer solution;

2. the use of the activities instead of concentration in the driving force equation to obtain more realistic correlation of the data;

3. the determination of an effective method for determining the resistances in the aqueous phase, in the organic phase, and at the interface; and

4. the simulation of the extraction process by means of a mathematical model.

CHAPTER 3

Experimental Method

The Lewis cell was modified by using an auto-titration mechanism and 'gravity leg' feed system. The kinetic experiments for cobalt extraction into HDTMPP were carried out under different conditions by varying: the aqueous phase cobalt concentration, the aqueous phase sodium sulfate concentration or the ionic strength, the pH, the interfacial area, the extractant concentration, the organic phase modifier, the aqueous phase stirrer speed, the organic phase stirrer speed and the temperature.

3.1 Apparatus

Design of the experimental apparatus in this study was based on the Type I Lewis cell as this type of equipment had been found to be useful in studying extraction kinetics. The extraction process of cobalt-HDTMPP system was likely

controlled by the diffusion from the bulk phase to the interface or by the chemical reaction at the interface or a combination of them both rather than by chemical reaction in the bulk phases because the interfacial area affected the extraction rate according to the pre-experiments. Figure 3-1 shows the equipment layout for the kinetic study of the cobalt extraction.

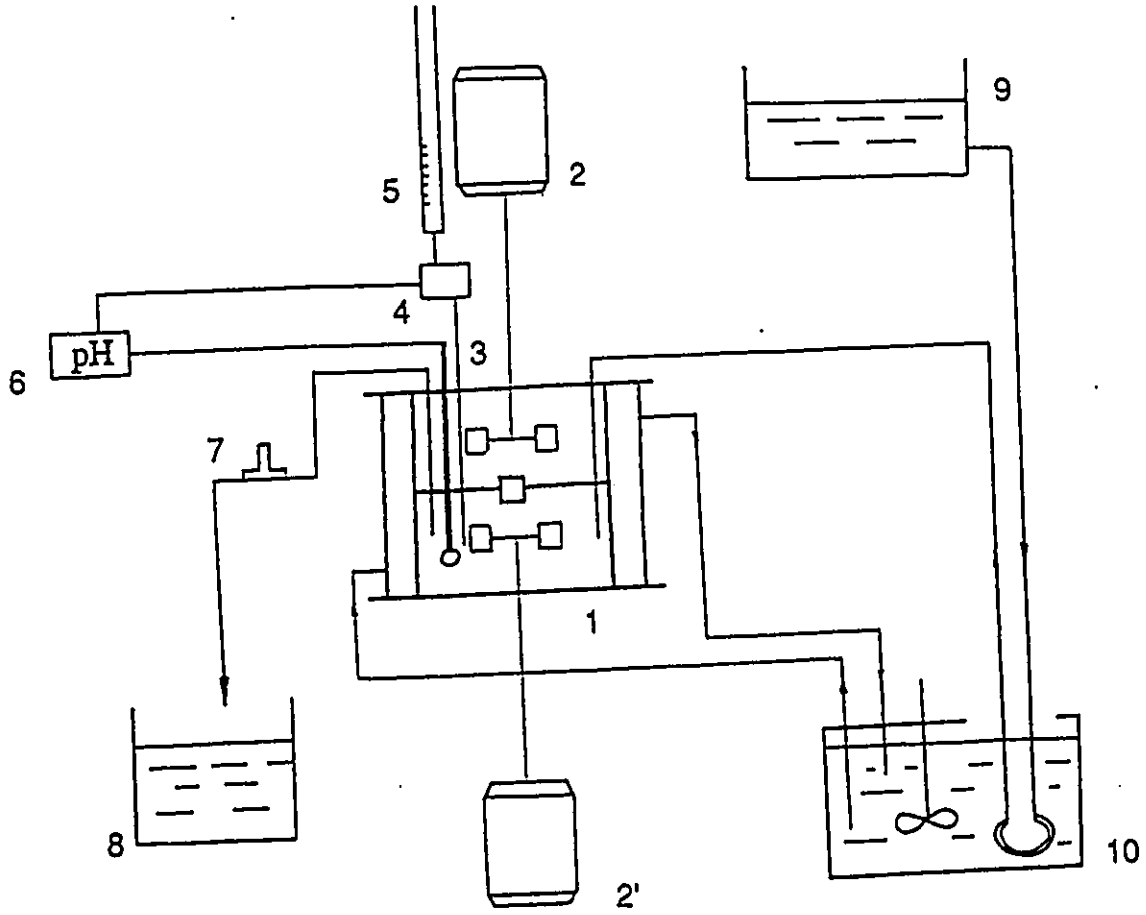

Figure 3-1: The experimental layout: 1. Lewis cell; 2 and 2'. servo motors; 3. pH electrode; 4. electro-magnetic valve; 5. NaOH buret; 6. pH meter; 7. "gravity leg"; 8. aqueous phase product tank; 9. aqueous phase reservoir; and 10. constant-temperature circulation bath.

The dimensions of the improved Lewis cell are shown in Table 3-1.

Table 3-1: The details of the improved Lewis cell.

Diameter of the cell = 100 mm
Height of the cell = 92.5 mm
Total volume of the cell = 700 ml
Diameter of the stirrers = 30 mm
Dimension of the vertical baffles: height = 40 mm; width = 10 mm
Dimension of the horizontal baffles: height = 40 mm; width = 10 mm

3.1.1 Design Considerations

The coaxial rotation of the phases was produced by the rotation of the stirrers. The vertical baffles and the horizontal baffles were used to increase the bulk turbulence. They were also useful to prevent the occurrence of eddies at the interface and to maintain an unrippled interface. The stirrers in both phases were driven by two servo motors which provided the steady rotation speeds in the range of 0 - 6 s^{-1} (0 - 350 rpm) with the error of ±1%.

3.1.2 Temperature Control

A thermometer was inserted into the Lewis cell and the temperature was controlled by the circulation of water in the water jacket. The temperature variation was ± 0.1 °C.

3.1.3 pH Control

A 6 mm diameter pH electrode was placed in the aqueous phase. A narrow tube was used to add the sodium hydroxide solution into the aqueous phase as the cobalt extraction experiments were carried out.

The flow of sodium hydroxide solution was controlled by a electromagnetic valve. As the pH fell, the electromagnetic valve opened automatically, and allowed the sodium hydroxide solution to flow into the aqueous phase. When the required pH was reached, the electromagnetic valve closed automatically. The pH could be controlled at a set value within an error of $\pm$ 0.1.

Choice of sodium hydroxide concentrations depended on the extraction rate. The sodium hydroxide concentration could not be so high as to cause the hydrolysis of $Co(OH)_2$ in the aqueous phase. Also, it could not be so low as to dilute the cobalt concentration in the aqueous phase. In this study, the NaOH concentration was maintained within the range from 0.01 to 0.1 kmol m^{-3}, depending on the cobalt extraction rate.

3.1.4 Aqueous Phase Cobalt Concentration Control

The aqueous phase cobalt concentrations were maintained constant during an experimental run by filling the fresh aqueous phase into the Lewis cell at a constant flow rate, while the aqueous phase flowed out of the cell at the same rate. Because of the very low extraction rate the aqueous phase cobalt concentration could be considered constant during an experimental run.

3.1.5 Interfacial Level Control

The interfacial level was maintained constant as any change of the level would affect the volume of the liquid in both phases as well as the hydrodynamic conditions in the cell. A "gravity leg" was used in the flow after the outlet of the aqueous phase. The "gravity leg" is a device to control the interfacial level by using the balance of the pressure difference between the liquid level in the improved Lewis cell and the level at the outlet. The interface level was kept constant even when the aqueous phase flow rate was varied.

In the kinetic experiments, the initial cobalt concentration in the organic phase was zero and the kinetic experimental runs were carried out at the low extraction rates. As a result, the organic phase cobalt concentrations were very low

during the experiments. Normally, the extraction rate was less then 1.0×10^{-6} mol s^{-1} and the experimental runs lasted less than 2 hours. The organic phase cobalt concentrations were less than 1.0×10^{-4} mol m^{-3}, which could be neglected compared to the aqueous phase cobalt concentrations. It could be considered then, that there was no effect of organic phase cobalt concentration on the extraction rate under the present experimental conditions. In addition, at such low organic phase cobalt concentrations it became convenient to analyze the organic phase cobalt concentration directly with the spectrophotometer, see Appendix 2.

3.2 Experimental System

3.2.1 Organic Phase Composition

3.2.1.1 Extractant

The bis (2.4, 4-trimethylpentyl) phosphinic acid (HDTMPP) is a recent solvent extraction reagent developed by the American Cyanamid Company. The commercial name is Cyanex 272. It exhibits a high degree of selectivity for cobalt against nickel in both sulphate and chloride media. Its chemical structure and properties are shown in Figure 3-2 and in Table 3-2 , respectively [Cyanamid, 1990].

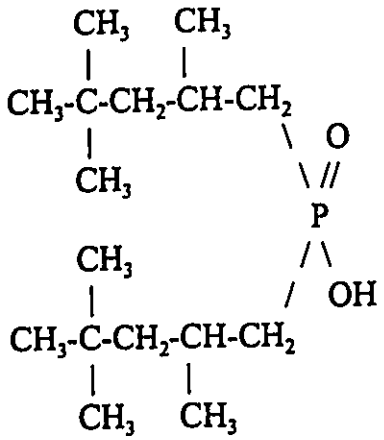

Figure 3-2: The structure of the HDTMPP extractant molecule.

Table 3-2: The chemical and physical properties of the HDTMPP extractant.

Appearance: Colourless to light amber liquid
Molecular Weight = 290.13
Specific Gravity = 0.92 at 24 °C
Viscosity (Brookfield) = 142 cp at 25 °C
= 37 cp at 50 °C
Solubility in distilled H_2O = 16 μg ml^{-1} at pH = 2.6
38 μg ml^{-1} at pH = 3.7
Pour Point = -32 °C

HDTMPP extractant is totally miscible with the common aromatic and aliphatic diluents and is stable to both heat and hydrolysis.

3.2.1.2 Modifier

Tributyl phosphate (TBP) was the first commercial extractant used in the

nuclear industry for the separation and refining of uranium. Today, it is widely used as an extractant or modifier in many extraction processes to prevent the third phase formation. The TBP used in this study was supplied by Albright and Wilson Company, America. The properties of TBP are showed in Table 3-3.

Table 3-3: The chemical and physical properties of the TBP modifier.

Appearance: Colourless
Molecular weight = 266.3
Viscosity = 3.32 cp at 25 ^{o}C
Specific gravity = 0.9727 at 25 ^{o}C

3.2.1.3 Diluent

The diluent used in the experiment was kerosene, commercially known as VARSOL DX3641, produced by ESSO Chemical, Canada. The properties of the diluent are shown in Table 3-4.

Table 3-4: The chemical and physical properties of the diluent.

Viscosity = 1.935 cp at 20 ^{o}C
Specific gravity = 0.750 at 20 ^{o}C

The properties of the organic phase used in the experiments are shown in

Table 3-5 and Table 3-6.

Table 3-5: The properties of the organic phase at different extractant concentrations.

H_2A_2	v/v	0.01	0.02	0.05	0.10	0.15
$[H_2A_2]$	kmol m^{-3}	0.0135	0.0230	0.0674	0.135	0.202
$\mu \times 10^3$	N m^{-2} s	3.44	4.88	9.01	16.0	23.0
ρ	kg m^{-3}	763.0	764.7	769.8	778.3	786.8

Table 3-6: The properties of the organic phase at different modifier concentrations at $[H_2A_2]$ = 0.135 kmol m^{-3}.

TBP	v/v	0.005	0.01	0.02	0.05	0.10
[TBP]	kmol m^{-3}	0.0183	0.0366	0.0733	0.183	0.366
$\mu \times 10^3$	N m^{-2} s	15.95	15.96	15.97	16.0	16.08
ρ	kg m^{-3}	768.1	769.3	780.3	778.3	789.6

Prior to the beginning of the experiment, the organic phase was pre-equilibrated by shaking it with distilled water at the phase ratio of 1:1. This process was repeated three times until the pH in the aqueous phase became greater than 4. It is considered that when the pH value in the aqueous phase is greater than 4 at equilibrium the extractant in the organic phase will be purified [Li, 1988]. The organic phases were allowed to sit for one week before being used to ensure the complete phase separation.

3.2.2 Aqueous Phase Composition

The $CoSO_4$ solutions were prepared using $CoSO_4.7H_2O$ and distilled water. $CoSO_4.7H_2O$ was abtained from the J.J. Baker Chemical Cooperation and the purity was greater than 99.4%. The solution was adjusted to the required pH by adding 2N H_2SO_4 or 1N NaOH solution. The added sodium ions did not affect the extraction. For instance, when the sodium solution was used to adjust the pH value of the aqueous phase from 4 to 7, the maximum sodium concentration in the aqueous phase was less than 1.0×10^{-4} kmol m^{-3}. The aqueous phase cobalt concentration was determined by the EDTA titration method, and is discussed in Appendix 3.

Organic phase cobalt concentration was measured directly by spectrophotometry. The spectrophotometer, Model 4050, was the product of LKB Biochrom Ltd, England. At 549 nm, there was a linear relationship between organic cobalt concentration and absorbance as shown in Appendix 2.

3.3 Operating Procedures

1. After the constant-temperature circulation bath was started and the temperature was set at the required value, both aqueous and organic phases were

kept in the bath at this temperature for one hour. Following this, water was circulated in the jacket of the Lewis cell and the cell was maintained at the design temperature.

2. The Lewis cell was then filled with the aqueous phase until the liquid level reached the middle point of the interfacial ring.

3. The stirrer speeds in both the aqueous phase and the organic phase were then set at the required value.

4. The pH was set at the required value.

5. The upper volume of the cell was filled with the organic phase. This prevented the cell from being disturbed by the eddy current. Also, care was taken to avoid a fast flow of the organic phase, which could lead to the entrapment of the organic phase into the aqueous phase.

6. As soon as the Lewis cell was filled with the organic phase, the motors and the timer were started simultaneously.

7. At the same time, the pH controller was started.

8. The organic phase cobalt concentration was analyzed at 15 minutes intervals by taking 2 ml samples of the organic phase. After analysis, the samples were returned to the cell.

9. The quantity of NaOH used was measured at the end of the experimental run.

10. The experimental runs were usually carried out for about 90 - 120

minutes.

The mean residence time of the aqueous phase in the cell is:

$$t = V/Q \qquad 3\text{-}1$$

here,

t = mean residence time, min;

V = aqueous phase volume, ml; and

Q = aqueous phase flow rate, 20 ml min^{-1}.

Assuming the aqueous phase in the improved Lewis cell is perfectly mixed, the mean residence time is 12 minutes. The cobalt extraction rate, J, is given by Equation 3-2:

$$J = Q(C_{in} - C_{out}) \qquad 3\text{-}2$$

C_{in} and C_{out} are the inlet and outlet aqueous phase cobalt concentrations, respectively and J is the extraction rate, mol s^{-1}.

Normally, $J < 1.0 \times 10^{-6}$ mol s^{-1}; so, $C_{in}-C_{out} < 1.0 \times 10^{-8}$ mol m^{-3}.

Therefore, it can be considered that the aqueous phase cobalt concentration is constant during an experimental run.

Figure 3-3 shows the study of the effect of varying aqueous phase cobalt concentration on the extraction rate. It can be seen that there is a linear relationship between the organic phase cobalt absorbance and time. All of the correlation coefficients were greater than 0.98. From the slope of the linear relationship, the extraction rate can be calculated exactly as:

$$J = V_{org} \times b_A \times b_L \qquad 3\text{-}3$$

where,

V_{org} = organic phase volume, m^3;

b_A = ratio of organic phase cobalt concentration to its absorbance, kmol m^{-3} (See Appendix 2); and

b_L = slope of the linear relationship of absorbance with time, s^{-1} (See Appendix 1).

3.4 Operation Variables

1. Stirrer rotation speeds

The stirrer rotation speeds in the aqueous phase ranged from 0.5 s^{-1} to 3.5 s^{-1} and in organic phase ranged from 0.5 s^{-1} to 5.0 s^{-1}.

The servo motors were used to keep the experimental agitation speeds steady. In the experimental rotation speed ranges, the error of the rotation speeds was less than 2.0%. When the rotation speeds were higher than 5.0 s^{-1}, the

interfacial rippling was observed.

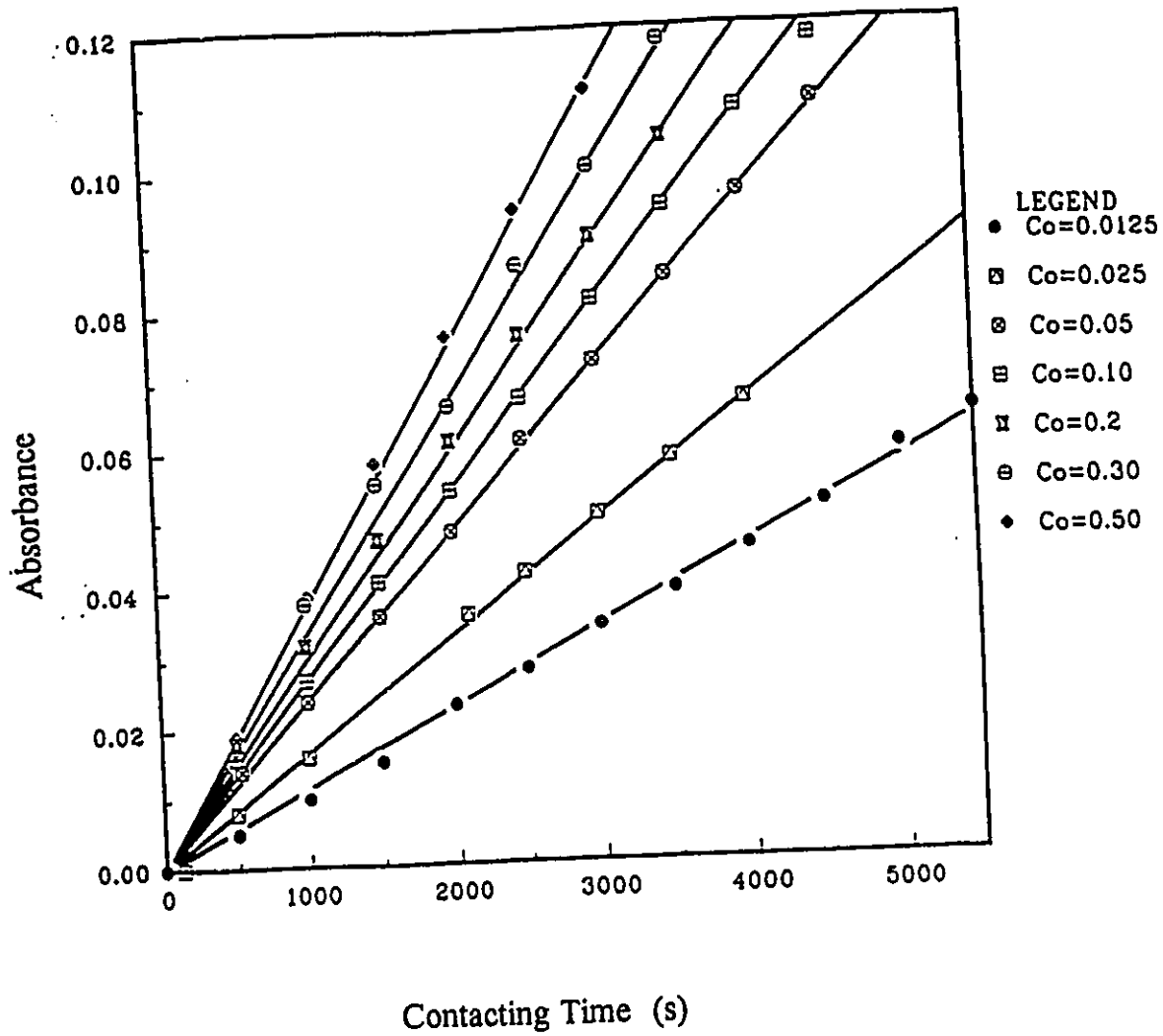

Figure 3-3: Variation of aqueous phase cobalt concentrations with extraction rates. Experimental condition: T = 25 °C; A = 7.775×10^{-3} m^2; C_{Na2SO4} = 0 kmol m^{-3}; pH = 5.0; C_{H2A2} = 0.2695 kmol m^{-3}; C_{TBP} = 0.1832 kmol m^{-3}; Re_{aq} = 2102.5; and Re_{org} = 110.5.

2. pH

The pH was in the range of 1.8 to 7.5. When the pH was higher than 7.5 the hydrolysis of $Co(OH)_2$ would like to take place.

3. Aqueous phase cobalt concentration

The aqueous phase cobalt concentrations ranged from 0.00125 to 0.5 kmol m^{-3}.

4. Flow rate of aqueous phase

The aqueous phase flow rates ranged from 0.0 to 23 ml min^{-1}.

5. Interfacial area

The interfacial areas ranged from 1.15×10^{-3} to 7.75×10^{-3} m^2.

6. Temperature

The extraction temperatures ranged from 14.3 to 56.0 ^{o}C.

7. Extractant concentration

The extractant concentrations ranged from 0.0 to 0.15 v/v, that is, from 0.0 to 0.202 kmol m^{-3} as H_2A_2.

8. Modifier concentration

The modifier concentrations ranged from 0.0 to 10% v/v (from 0 to 0.366 kmol m^{-3}).

3.5 Analysis of the Experimental Error

In order to provide a basis to determine the effects of the kinetic variables on the extraction rates and to obtain an estimate of the error, the standard condition for the experiment was chosen as follows, see Table 3-7.

Table 3-7: Standard experimental conditions.

$T = 25\ ^{o}C$
$A = 7.775 \times 10^{-3}\ m^2$
$C_{Co2SO4} = 0.10\ kmol\ m^{-3}$
$C_{Na2SO4} = 0.0\ kmol\ m^{-3}$
$pH = 5.0$
$C_{H2A2} = 0.2695\ kmol\ m^{-3}$
$C_{TBP} = 0.1832\ kmol\ m^{-3}$
$Re_{aq} = 2102.5$
$Re_{org} = 110.5$

Experimental runs were carried out to determine the effects of (1) the aqueous phase cobalt concentration, (2) the pH, (3) the temperature, (4) the aqueous phase sodium sulphate concentration and (5) the organic phase extractant concentration on the extraction rates. The extraction rates and the experimental error for the runs carried out under standard conditions are shown in Table 3-8.

Table 3-8: The extraction rates under the standard conditions and the experimental errors.

		(1)	(2)	(3)	(4)	(5)
$J \times 10^7$	mol s^{-1}	1.099	1.10	1.15	1.11	1.28
e	%	4.3	3.5	0.1	3.6	11.3

here, J is the extraction rate and e is the experimental error.

$J_{average} = 1.15 \times 10^{-7}$ mol s^{-1}.

The errors were calculated by using Equation 3-4:

$$e = \frac{|J - J_{average}|}{J_{average}} \times 100\% \qquad 3\text{-}4$$

The average of the errors was 4.52%. As a result, the majority of the runs were not duplicated.

CHAPTER 4

Results and Discussion

The effects of the different variables on the extraction rate, that is, the aqueous phase cobalt concentration, the ionic strength, the interfacial area, the extractant concentration, the modifier concentration, the pH, the aqueous phase stirrer speed, the organic phase stirrer speed and the temperature, were investigated. Each variable was changed independently while keeping the remaining variables constant. Both activity and concentration were used in the driving force to interpret the results. Based on the two film-theory the extraction resistances in the aqueous phase, in the organic phase and at the interface were estimated.

4.1 Effect of Aqueous Phase Cobalt Concentration

Figure 4-1 shows the effect of the aqueous phase cobalt concentration on the extraction rate. At the lower cobalt concentrations (Co_{aq} < 0.05 kmol m^{-3}), the

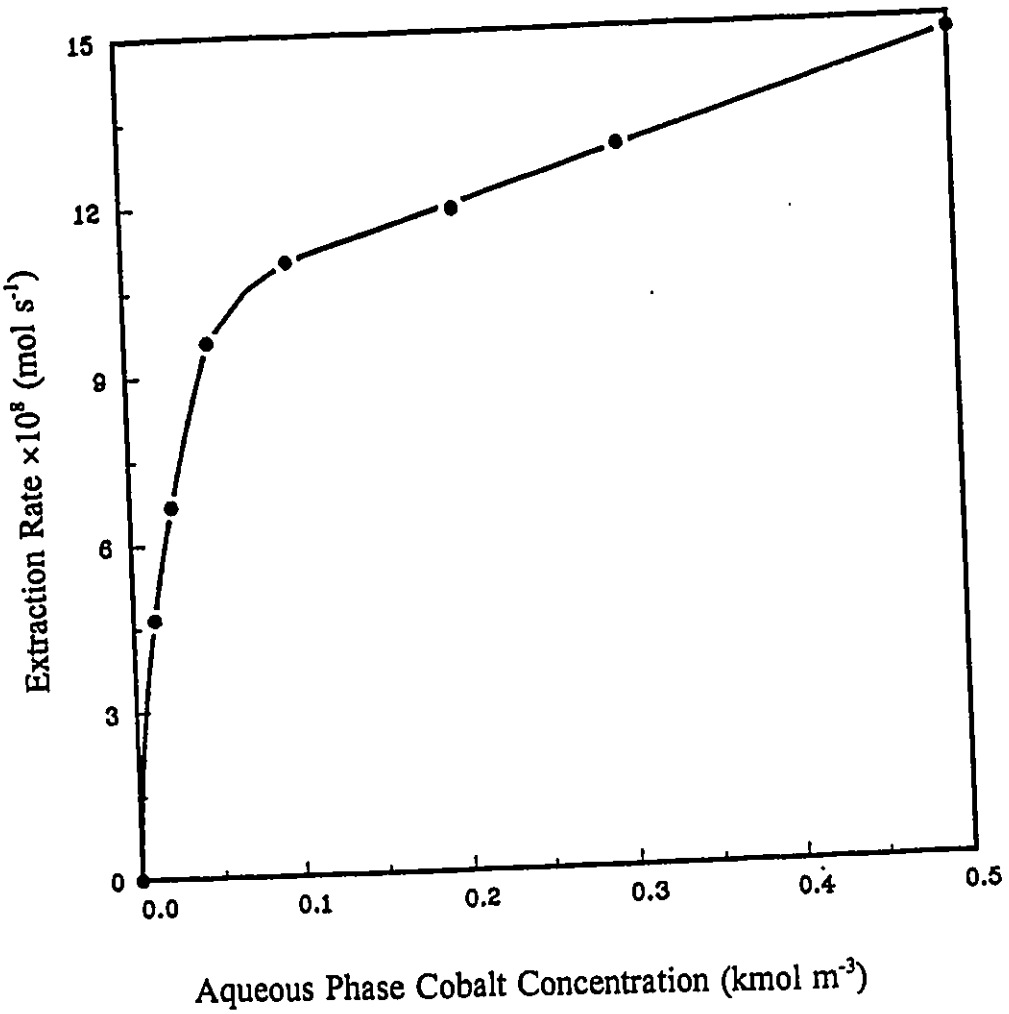

Figure 4-1: Effect of aqueous phase cobalt concentrations on extraction rates.
Experimental Conditions: T = 25 °C; A = 7.775×10^{-3} m^2; C_{Na2SO4} = 0.0 kmol m^{-3}; pH = 5.0; C_{H2A2} = 0.2695 kmol m^{-3}; C_{TBP} = 0.1832 kmol m^{-3}; Re_{aq} = 2102.5; and Re_{org} = 110.5.

increase in the extraction rate was directly proportional to the increase in the aqueous phase cobalt concentration. At higher cobalt concentrations, this relationship did not hold.

Unlike Figure 4-1, where the linearity existed only in the range of 0 to 0.05 kmol m^{-3} with respect to the aqueous phase cobalt concentration, when activities were used the extraction rate was directly proportional to the cobalt activity over a wider range, i.e., from 0 to 0.012 kmol m^{-3} Co_2SO_4 activity, see Figure 4-2. The extraction rate can be written in the following form for the aqueous phase cobalt concentrations less than 0.05 kmol m^{-3}:

$$J = K_{aq,Co}A(C-C^*) \qquad 4\text{-}1$$

where,

J = extraction rate, mol s^{-1};

$K_{aq,Co}$ = overall extraction rate coefficient in terms of the aqueous phase cobalt concentration, m s^{-1};

A = interfacial area, m^2;

C = aqueous phase cobalt concentration, kmol m^{-3}; and

C* = aqueous phase cobalt concentration in equilibrium with organic phase cobalt concentration, kmol m^{-3}.

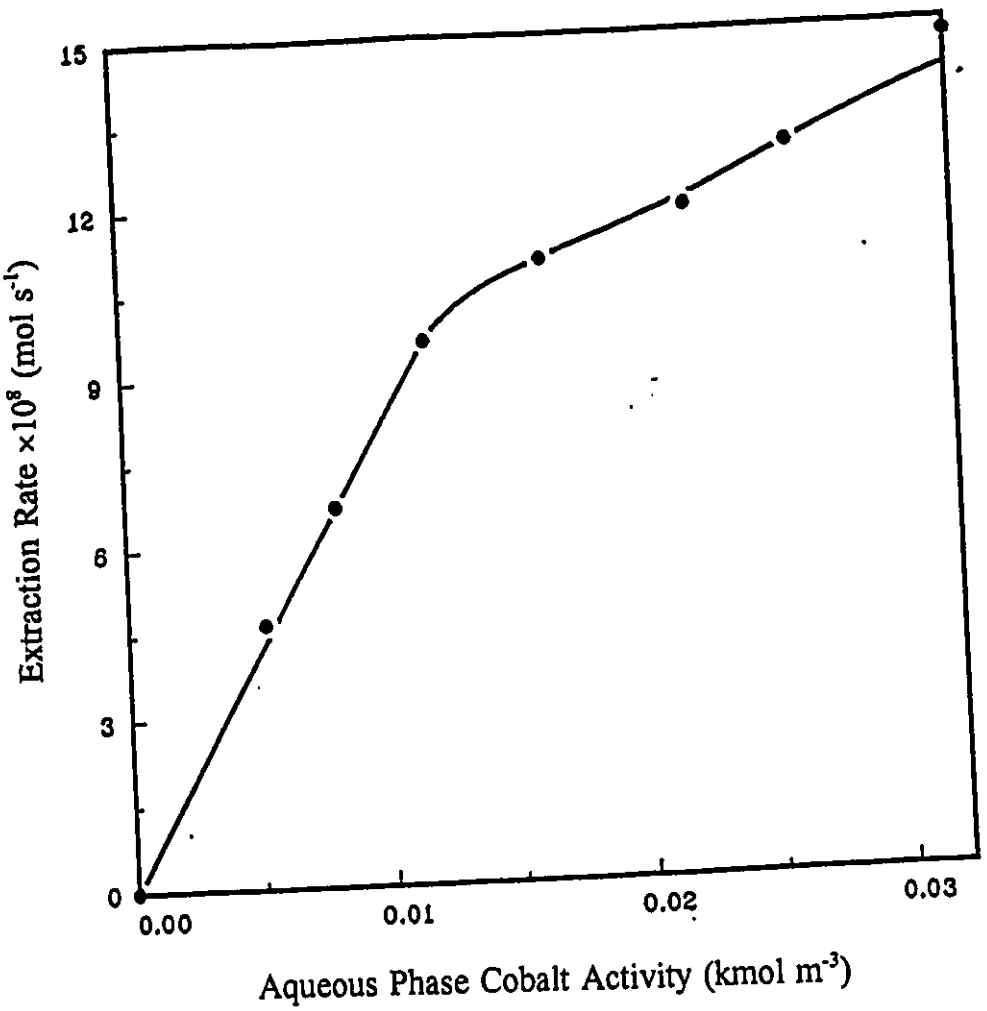

Figure 4-2: Effect of aqueous phase cobalt activities on extraction rates. Experimental Conditions: T = 25 ^{0}C; A = 7.775×10^{-3} m^2; C_{Na2SO4} = 0.0 kmol m^{-3}; pH = 5.0; C_{H2A2} = 0.2695 kmol m^{-3}; C_{TBP} = 0.1832 kmol m^{-3}; Re_{aq} = 2102.5; and Re_{org} = 110.5.

Using activity instead of concentration for the aqueous phase cobalt activities below 0.07 kmol m^{-3} , there is the following equation:

$$J=K_{aq,a}A(a-a^*) \qquad 4\text{-}2$$

here,

$K_{aq,a}$ = overall extraction coefficient in terms of aqueous phase cobalt activity;

a = aqueous phase cobalt activity, kmol m^{-3}; and

a* = aqueous phase cobalt activity in equilibrium with organic phase cobalt activity, kmol m^{-3}.

In this study, the systems were not at equilibrium and the experiments normally lasted less than 2 hours. Under these conditions, all of the final organic phase cobalt concentrations were less than 2.0×10^{-3} kmol m^{-3}. The distribution factor at a pH of 5 is greater than 1.0×10^{4} [Fu et al., 1990], so the equivalent cobalt activity values in the aqueous phase at these conditions are less than 2.0×10^{-7} kmol m^{-3}, i.e., $a^* \ll a$. Therefore, Equation 4-2 can be simplified to:

$$J=K_{aq,a}\times A\times a \qquad 4\text{-}3$$

At the low cobalt concentrations, it can be seen that Equation 4-3 represents the extraction driving force; however, at the high cobalt concentrations in the

aqueous phase both Equations 4-1 and 4-3 do not hold. Similar results were found by Yang et al. [Yang et al., 1993] when studying the cobalt-dithizone system. They considered this to be due to the complexity of the aqueous system at high concentrations or high ionic strengths. At the high aqueous phase concentration the interaction between the ions was believed to affect the extraction coefficient for the cobalt ion. These results were similar to those observed in the present study, as seen in Figures 4-1 and 4-2.

Using activities instead of concentrations as the driving forces the results can be explained over a wider range of the aqueous phase cobalt concentrations. However, because of the difficulty in estimating activities many researchers have preferred to study extractions at low aqueous phase concentrations.

It is difficult to measure the activity coefficients for ions in the aqueous phases solution. Researchers have used buffer solutions [Dreisinger and Cooper, 1986 and Chen, 1986], i.e., a large concentration of inert electrolytes, in the aqueous phase to maintain ionic strengths. But when inert electrolytes are added, because absolute activity coefficients become very low so that the real extraction mechanism for the systems could be disguised or changed.

This can be shown by considering the activity coefficients of the aqueous phase systems given in Dreisinger's [Dreisinger and Cooper, 1986] and Chen's [Chen, 1986] investigations as shown in Tables 4-1 and 4-2 below:

Table 4-1: Dreisinger's aqueous phase system [Dreisinger and Cooper, 1986].

0.5 kmol m^{-3} Na_2SO_4 buffer solution
$C_{Co} = 0.0016 - 0.1973$ kmol m^{-3}
$\gamma_{Co} = 0.0755 - 0.0595$
$a_{Co} = 1.21\times10^{-4} - 1.17\times10^{-2}$ kmol m^{-3}

Table 4-2: Chen's aqueous phase system [Chen, 1986].

Sodium acetate - acetic acid buffer solution
$C_{Co} = 0.002 - 0.060$ kmol m^{-3}
$\gamma_{Co} = 0.2724 - 0.1832$
$a_{Co} = 5.45\times10^{-4} - 1.10\times10^{-2}$ kmol m^{-3}

It can be seen that when the composition of the aqueous system was changed by adding the buffer solutions it results in smaller cobalt activities while in addition, the activity coefficients vary with the ionic strength.

4.2 The Effect of Ionic Strength on Extraction Rates

A large amount of non-extracted ions added to the aqueous phase can affect the mechanism of the extraction process. Shen et al.'s [Shen et al., 1984] study showed that with the increase in the aqueous phase Na_2SO_4 concentration, the cobalt extraction rate decreased.

In order to study the effect of the ionic strength on the extraction rate, different concentrations of sodium sulphate were used. Table 4-3 shows that both activity coefficients and activities vary with an increase in the Na_2SO_4 concentration for a $CoSO_4$ concentration of 0.1 kmol m^{-3}. As shown in Table 4-3, when the Na_2SO_4 concentration increased to 0.5 kmol m^{-3}, the cobalt activity coefficient is as low as 0.06815, which means that the ratio of the cobalt concentration to the activity would be 14.67. The extraction mechanism at such high ionic strengths could be quite different from the mechanism found at the lower ionic strengths.

Table 4-3: The variation of the cobalt activity and its coefficient at different Na_2SO_4 concentrations at $[CoSO_4]$ = 0.10 kmol m^{-3}.

Na_2SO_4	kmol m^{-3}	0.00	0.01	0.02	0.05	0.10	0.20	0.50
I	kmol m^{-3}	0.40	0.43	0.48	0.55	0.70	1.00	1.90
γ_{Co}	/	0.163	0.156	0.147	0.136	0.118	0.096	0.068
a_{Co}	mol m^{-3}	16.26	15.62	14.68	13.58	11.82	9.96	6.81

Figure 4-3 shows the effect of Na_2SO_4 concentration on the extraction rate. As the Na_2SO_4 concentration was increased the extraction rate decreased. Similarly, the extraction rate varied with the ionic strength, as shown in Figure 4-4 , the extraction rate decreasing as the ionic strength was increased.

4.3 Effect of Interfacial Area on Extraction Rates

Figure 4-5 shows the effect of the interfacial area on the extraction rate. It was observed that the extraction rate was directly proportional to the interfacial area. This result was in agreement with Golding et al. [Golding and Pushparajah, 1985 and Fu et al., 1990] in their investigations of cobalt extraction into HDEHP. According to their results, the controlling steps under the experimental conditions were close to, or at, the interface and not in the bulk phases. Therefore, the extraction rates were not dominated by the chemical reactions either in the aqueous phase or in the organic phase. The controlling mechanism is due to either the diffusion across the interface or a reaction at or close to the interface. The turbulence in the centre of the interface was greater than at the edges. As a result, the extraction rates did not show an exact linear relationship with an increase in the interfacial area at the highest values.

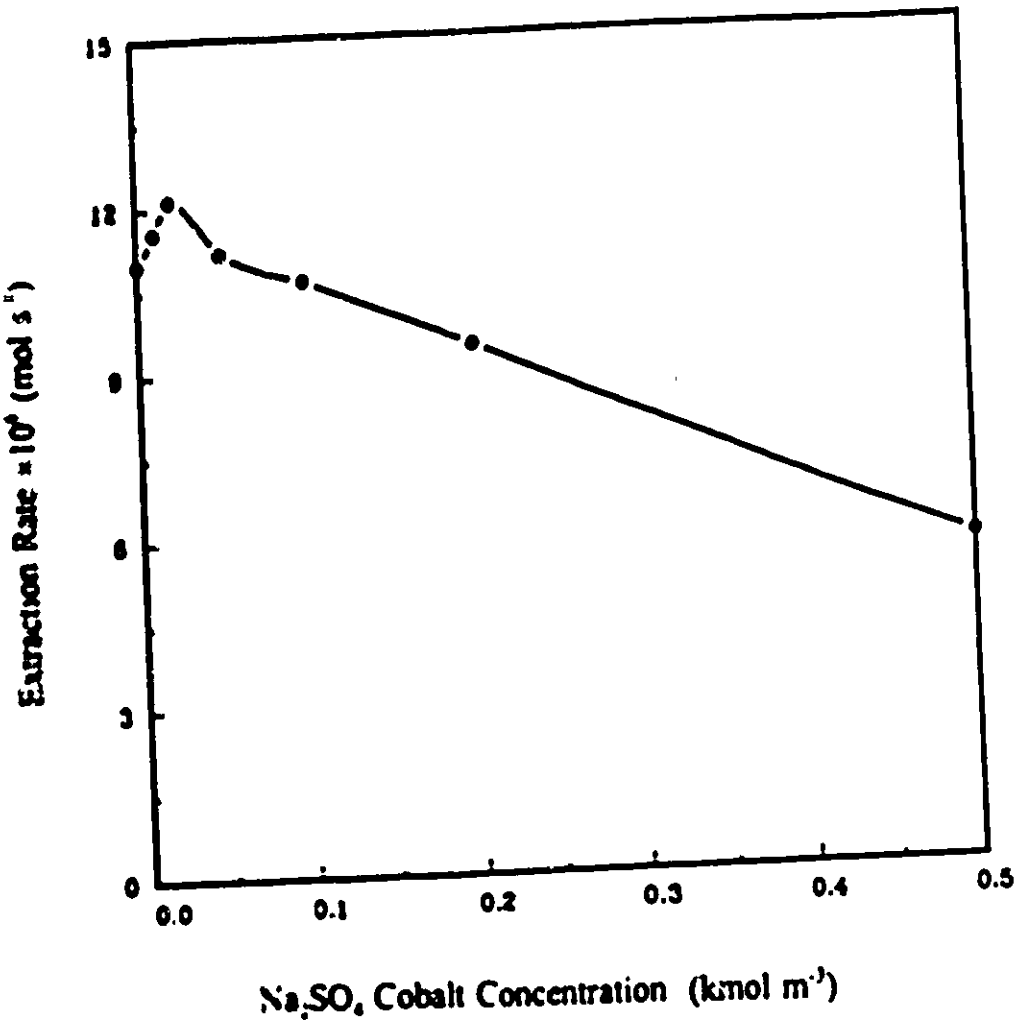

Figure 4-3: Effect of aqueous phase Na_2SO_4 concentrations on extraction rates.
Experimental Conditions: T = 25 °C; A = 7.775×10^{-3} m^2; $C_{Co(II)}$ = 0.10 kmol m^{-3}; pH = 5.0; $C_{H(A)}$ = 0.2695 kmol m^{-3}; C_{TBP} = 0.1832 kmol m^{-3}; Re_{aq} = 2102.5; and Re_{org} = 110.5.

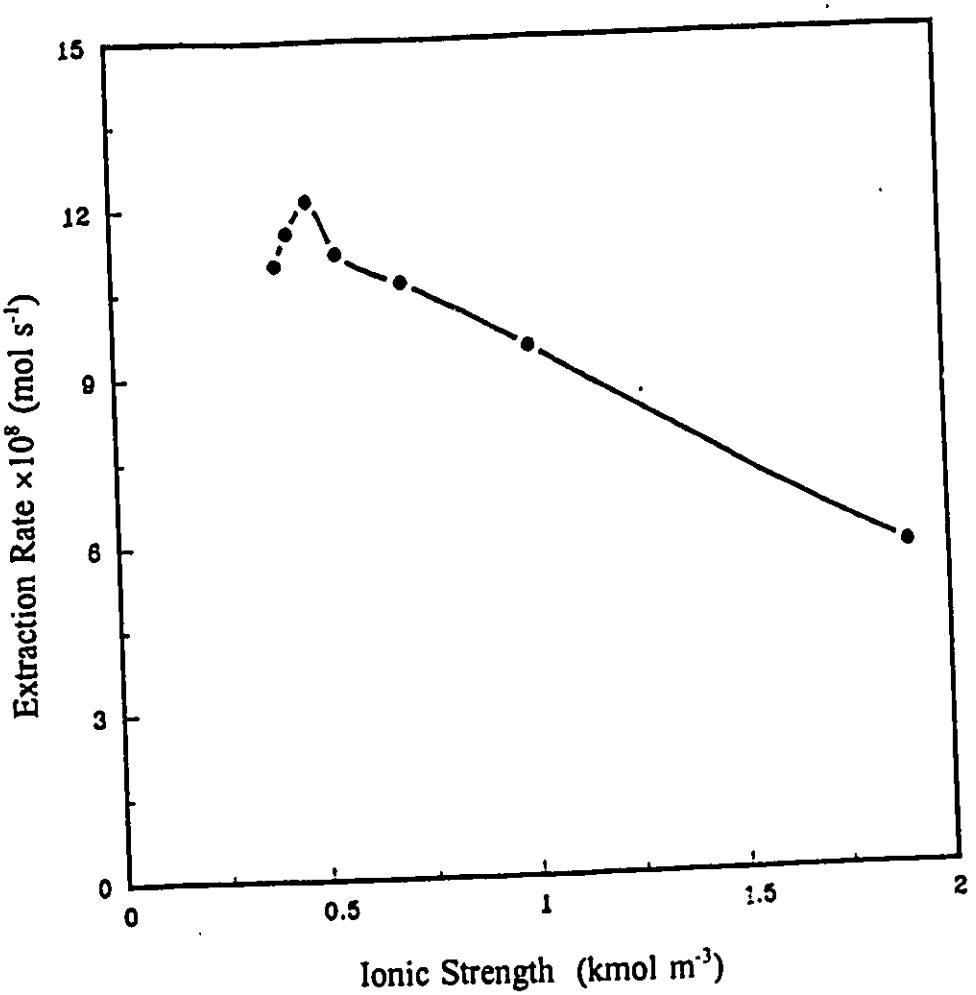

Figure 4-4: Effect of aqueous phase ionic strength on extraction rates.
Experimental Conditions: T = 25 °C; A = 7.775×10^{-3} m^2;
C_{CoSO_4} = 0.10 kmol m^{-3}; $C_{H_2A_2}$ = 0.2695 kmol m^{-3};
C_{TBP} = 0.1832 kmol m^{-3}; pH = 5.0; Re_{aq} = 2102.5; and Re_{org} = 110.5.

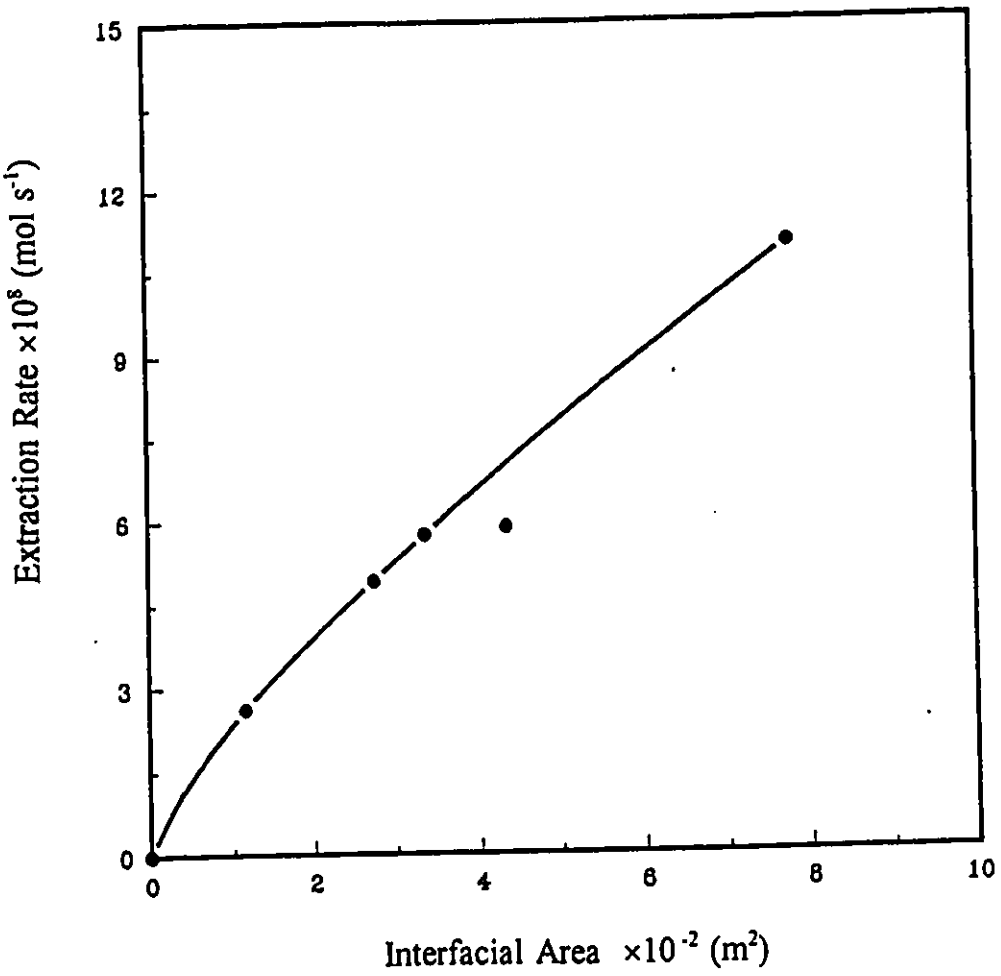

Figure 4-5: Effect of interfacial area on extraction rates.
Experimental Conditions: T = 25 ^{0}C; C_{CoSO_4} = 0.10 kmol m^{-3}; $C_{Na_2SO_4}$ = 0.0 kmol m^{-3}; pH = 5.0; $C_{H_2A_2}$ = 0.2695 kmol m^{-3}; C_{TBP} = 0.1832 kmol m^{-3}; Re_{aq} = 2102.5; and Re_{org} = 110.5.

4.4 Effect of the Extractant Concentration on Extraction Rates

The results showed that the extraction rate had an approximate linear relationship with the extractant concentration; see Figure 4-6. The extraction rate did not increase exactly proportionally with an increase in the extractant concentration due to the increase in viscosity of the organic phase, see Table 3-5. This would lower the extraction rate as the runs were carried out at constant stirrer speed and not at a constant organic phase Reynolds number. Under these conditions the organic phase resistance could increase. It should be noted that the extractant exists in the dimer form in the organic phase [Komasawa, 1983]. It can be seen from these results that the extractant also plays a role in the kinetics of cobalt extraction from the aqueous phase to the organic phase.

4.5 Effect of Modifier Concentration on Extraction Rates

Figure 4-7 shows the effect of the concentration of the modifier, TBP, on the extraction rate. For TBP concentrations in the range of 0 to 0.36 kmol m^{-3} (0% to 10% v/v), almost no change was observed in the extraction rate with an increase in the TBP concentration. Therefore, the TBP modifier in this system did not influence the extraction rate even at the highest TBP concentration of 10% v/v.

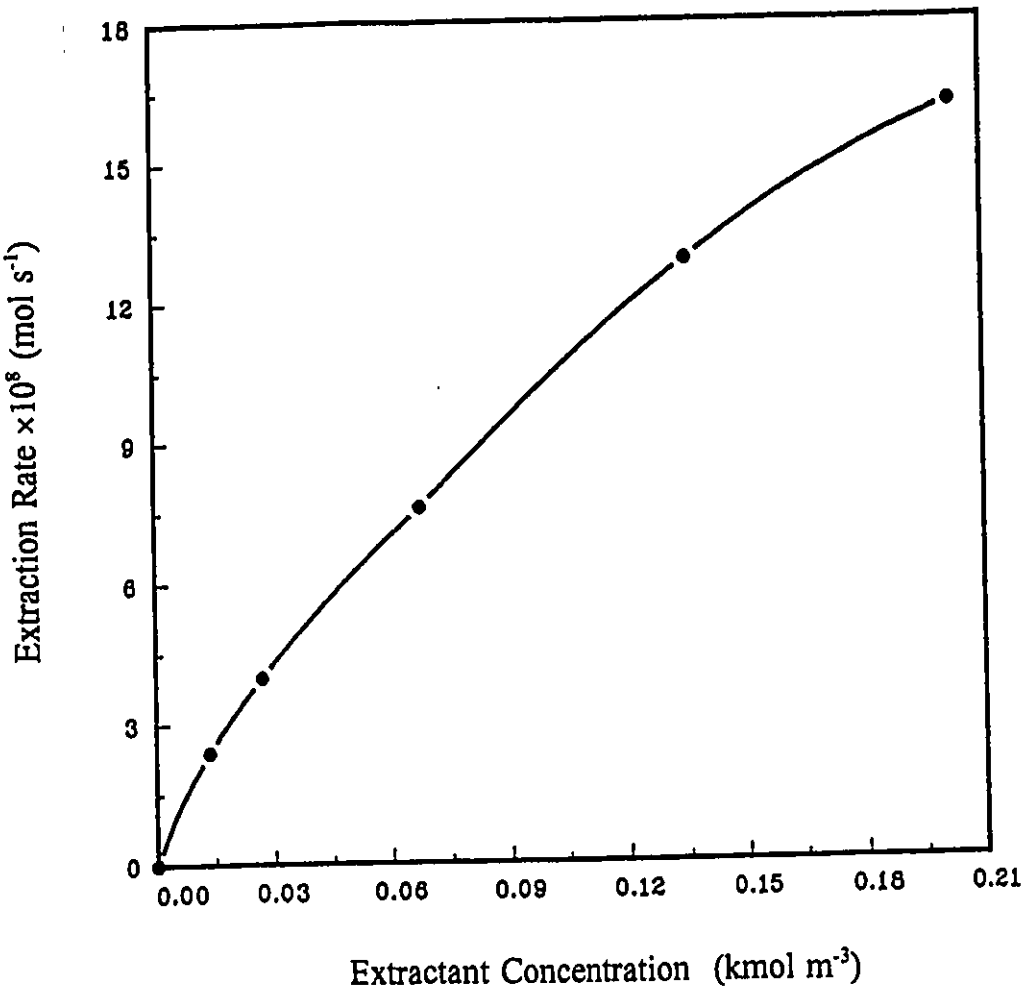

Figure 4-6: Effect of extractant concentrations on extraction rates. Experimental Conditions: T = 25 ^{0}C; A =7.775×10^{-3} m^{2}; C_{CoSO_4} = 0.10 kmol m^{-3}; $C_{Na_2SO_4}$ = 0.0 kmol m^{-3}; pH = 5.0; C_{TBP} = 0.1832 kmol m^{-3}; Re_{aq} = 2102.5; and n_{org}= 2.7 s^{-1}.

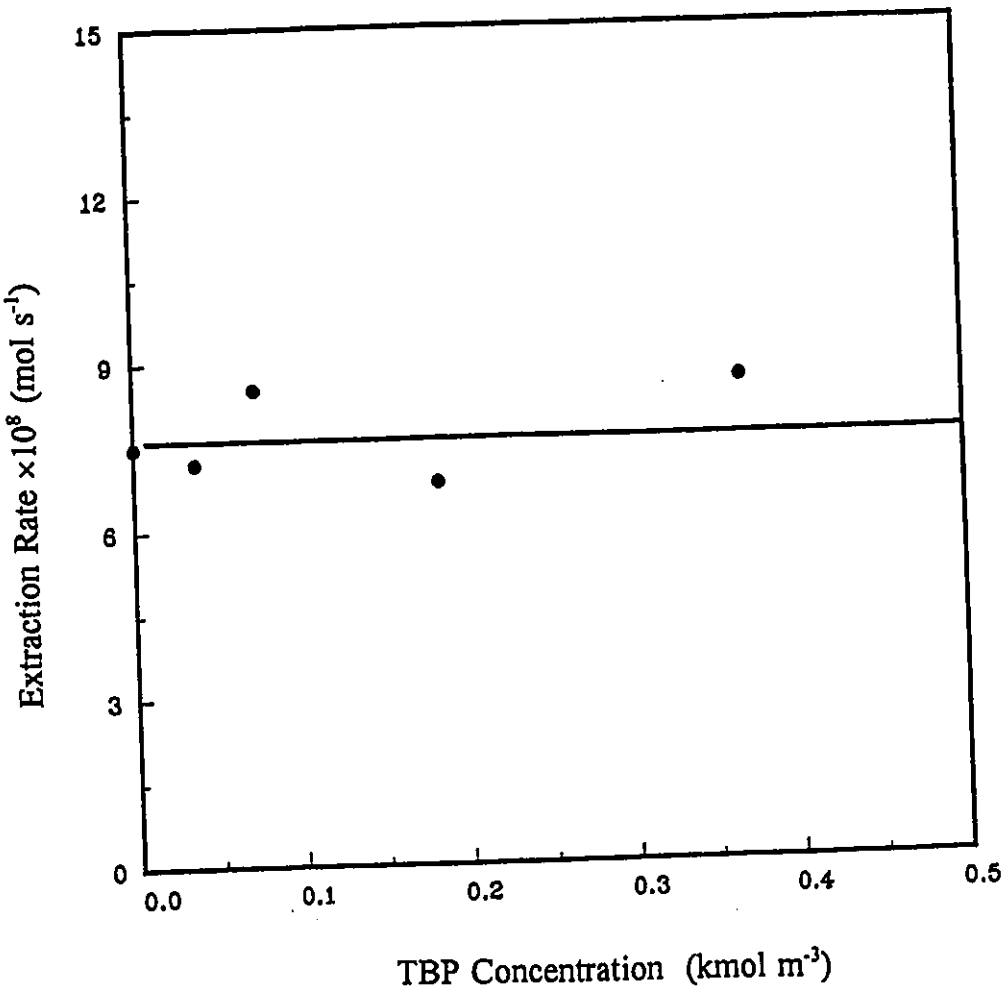

Figure 4-7: Effect of TBP concentrations on extraction rates.
Experimental Conditions: T = 25 ^{0}C; A = 7.775×10^{-3} m^2;
C_{CoSO_4} = 0.10 kmol m^{-3}; C_{Na2SO_4} = 0.0 kmol m^{-3}; pH = 5.0;
C_{H2A2} = 0.2695 kmol m^{-3}; Re_{aq} = 2102.5; and Re_{org} = 110.5.

4.6 Effect of pH on Extraction Rates

The pH was found to play a very important role in the kinetics of cobalt extraction, see Figure 4-8. At pH values lower than 3.1, the direction of the cobalt extraction took place from the organic phase to the aqueous phase, even though the cobalt concentration in the organic phase was very low ($C_{Coorg} < 2.5\times10^{-3}$ kmol m^{-3}). In this pH range the extraction process was reversed, that is, a stripping process was taking place which is recovery of the metal ions from the organic phase into the aqueous phase. The mass transfer rate did not seem to vary with pH over the range of 1.8 to 3. The extraction rate under these conditions was so low that the extraction was likely controlled by a chemical reaction extraction, but further work needs to be carried out in this area.

The extraction rate increased as the pH was raised from 3.0 to 5.5. This indicated that for pH values lower than 5.5, the extraction rate was controlled by a chemical reaction in which hydrogen ions took part. At pH values greater than 5.5, the effect of the pH on the extraction rates gradually disappeared. At this pH range, the diffusion resistances in the aqueous and organic phases would appear to dominate the extraction rate.

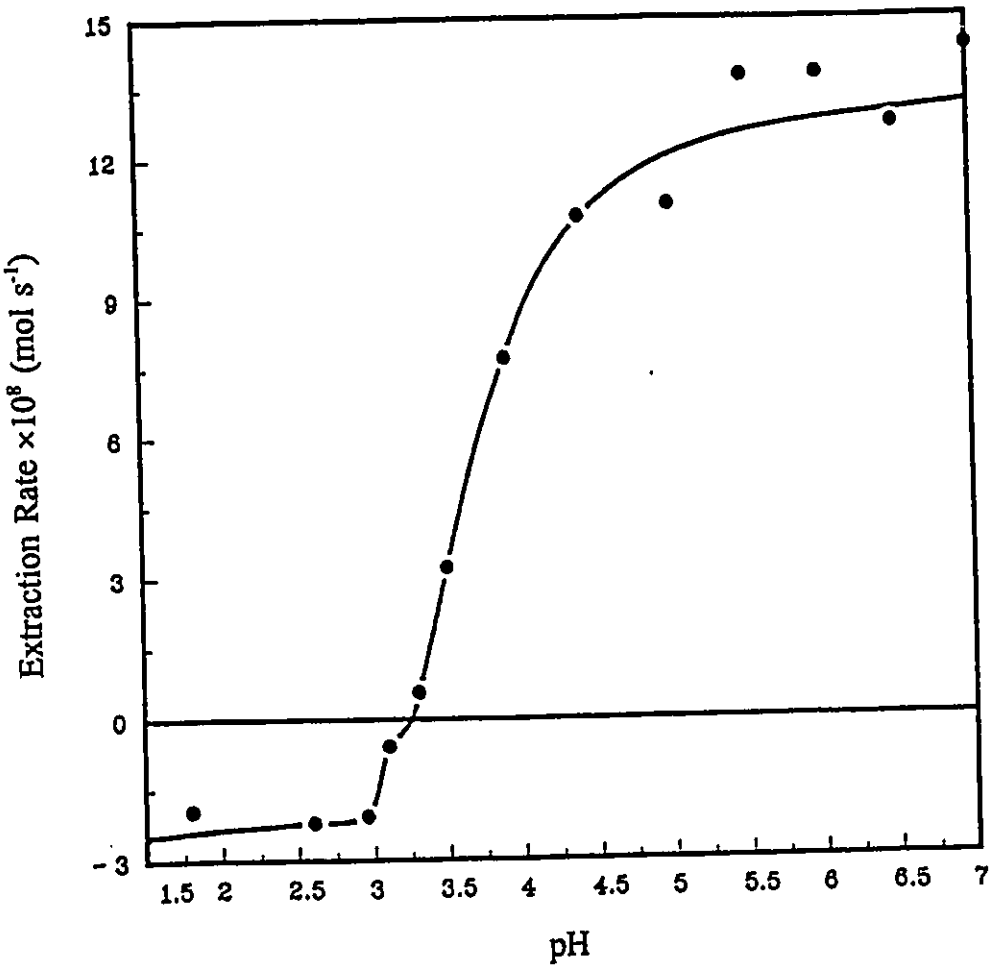

Figure 4-8: Effect of pH on extraction rates.
Experimental Conditions: T = 25 ^{0}C; A = 7.775×10^{-3} m^2;
C_{CoSO_4} = 0.10 kmol m^{-3}; $C_{Na_2SO_4}$ = 0.0 kmol m^{-3}; pH = 5.0;
$C_{H_2A_2}$ = 0.2695 kmol m^{-3}; C_{TBP} = 0.1832 kmol m^{-3};
Re_{aq} = 2102.5; and Re_{org} = 110.5.

4.7 Extraction Resistances

As noted previously the overall extraction rate coefficient can be obtained from Equation 4-1 for any given extraction concentration, i.e.,

$$J = \frac{A(a-a^*)}{K_{aq,a}^{-1}} = \frac{A(a-a^*)}{R} \qquad 4\text{-}4$$

where,

$$R = K_{aq,a}^{-1} \qquad 4\text{-}5$$

and R is defined as the overall extraction resistance.

At the steady state conditions, mass transfer coefficients can be defined as follows:

$$J = k_{aq,a}A(a_{aq} - a_{aq,i}) = k_{org,a}A(a_{org,i} - a_{org}) \qquad 4\text{-}6$$

where $k_{aq,a}$ and $k_{org,a}$ are the mass transfer coefficients in the aqueous and the organic phases, respectively, defined in terms of activity. Also, mass transfer

resistances can be defined as follows:

$$R_{aq}=k_{aq}^{-1}$$

and

$$R_{org}=k_{org}^{-1}$$

where R_{aq} and R_{org} are mass transfer resistances in the aqueous and the organic phases, respectively.

Considering the chemical reaction at the interface R_r is defined as the interfacial resistance, such that:

$$R=R_{aq}+R_r+R_{org} \qquad 4\text{-}7$$

According to this definition, R_r is dependent only on the chemical reaction at the interface, while R_{aq} and R_{org} are dependent on the hydrodynamic conditions in the aqueous and organic phases, respectively.

Assuming R_r, R_{aq}, and R_{org} are independent of each other it is possible to determine the kinetic mechanism for cobalt extraction into HDTMPP by considering the effects of the process variables on the overall extraction rate.

Figure 4-9 shows the variation of the overall extraction rate resistance with pH. It is seen that at low pH values, the overall extraction resistance was initially very high. For pH values in the range of 3.3 to 5.5 the overall extraction resistance decreased with increase in pH. Meanwhile at pH values greater than 5.5, the resistance did not change with pH and assumed a constant value of 0.134×10^{7} s m^{-1}.

From Equation 4-7, it was possible to define a diffusion resistance, R_d, as follows:

$$R_d = R_{aq} + R_{org} \qquad 4\text{-}8$$

such that,

$$R = R_d + R_r \qquad 4\text{-}9$$

R_d is a function of the hydrodynamic conditions of the system and is independent of the pH. R_r is a function of the reaction close to, or at, the interface, as well as the pH. Also, R_r and R_d are considered to be independent of each other.

So that, for the condition of pH > 5.5 , $n_{aq} = 2.5\ s^{-1}$ and $n_{org} = 2.7\ s^{-1}$, R_d is 0.134×10^{7} s m^{-1}. R_r can be neglected as the diffusion resistance controlled the

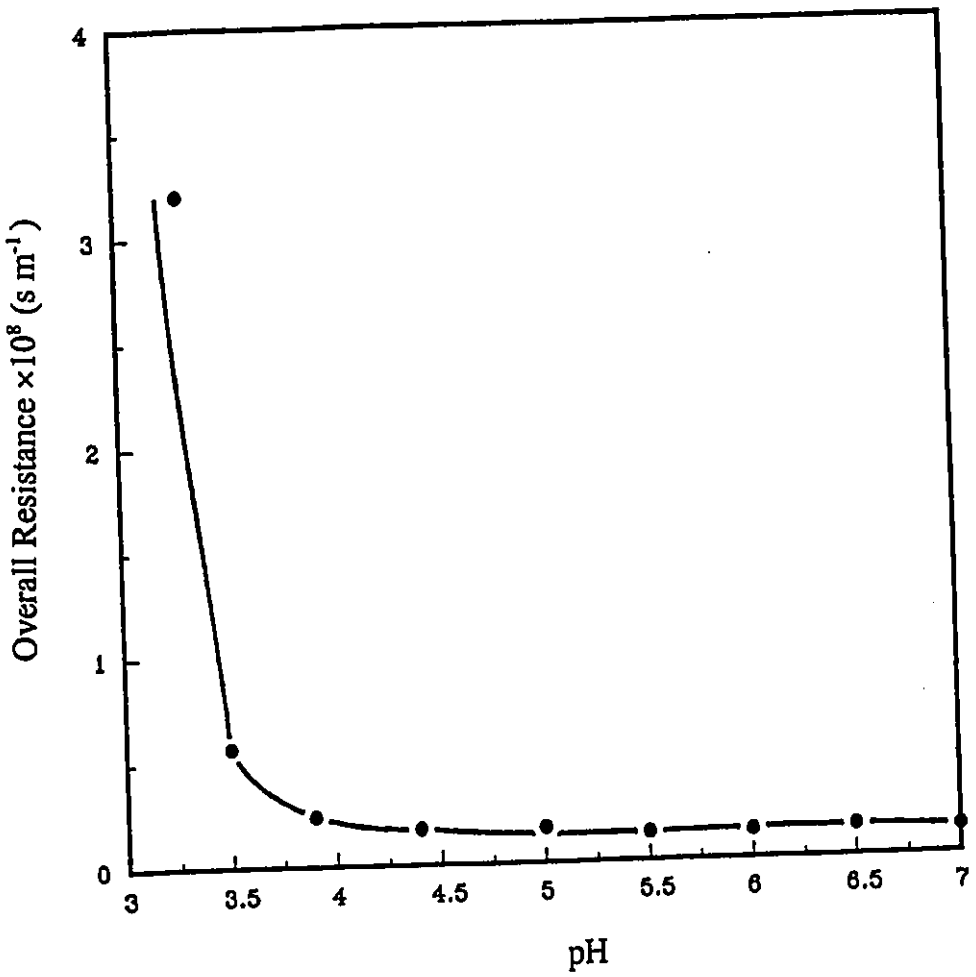

Figure 4-9: Effect of pH on the overall extraction resistance.
Experimental Conditions: T = 25 ^{0}C; A = 7.775×10^{-3} m^2;
C_{CoSO4} = 0.10 kmol m^{-3}; C_{Na2SO4} = 0.0 kmol m^{-3};
C_{H2A2} = 0.2695 kmol m^{-3}; C_{TBP} = 0.1832 kmol m^{-3}; Re_{aq} = 2102.5; and
Re_{org} = 110.5.

extraction process.

Using Equation 4-9:

$$R_r = R - R_d \qquad 4\text{-}10$$

and

$$k_r = R_r^{-1} \qquad 4\text{-}11$$

The interfacial resistance and the reaction coefficient rate can be obtained for the different pH values using Equations 4-10 and 4-11, respectively.

Figure 4-10 shows the relationship between log k_r and pH. It can be seen that there was a linear dependence on pH, with the slope being 1.027. This implies that the extraction rate, in the pH range of 3.3 to 5.5, was controlled by the chemical reaction and the order of the reaction was one, with respect to the hydrogen ion concentration.

In order to study the diffusion resistance in the two phases, experimental runs were carried out at varying stirrer speeds in both the aqueous and organic phases, respectively, at a pH value of 5.0.

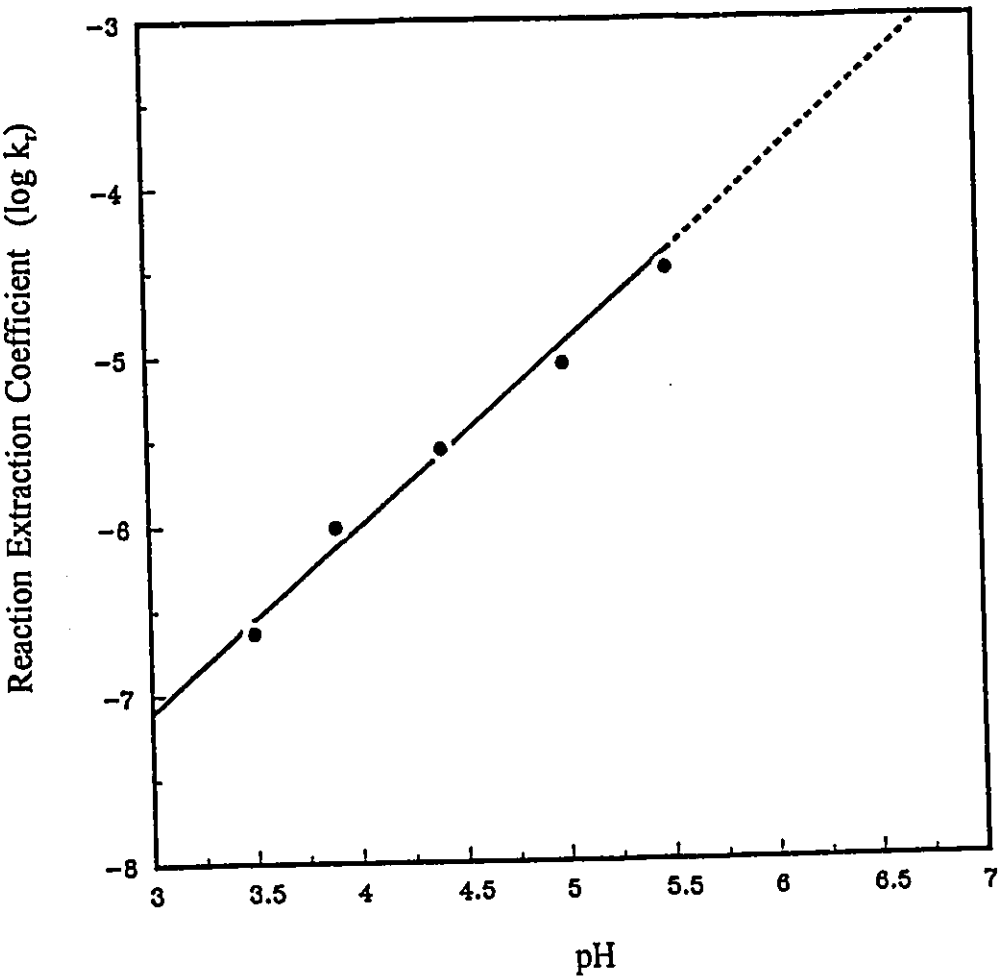

Figure 4-10: Effect of pH on the interfacial extraction coefficient.
Experimental Conditions: T = 25 ^{0}C; A = 7.775×10^{-3} m^2;
C_{CoSO_4} = 0.10 kmol m^{-3}; $C_{Na_2SO_4}$ = 0.0 kmol m^{-3};
$C_{H_2A_2}$ = 0.2695 kmol m^{-3}; C_{TBP} = 0.1832 kmol m^{-3}; Re_{aq} = 2102.5; and
Re_{org} = 110.5.

Figures 4-11 and 4-12 show the effects of the stirrer speeds on the extraction rates. When the stirrer speeds in the aqueous and organic phases were increased, the extraction rates also increased. Ideally if the stirrer speeds in both phases are high enough the diffusion resistances in both phases can be neglected; that is, only chemical reaction resistance would control the process. In practice this was not possible as rippling of the interface took place when the stirrer speeds in both phases were greater than 5 s^{-1}. However an estimate of diffusion resistance can be made using the following relationship when at pH = 5.0, $R_r = 0.0125 \times 10^7$ s m^{-1}, see Figure 4-9.

Using the equation:

$$R_d = R - R_r \qquad 4\text{-}12$$

the values of the diffusion resistance under the different hydrodynamic conditions were obtained by varying the stirrer speeds in the aqueous and organic phases. The extraction resistance has been found to vary with the square root of the Reynolds number for both of the phases, under the low stirrer speeds, by several investigators [Lewis, 1954 and Yan, 1989]. The effect of the Reynolds number on the extraction rates, for the aqueous and organic phases, are shown in equation 4-13 and 4-14,

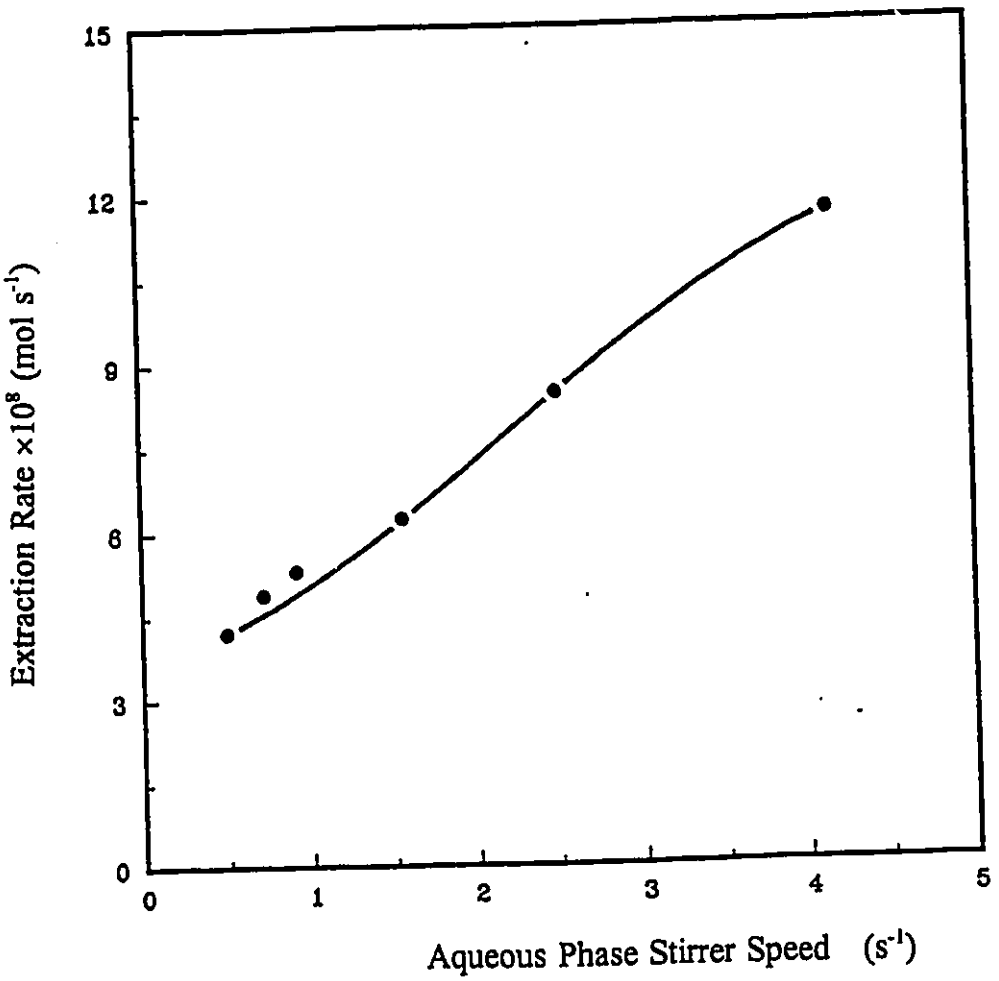

Figure 4-11: Effect of aqueous phase stirrer speed on extraction rates. Experimental Conditions: T = 25 °C; A = 7.775×10^{-3} m^2; C_{CoSO_4} = 0.050 kmol m^{-3}; C_{Na2SO4} = 0.0 kmol m^{-3}; pH = 5.0;); C_{H2A2} = 0.2695 kmol m^{-3}; C_{TBP} = 0.1832 kmol m^{-3} ; and Re_{org} = 110.5.

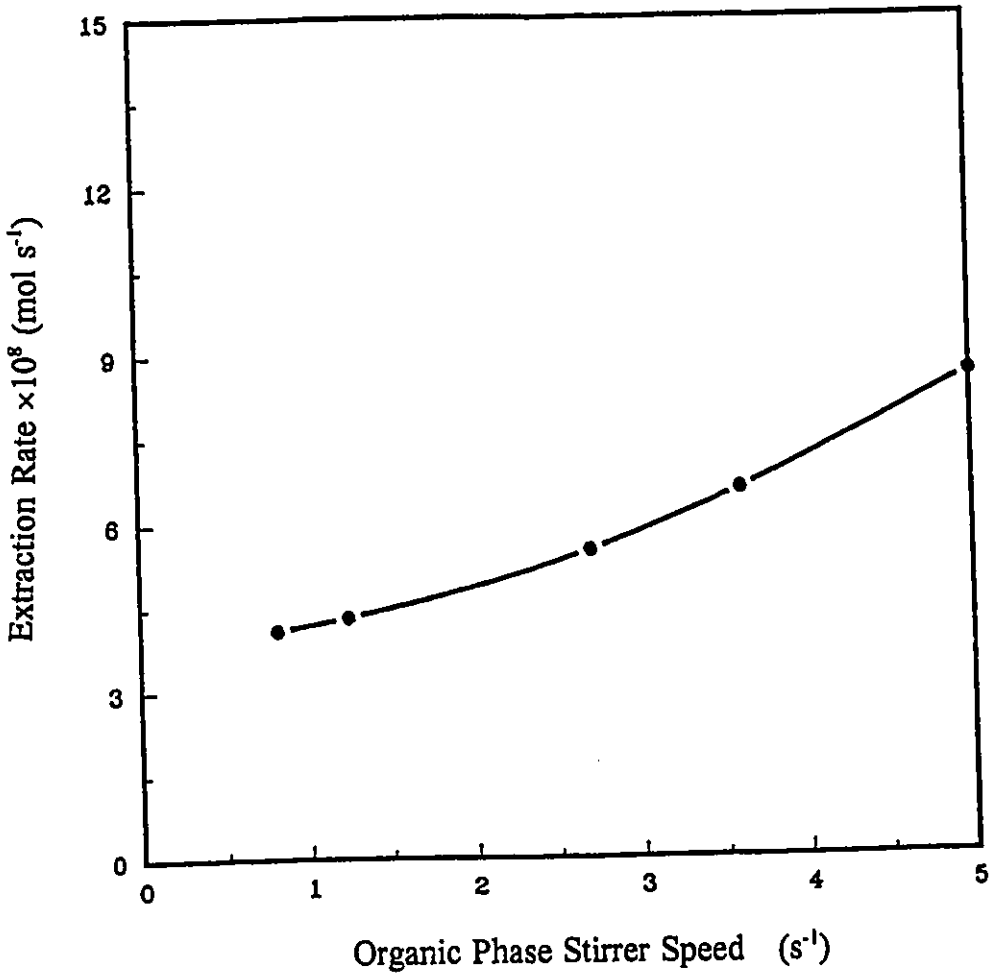

Figure 4-12: Effect of organic phase stirrer speed on extraction rates. Experimental Conditions: T = 25 ^{0}C; A = 7.775×10^{-3} m^2; C_{CoSO_4} = 0.050 kmol m^{-3}; $C_{Na_2SO_4}$ = 0.0 kmol m^{-3}; pH = 5.0; $C_{H_2A_2}$ = 0.2695 kmol m^{-3}; C_{TBP} = 0.1832 kmol m^{-3}; and Re_{aq} = 2102.5.

respectively. There are:

$$R_{aq}=\alpha_1 Re_{aq}^{-1/2} \qquad 4\text{-}13$$

and

$$R_{org}=\alpha_2 Re_{org}^{-1/2} \qquad 4\text{-}14$$

where α_1 and α_2 are constants which are independent of the hydrodynamic conditions in the individual phase, see Figure 4-13 and Figure 4-14; that is:

$$R_d=\alpha_1 Re_{aq}^{-1/2}+\alpha_2 Re_{org}^{-1/2} \qquad 4\text{-}15$$

The magnitudes of the organic and aqueous phase resistances for a particular Reynolds number were estimated from the plots of extraction resistance vs $Re^{-1/2}$. When the organic phase stirrer speed was fixed, then by varying the aqueous phase stirrer speeds, it was observed that the diffusion resistance was proportional to $Re_{aq}^{-1/2}$, as seen in Figure 4-15. Extrapolating the line in Figure 4-15 to the zero point of the horizontal axis, when, the aqueous phase Reynolds number was infinite, that is no diffusion resistance in the aqueous phase. An estimate of the organic phase diffusion resistance can be made. Under the conditions of $n_{org} = 2.7$ s^{-1} ($Re_{org} = 110.5$), the organic phase diffusion resistance, R_{org}, was 0.596×10^{6} s m^{-1} and the mass transfer coefficient in the organic phase, k_{org}, was 1.68×10^{-6} m s^{-1}.

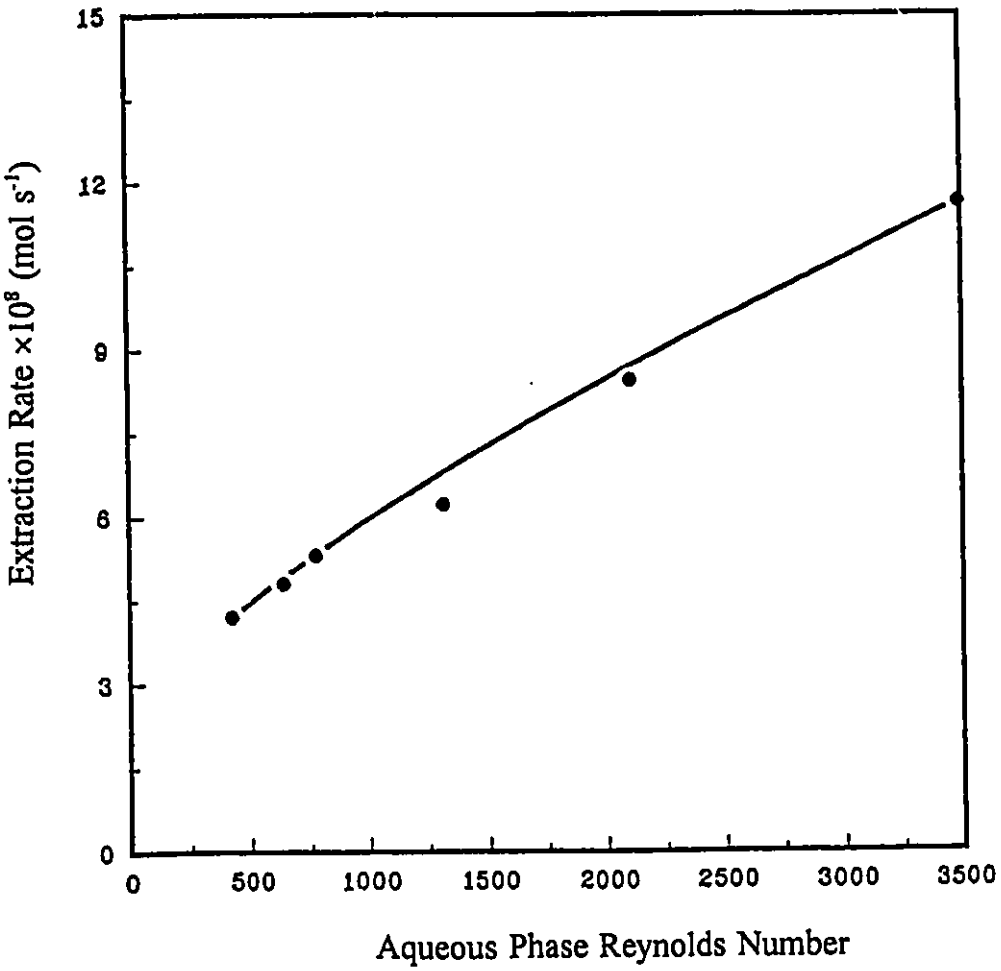

Figure 4-13: Effect of aqueous phase Reynolds number on extraction rates. Experimental Conditions: T = 25 ^{0}C; A = 7.775×10^{-3} m^{2}; C_{CoSO_4} = 0.050 kmol m^{-3}; $C_{Na_2SO_4}$ = 0.0 kmol m^{-3}; pH = 5.0; $C_{H_2A_2}$ = 0.2695 kmol m^{-3}; C_{TBP} = 0.1832 kmol m^{-3} ; and Re_{org} = 110.5.

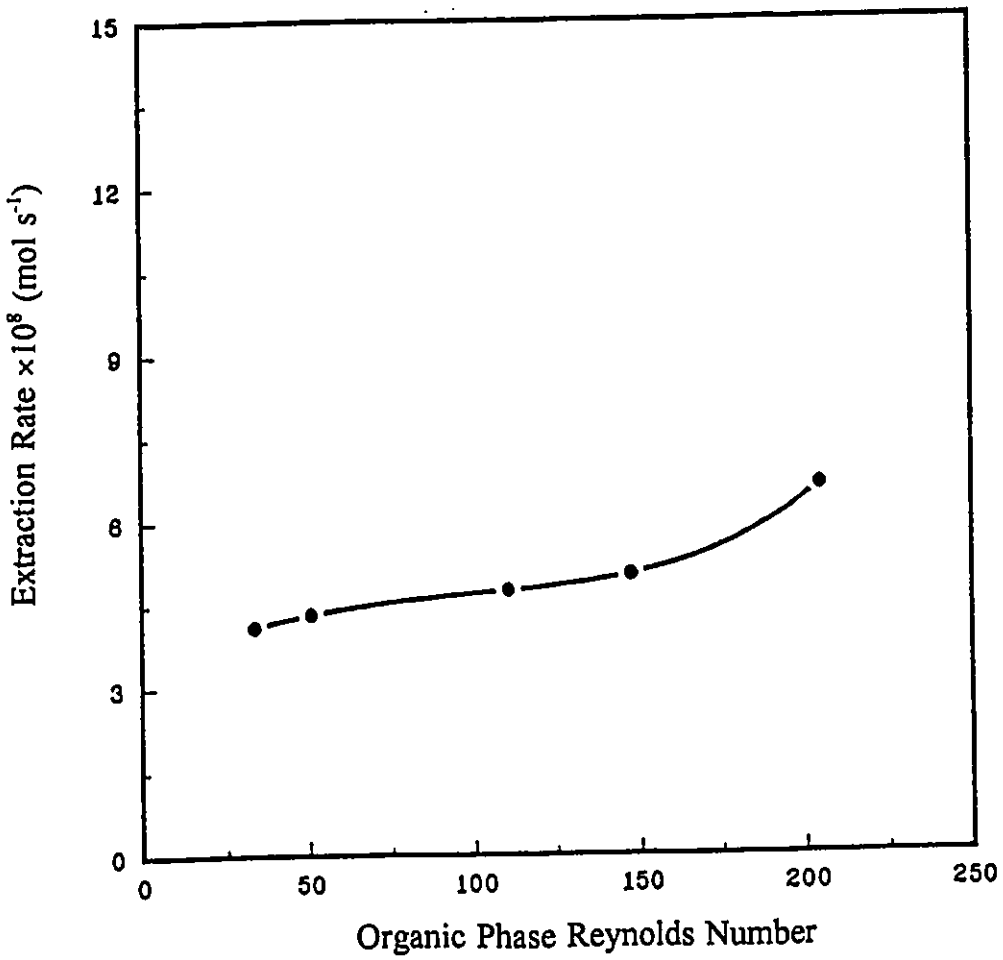

Figure 4-14: Effect of organic phase Reynolds number on extraction rates. Experimental Conditions: T = 25 ^{0}C; A = 7.775×10^{-3} m^2; C_{CoSO_4} = 0.050 kmol m^{-3}; $C_{Na_2SO_4}$ = 0.0 kmol m^{-3}; $C_{H_2A_2}$ = 0.2695 kmol m^{-3}; C_{TBP} = 0.1832 kmol m^{-3}; pH = 5.0; and Re_{aq} = 2102.5.

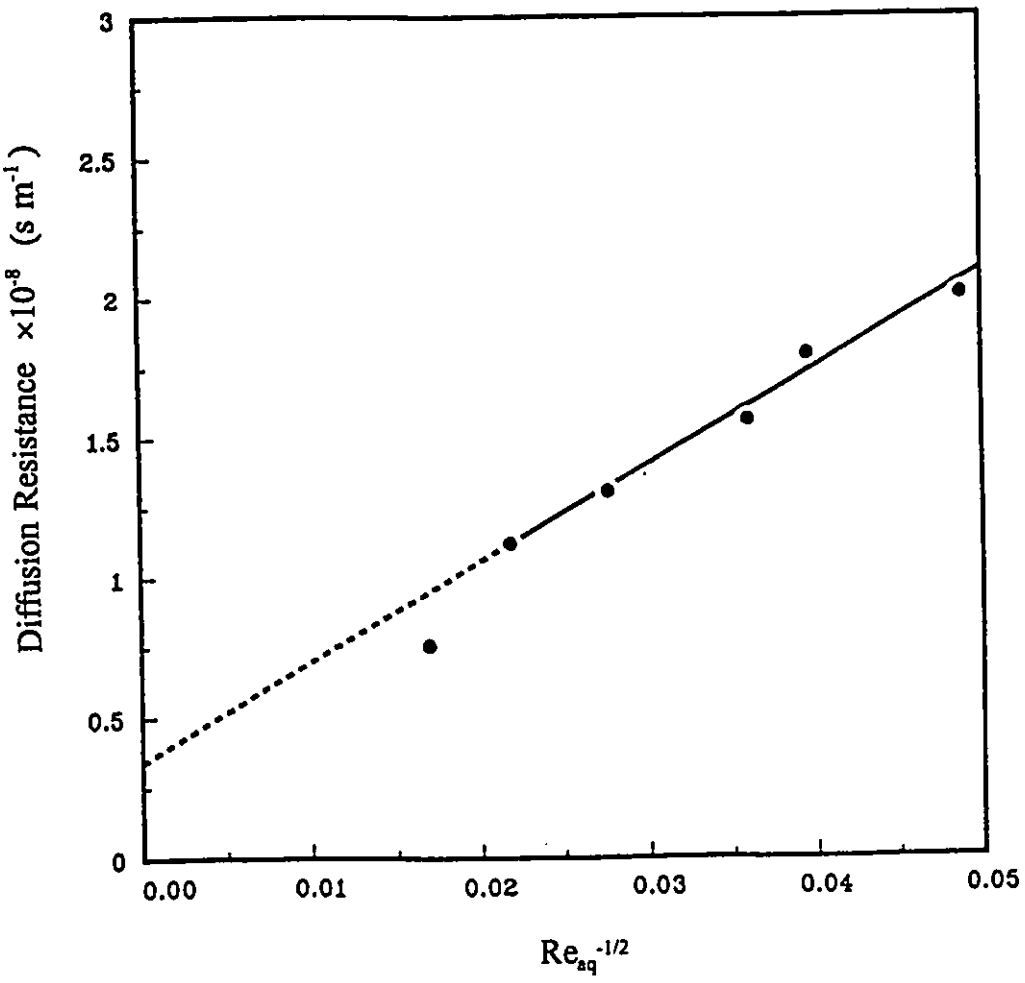

Figure 4-15: Relationship between aqueous phase Reynolds number and diffusion resistance.
Experimental Conditions: T = 25 ^{0}C; A = 7.775×10^{-3} m^2; C_{CoSO_4} = 0.050 kmol m^{-3}; C_{Na2SO4} = 0.0 kmol m^{-3}; pH = 5.0; C_{H2A2} = 0.2695 kmol m^{-3}; C_{TBP} = 0.1832 kmol m^{-3} ; and Re_{org} = 110.5.

A Similar procedure was carried out to estimate the aqueous phase resistance, see Figure 4-16. At the conditions of n_{aq} = 2.5 s^{-1} (Re_{aq} = 2102.5), R_{aq} was $0.847\times10^{+6}$ s m^{-1}. The mass transfer coefficient in the aqueous phase, k_{aq}, was 1.181×10^{-6} m s^{-1}.

The aqueous phase boundary layer thickness can also be estimated. At steady state, the equations for the mass transfer of cobalt and hydrogen ions are [Komasawa, 1980]:

$$N_{Co}=k_{Co}(a-a_i) \qquad 4\text{-}16$$

$$N_H=-k_H(a_H-a_{H_i}) \qquad 4\text{-}17$$

where N_{Co} and N_H are the mass transfer rates per unit area for the cobalt and hydrogen ions, respectively; then, $2N_{Co} = N_H$. k_H is the diffusion mass transfer coefficient for hydrogen ion.

According to the two-film theory, the mass transfer coefficient is given by:

$$k_d=D_j/\delta_{aq} \qquad 4\text{-}18$$

where D_j is the diffusion coefficient for the j ion and δ_{aq} is the thickness of boundary layer at the interface in the aqueous phase, Also D_{Co} = 0.85×10^{-9} m^2 s^{-1}

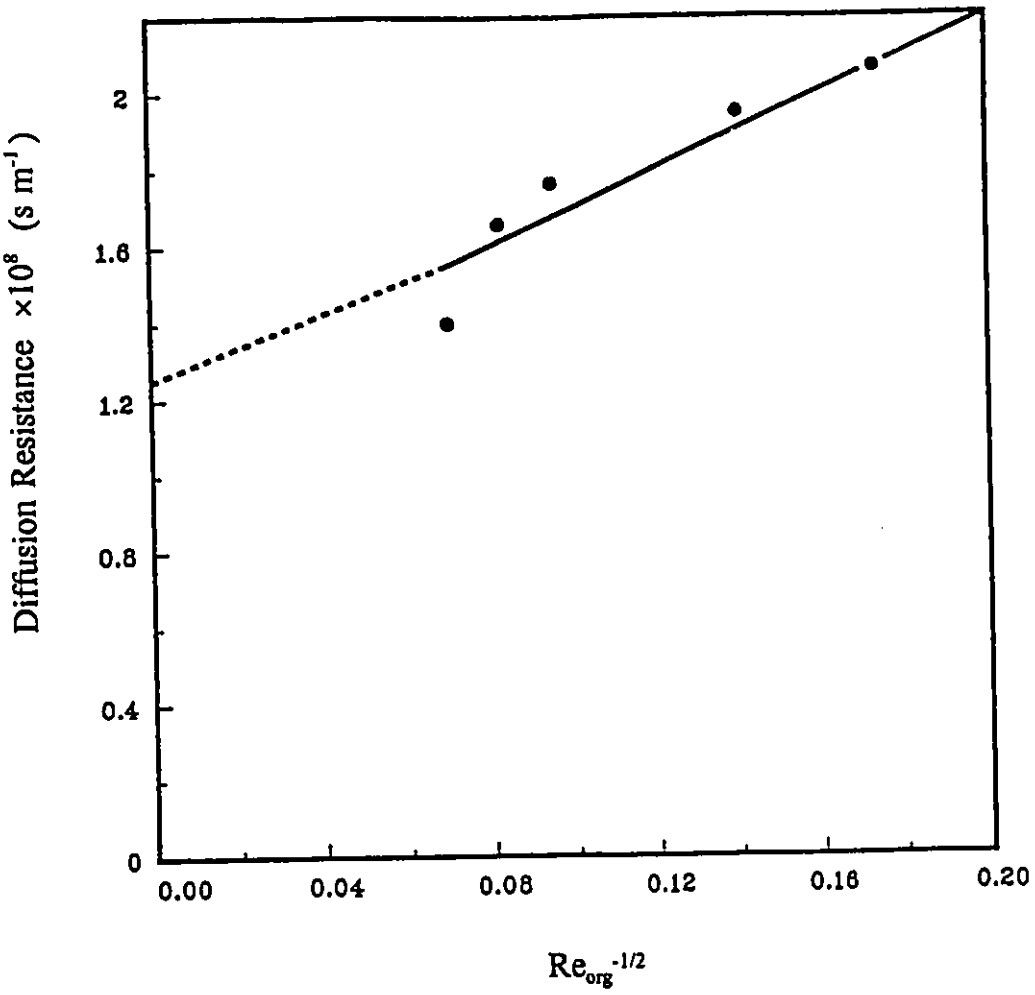

Figure 4-16: Relationship between organic phase Reynolds number and diffusion resistance.
Experimental Conditions: T = 25 ^{0}C; A = 7.775×10^{-3} m^2;
C_{CoSO_4} = 0.050 kmol m^{-3}; $C_{Na_2SO_4}$ = 0.0 kmol m^{-3};
$C_{H_2A_2}$ = 0.2695 kmol m^{-3}; pH = 5.0; C_{TBP} = 0.1832 kmol m^{-3} ; and
Re_{aq} = 2102.5.

and $D_H = 5.89\times10^{-8}$ $m^2 s^{-1}$ [Komasawa, 1980].

Then substituting in Equation 4-18,

$$\delta_{aq}=D_{Co}/k_{Co}=1.306\times10^{-3}m$$

at $Re_{aq} = 77.37$ or $n_{aq} = 0.92$ s^{-1}.

Considering the hydrogen ion transfer across the boundary layer it is possible to estimate the values of the hydrogen ion mass transfer coefficient:

$$k_H=D_H/\delta_{aq}=4.51\times10^{-5}m\ s^{-1}$$

that is, k_H has a much high value than found for cobalt ion transfer.

Rewriting Equation 4-2:

$$a_i=a_{aq}-J/K_{aq}A \qquad 4\text{-}19$$

the thickness of the boundary layer in the aqueous phase and the cobalt activities near the interface in the aqueous phase, can then be calculated, see Table 4-4.

Table 4-4: Boundary layer thickness and cobalt activities at the aqueous phase boundary under different hydrodynamic conditions.

n_{aq}	s^{-1}	0.50	0.76	0.92	1.56	2.5	4.15	inf.
Re_{aq}	/	42.05	64.00	77.37	131.2	210.3	349.0	inf.
δ_{aq}	$m \times 10^3$	1.938	1.683	1.468	1.107	1.048	0.308	0.0
a_i	mol m^{-3}	5.64	6.27	7.12	8.37	8.67	15.63	23.49

Table 4-4 shows the cobalt activities at the interface for the different stirrer speeds and Reynolds numbers. When the aqueous phase Reynolds number increases the aqueous phase cobalt activity near the interface increased. As the Reynolds number approaches infinity the boundary layer near the interface tends to zero. Under these conditions the cobalt activity near the interface can be assumed to be equal to the cobalt activity in the bulk aqueous phase.

4.8 Study on the Apparent Activation Energy

The effect of temperature on the extraction rate is shown in Figure 4-17. The extraction rate increases with increases in the temperature. According to the Arrhenius Equation:

$$N=Ae^{-E/RT} \qquad 4\text{-}20$$

$$\ln N = -E/RT + B \qquad (4\text{-}21)$$

where,

N = the extraction rate per unit area, mol s^{-1} m^{-2};

A = constant;

E = apparent activation energy in the extraction; and

R = 8.314 J $mol^{-1}k^{-1}$ (gas constant).

Using Figure 4-18 the apparent activation energy for cobalt extraction into HDTMPP was estimated as 39.4 kJ mol^{-1} at pH of 5.0.

Usually, when an extraction process is controlled by the diffusion mechanism, the value of the apparent activation energy is lower than when the extraction process is controlled by the chemical reaction mechanism. Consequently the value of the apparent activation energy is used as an indication of the controlling step in an the extraction.

The values of the apparent activation energy for different systems obtained by some previous studies and the present work are shown in Table 4-5.

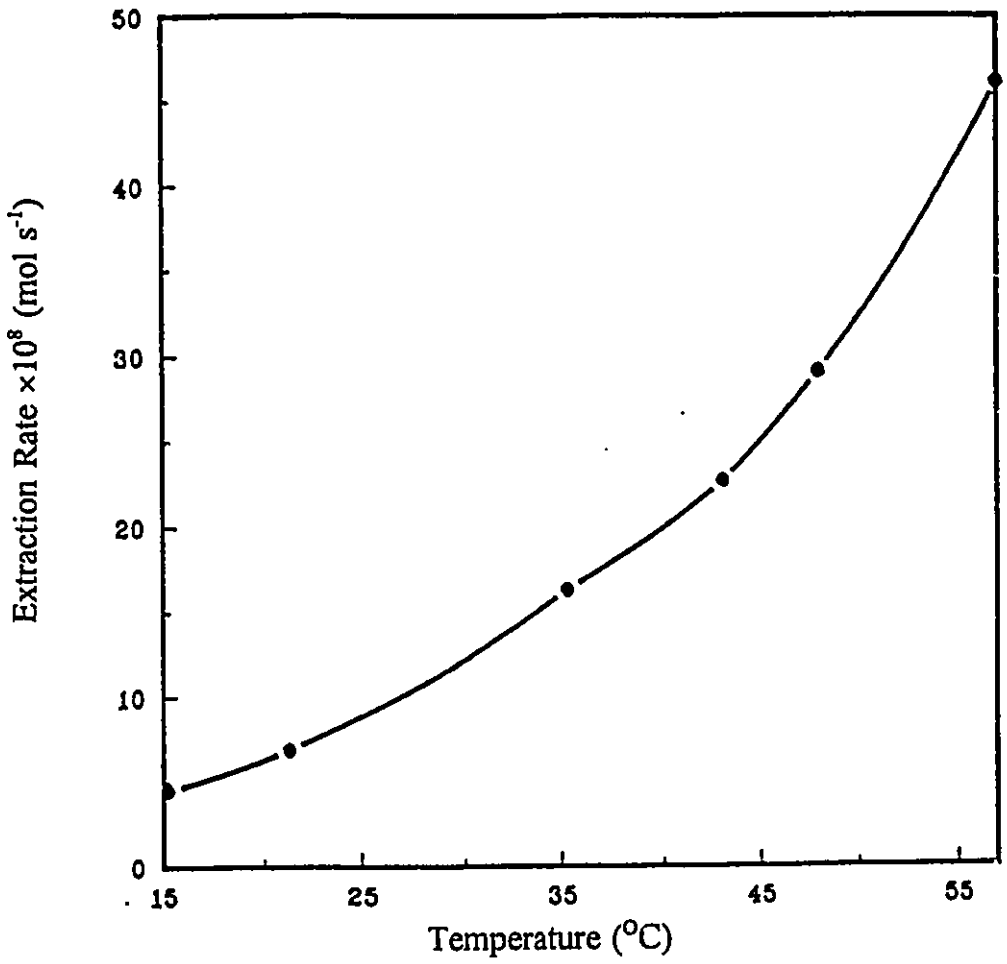

Figure 4-17: Effect of temperature on extraction rates.
Experimental Conditions: $A = 7.775\times10^{-3}$ m^2;
$C_{CoSO_4} = 0.050$ kmol m^{-3}; $C_{Na_2SO_4} = 0.0$ kmol m^{-3}; pH = 5.0;
$C_{H_2A_2} = 0.2695$ kmol m^{-3}; $C_{TBP} = 0.1832$ kmol m^{-3}; $Re_{aq} = 2102.5$;
and $Re_{org} = 110.5$.

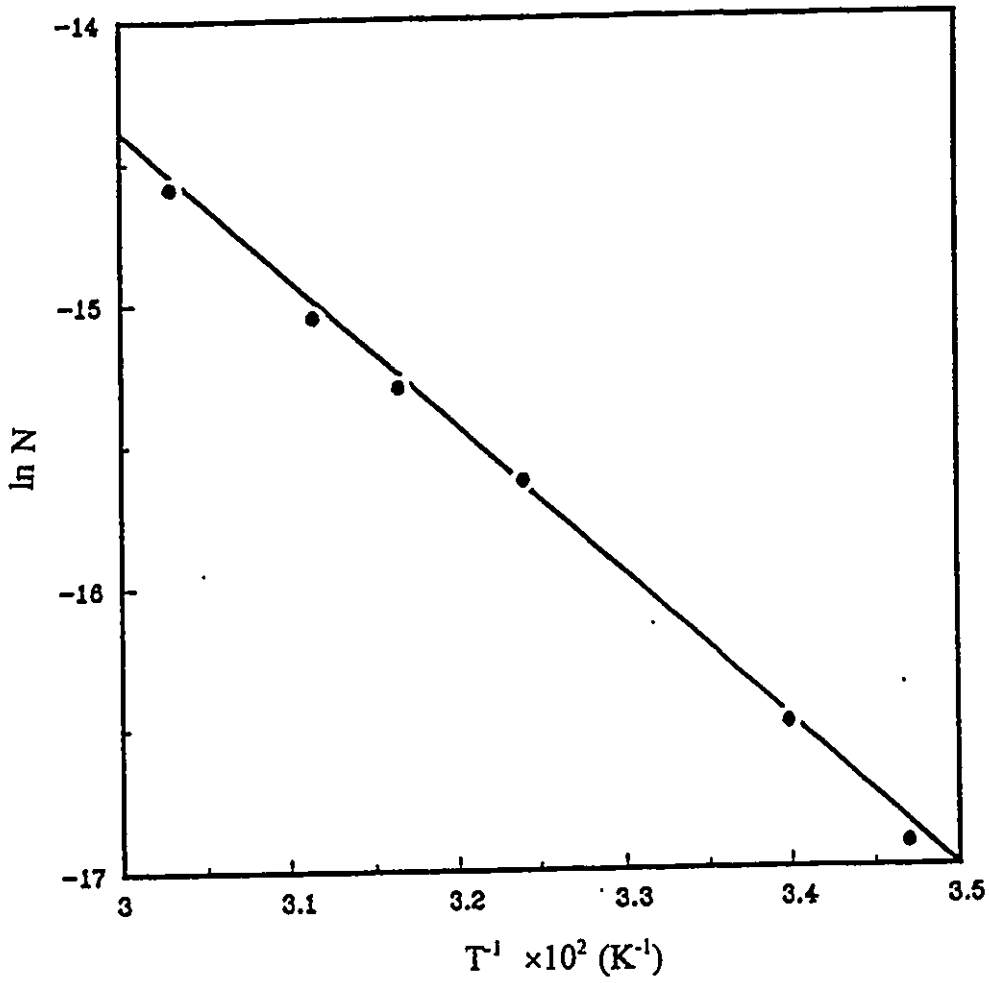

Figure 4-18: Relationship between temperature and extraction rates.
Experimental Conditions: $A = 7.775\times10^{-3}$ m^2;
$C_{CoSO_4} = 0.050$ kmol m^{-3}; $C_{Na_2SO_4} = 0.0$ kmol m^{-3}; pH = 5.0;
$C_{H_2A_2} = 0.2695$ kmol m^{-3}; $C_{TBP} = 0.1832$ kmol m^{-3}; $Re_{aq} = 2102.5$;
and $Re_{org} = 110.5$.

Table 4-5: Apparent activation energy for different cobalt extraction systems.

Author	Zhuo	Gai	Dreisinger	Yan	Chen	Present
System	5709	HEHEHP	HEHEHP	HMHHP	HEHEHP	HDTMPP
E, $kJmol^{-1}$	16.8	45.3	27.2	35.9	31.1	39.4
Mechanism	D	R	D-R	D-R	D	D-R

The value of the apparent activation energy obtained in this investigation was compared with the values obtained by the other authors. The experimental results indicated that at pH = 5, the extraction process was probably controlled by a combined chemical reaction and diffusion mechanism, however the present value of the activation energy was high making it an unreliable indicator of a chemical reaction or diffusion controlled extraction.

CHAPTER 5

Extraction Mechanism

A kinetic mechanism for the extraction of cobalt into HDTMPP has been developed based on the results seen in Chapter 4. This was carried out by considering all possible extraction steps in the extraction process and by examing the experimental results, the rate-controlling steps were determined for this process.

Under steady extraction conditions, the extraction resistance arises from: 1. the aqueous phase boundary layer, 2. chemical reaction at the interface, and 3. the organic phase boundary layer. Figure 5-1 shows the assumed distribution of cobalt activity close to the interface in a liquid-liquid extraction process.

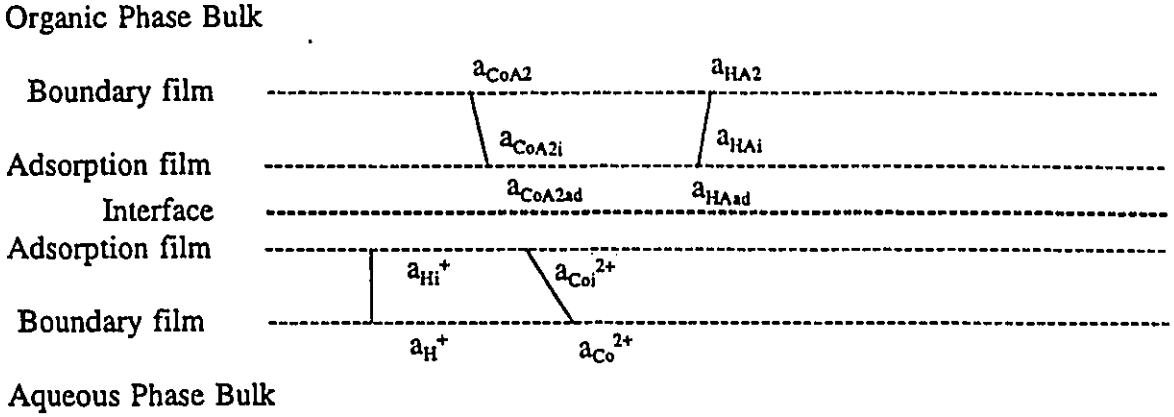

Figure 5-1: Activity profile near the interface for cobalt extraction.

The mass transfer rates in the boundary layers can be assumed to be dependent on the hydrodynamic conditions, that is, the thickness of the boundary layers of the two phases and the interfacial area. The chemical reaction rate is dependent on the reaction constant, the factors influencing the reaction such as the pH, the aqueous phase cobalt concentration and the extractant concentration, and the interfacial area if the chemical reaction takes place at the interface.

These three resistances (aqueous phase diffusion resistance, organic phase diffusion resistance and interfacial chemical reaction resistance) would control the overall extraction rate. They are assumed to be independent of each other. It is

possible to study the location of the controlling step or steps by considering all the possible steps in the extraction process.

5.1 Extraction Mechanism Steps

The possible steps in the extraction of cobalt into HDTMPP are shown below:

Step 1 $Co^{2+} \rightarrow Co_i^{2+}$

Step 2 $\overline{H_2A_2} = 2\overline{HA}$

Step 3 $\overline{HA} = \overline{HA_i}$

Step 4 $\overline{HA_i} \rightarrow HA_{ad}$

Step 5 $Co_i^{2+} + HA_{ad} = CoA_{ad}^{+} + H_i^{+}$

Step 6 $CoA_{ad}^{+} + \overline{HA_i} = CoA_{2ad} + H_i^{+}$

Step 7 $CoA_{2ad} = \overline{CoA_{2i}}$

Step 8 $\overline{CoA_{2i}} \rightarrow \overline{CoA_2}$

Step 9 $\overline{CoA_2} + \overline{H_2A_2} = \overline{CoA_2.2HA}$

Of these steps, some represent diffusion of ions in the extraction process, while others represent the chemical reactions taking place in the extraction process. These are described further below.

Step 1 describes the diffusion process of the cobalt ions from the aqueous bulk phase to the boundary layer near the interface:

$$N=k_{aq}(a_{Co^{2+}}-a_{Co_i^{2+}}) \qquad 5\text{-}1$$

Step 2 represents the formation of monomer from dimer. It is a fast reaction. The equilibrium distribution equation can be written as:

$$D_b=\frac{a_{\overline{HA}}^{\,2}}{a_{\overline{H_2A_2}}} \qquad 5\text{-}2$$

Step 3 is the diffusion of the extractant monomer from the organic bulk phase to the interface:

$$N=k_{org(HA)}(a_{\overline{HA}}-a_{\overline{HA_i}}) \qquad 5\text{-}3$$

Step 4 is the adsorption of the extractant in the reaction zone at the interface. Because of the surface activity, the extractant is situated at the interface and its concentration is very high, therefore, a_{HAad} is constant.

Step 5 is the first order chelation. If this step is assumed to be the rate-controlling step, all others being fast reactions, then

$$\frac{d[CoA_2.2HA]}{dt} = k\, a_{HA_{ad}} a_{Co_i^{2+}} \qquad 5\text{-}4$$

However, Equation 5-4 shows that the extraction rate is not dependent on the pH, which is contrary to the experimental results. Consequently, this step can be assumed to be at equilibrium and not rate controlling. At equlibrium there is:

$$D = \frac{a_{CoA_{ad}} \cdot a_{H_i}^{+}}{a_{Co_i^{2+}} \cdot a_{HA_{ad}}} \qquad 5\text{-}5$$

Step 6 is the second order chelation. Assuming this step is the controlling step, then

$$\frac{d[CoA_2.2HA]}{dt} = k a_{\overline{HA}} a_{HA_{ad}} a_{Co_i^{2+}} a_{H^+}^{-1} \qquad 5\text{-}6$$

This equation involves the pH and is in agreement with the experimental results, hence this is a possible rate controlling step.

Step 7 is the desorption of the chelated molecule at the interface.

Assuming this step is the only controlling step, then

$$\frac{d[CoA_2.2HA]}{dt} = k a_{\overline{HA_l}} a_{HA_{ad}} a_{Co^{2+}} a_{H^+}^{-2} \qquad 5\text{-}7$$

Equation 5-7 shows a second order relationship between pH and the extraction rate. Since this is not in agreement with the experimental data this step should be fast and not rate controlling.

Step 8 is the diffusion of the chelated molecules from the interface to the organic bulk phase. This step is expressed as:

$$N = k_{org}(a_{CoA_2 i} - a_{CoA_2}) \qquad 5\text{-}8$$

Step 9 is the combination of the organic cobalt compounds with extractant dimers in the organic phase. This is considered to be a fast reaction [Komasawa, 1984].

5.2 Simulation of the Extraction Rates

From the results discussed earlier, the overall resistance of the extraction rate is assumed to arise from three regions:

1) diffusion of cobalt ion from the aqueous bulk phase to the interface,

Step 1 $$Co^{2+} \rightarrow Co_i^{2+}$$

2) the second order chelation of cobalt at the interface,

Step 2 $$CoA_{ad}^{+} + HA_i = CoA_{2ad} + H_i^{+}$$

and 3) diffusion of the organic cobalt compounds from the interface to the organic bulk phase.

Step 3 $$\overline{CoA_{2i}} \rightarrow \overline{CoA_2}$$

From the previous discussion, it is assumed that

$$R_{overall} = R_{aq} + R_r + R_{org} \qquad 5\text{-}9$$

where,

$$R_{aq} = \alpha_1 Re_{aq}^{-1/2} \qquad 5\text{-}10$$

$$R_{org} = \alpha_2 Re_{org}^{-1/2} \qquad 5\text{-}11$$

and

$$Rr = 1/k_r = \alpha_3 a_H \qquad 5\text{-}12$$

α_1, α_2 and α_3 are constants. Using all the experimental data, an expression for the prediction of the extraction rate can be obtained as follows:

$$J=\frac{A\times a_{Co}\times a_{H_2A_2}}{3.69\times10^{6}Re_{aq}^{-1/2}+4.89\times10^{5}Re_{org}^{-1/2}+1.52\times10^{9}a_{H}} \qquad 5\text{-}13$$

The average error of Equation 5-13 was found to be less than 10% over the range of the variables studied.

5.3 Discussion of the Proposed Model

The extraction process of cobalt with HDTMPP was found to be a diffusion-chemical reaction combined controlled mechanism. The mechanism, however, was dependent on the actual experimental conditions. When the experimental conditions were changed, the resistances from the three regions, namely, in the aqueous phase, in the organic phase and at the interface, were affected. Also, the distribution of the resistance would be changed, causing the mechanism pattern to be altered.

When pH < 5, the extraction was controlled by the chemical reaction and the

extraction resistance only came from the chemical reaction. so Equation 5-13 becomes

$$J=6.57\times10^{-10}A\ a_{Co}a_{H_2A_2}a_H^{-1} \qquad 5\text{-}14$$

When pH > 5, the chemical resistance disappeared gradually with an increase in pH and the diffusion resistance played a major role in affecting the overall extraction rate. Under these conditions extraction was diffusion controlled and Equation 5-15 becomes:

$$J = A\ a_{Co}a_{\overline{H_2A_2}}(3.69\times10^{6}Re_{aq}^{-1/2}+4.89\times10^{5}Re_{org}^{-1/2})^{-1} \qquad 5\text{-}15$$

The diffusion resistance consisted of two parts, one from the aqueous phase, the other from the organic phase. The phase diffusion resistances are dependent on the hydrodynamic conditions of the two phases.

The apparent activation energy of the cobalt-HDTMPP system at pH = 5.0 was found to be 39.4 kJ mol^{-1}. As noted previously, further investigation is required at pH values less than 5.0.

5.4 Comparison of the Predicted Value with the Experimental Data

Errors was calculated by means of Equation 5-16:

$$e = \frac{|J_{pre.} - J_{exp.}|}{J_{exp.}} \times 100\% \qquad 5\text{-}16$$

For all the comparisons shown from Figure 5-2 to Figure 5-8, the predicted values were in good agreement with the experimental data for the majority of the runs. Major deviations occur when there was a marked from a linear dependence of extraction rate, for example, the effects of extraction on concentration, see Figure 5-2. Under these conditions good agreement was only observed up to the cobalt concentration of 0.07 kmol m^{-3}. At high concentrations deviation can be attributed to difficulties in evaluation of activities.

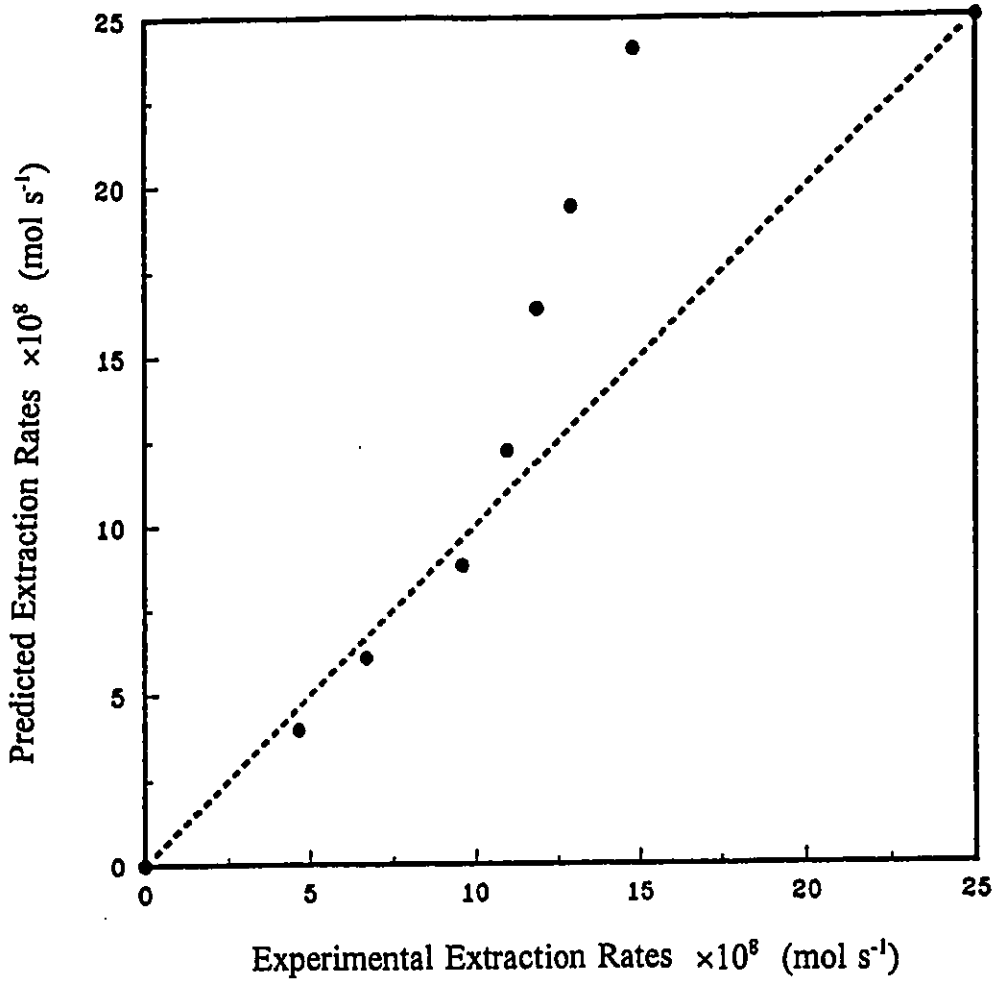

Figure 5-2: Comparison of experimental and predicted extraction rates at different aqueous phase cobalt concentrations.
Experimental Conditions: T = 25 °C; A = 7.775×10^{-3} m^2; pH = 5.0;
C_{Na2SO4} = 0.0 kmol m^{-3}; C_{H2A2}= 0.2695 kmol m^{-3};
C_{TBP}= 0.1832 kmol m^{-3}; n_{aq} = 2.5 s^{-1}; and n_{org}= 2.7 s^{-1}.

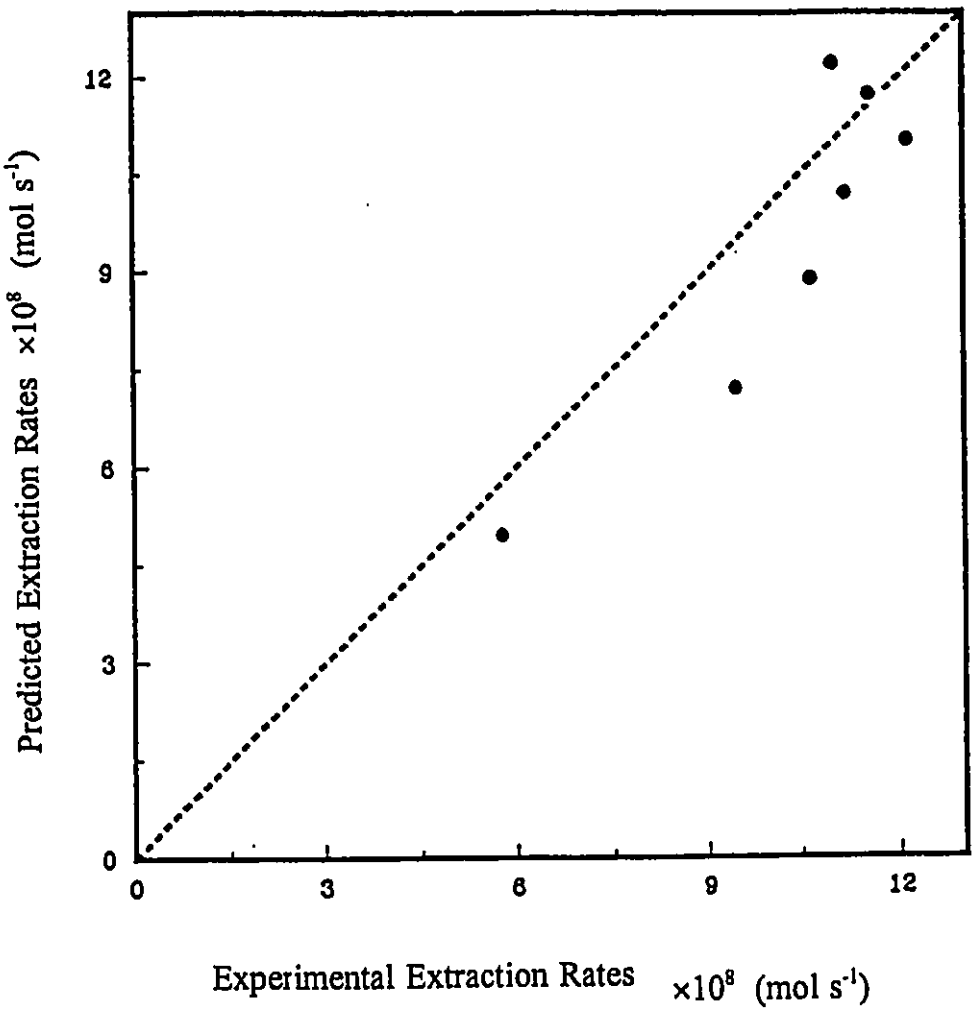

Figure 5-3: Comparison of experimental and predicted extraction rates at different aqueous phase Na_2SO_4 concentrations.
Experimental Conditions: T = 25 ^{o}C; A = 7.775×10^{-3} m^2; pH = 5.0;
C_{Co2SO4} = 0.01 kmol m^{-3}; C_{H2A2}= 0.2695 kmol m^{-3};
C_{TBP}= 0.1832 kmol m^{-3}; n_{aq} = 2.5 s^{-1}; and n_{org}= 2.7 s^{-1}.

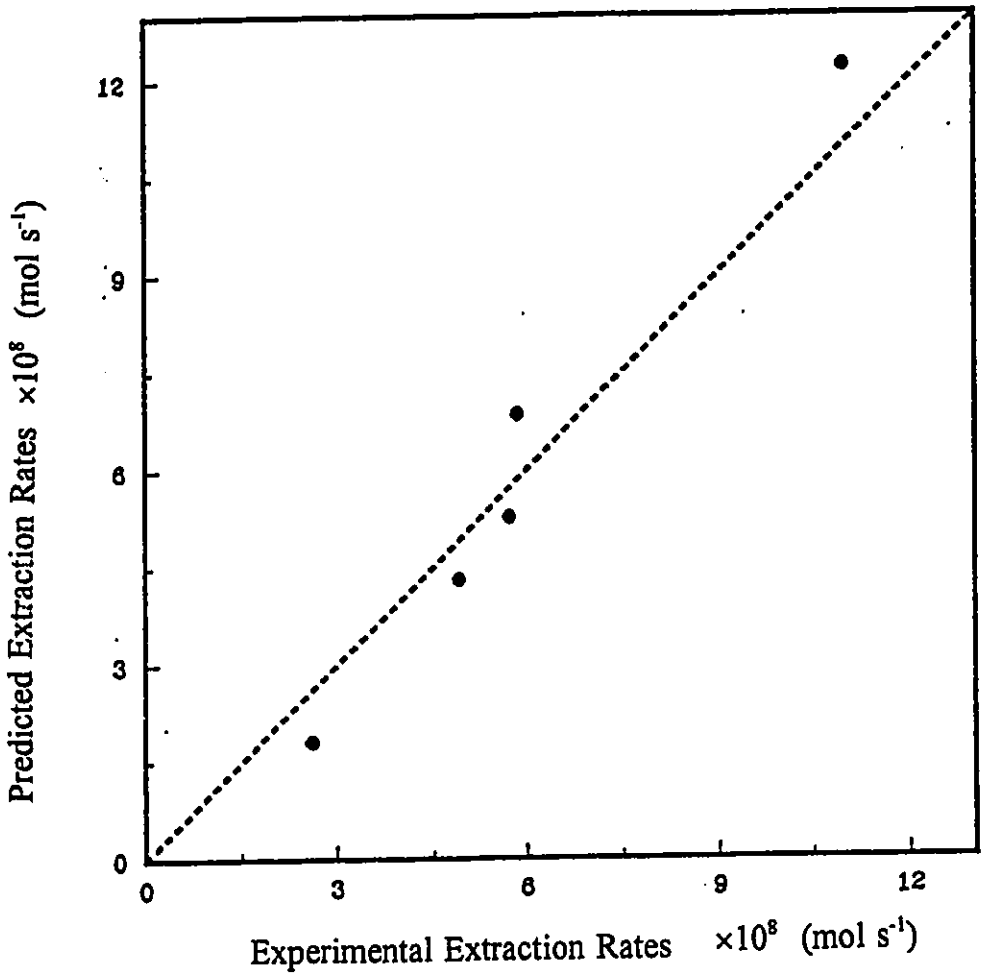

Figure 5-4: Comparison of experimental and predicted extraction rates at Different Interfacial Areas.
Experimental Conditions: T = 25 ^{O}C; pH = 5.0;
C_{Co2SO4} = 0.01 kmol m^{-3}; C_{Na2SO4} = 0.0 kmol m^{-3};
C_{H2A2} = 0.2695 kmol m^{-3}; C_{TBP}= 0.1832 kmol m^{-3}; n_{aq} = 2.5 s^{-1}; and
n_{org} = 2.7 s^{-1}.

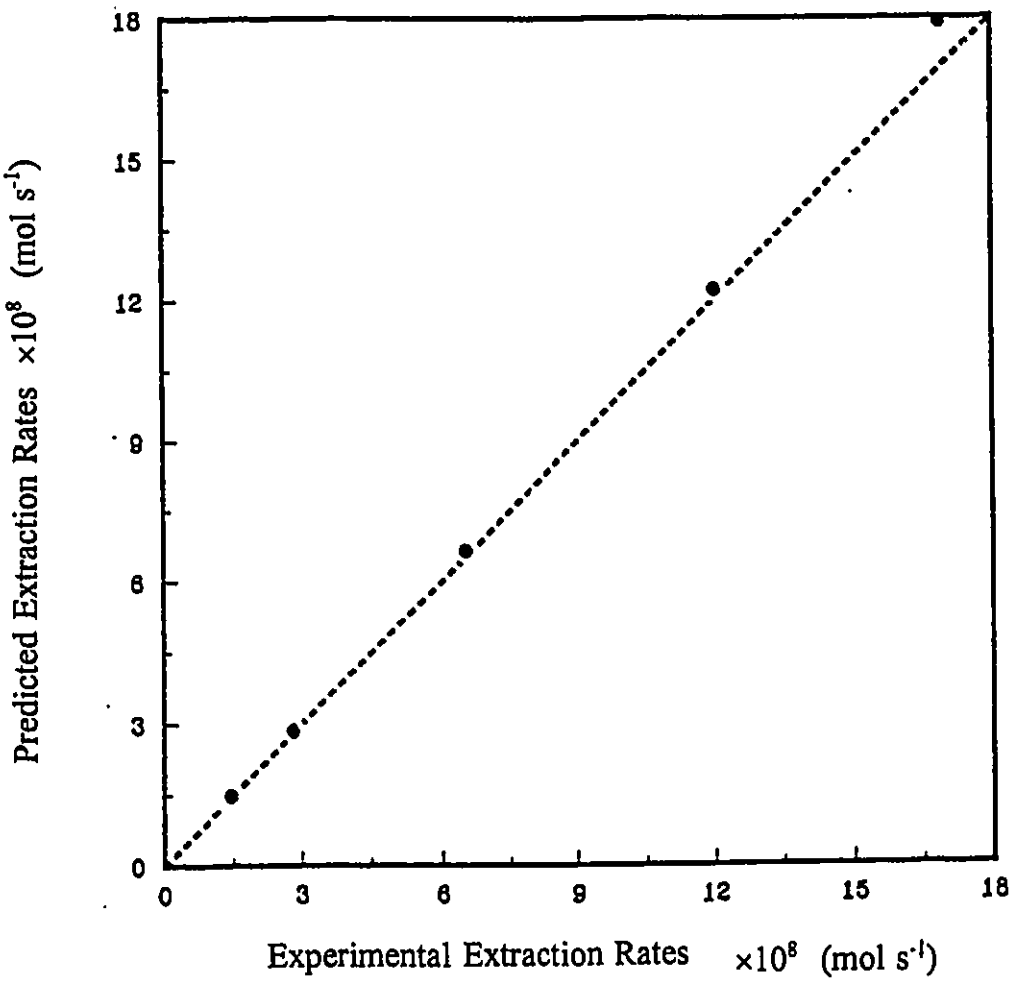

Figure 5-5: Comparison of experimental and predicted extraction rates at different extractant concentrations.
Experimental Conditions: T = 25 °C; A = 7.775×10^{-3} m^2; pH = 5.0;
C_{Co2SO4} = 0.01 kmol m^{-3}; C_{Na2SO4} = 0.0 kmol m^{-3};
C_{TBP}= 0.1832 kmol m^{-3}; n_{aq} = 2.5 s^{-1} ; and n_{org}= 2.7 s^{-1}.

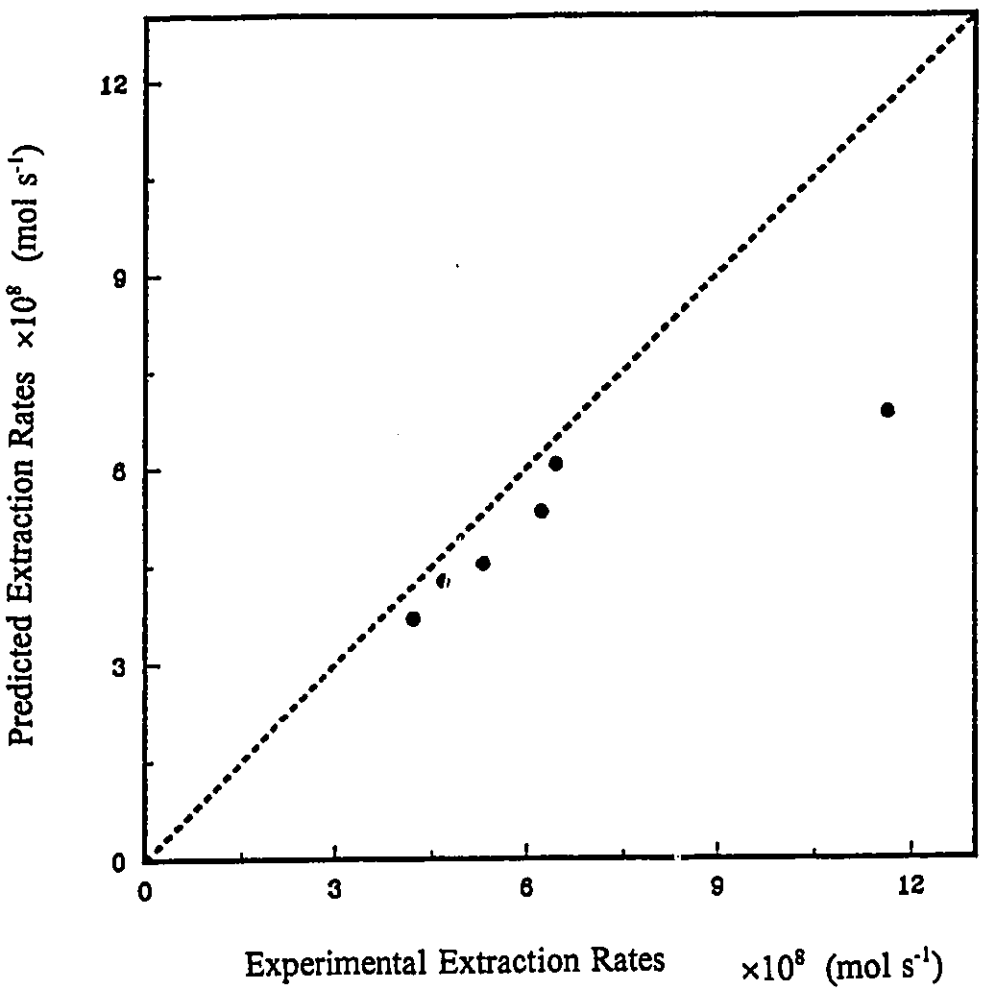

Figure 5-6: Comparison of experimental and predicted extraction rates at different aqueous phase rotation speeds.
Experimental Conditions: T = 25 °C; A = 7.775×10^{-3} m^2; pH = 5.0;
C_{Co2SO4} = 0.01 kmol m^{-3}; C_{Na2SO4} = 0.0 kmol m^{-3};
C_{H2A2}= 0.2695 kmol m^{-3}; C_{TBP}= 0.1832 kmol m^{-3} ; and n_{aq} = 2.5 s^{-1};
and n_{org}= 2.7 s^{-1}.

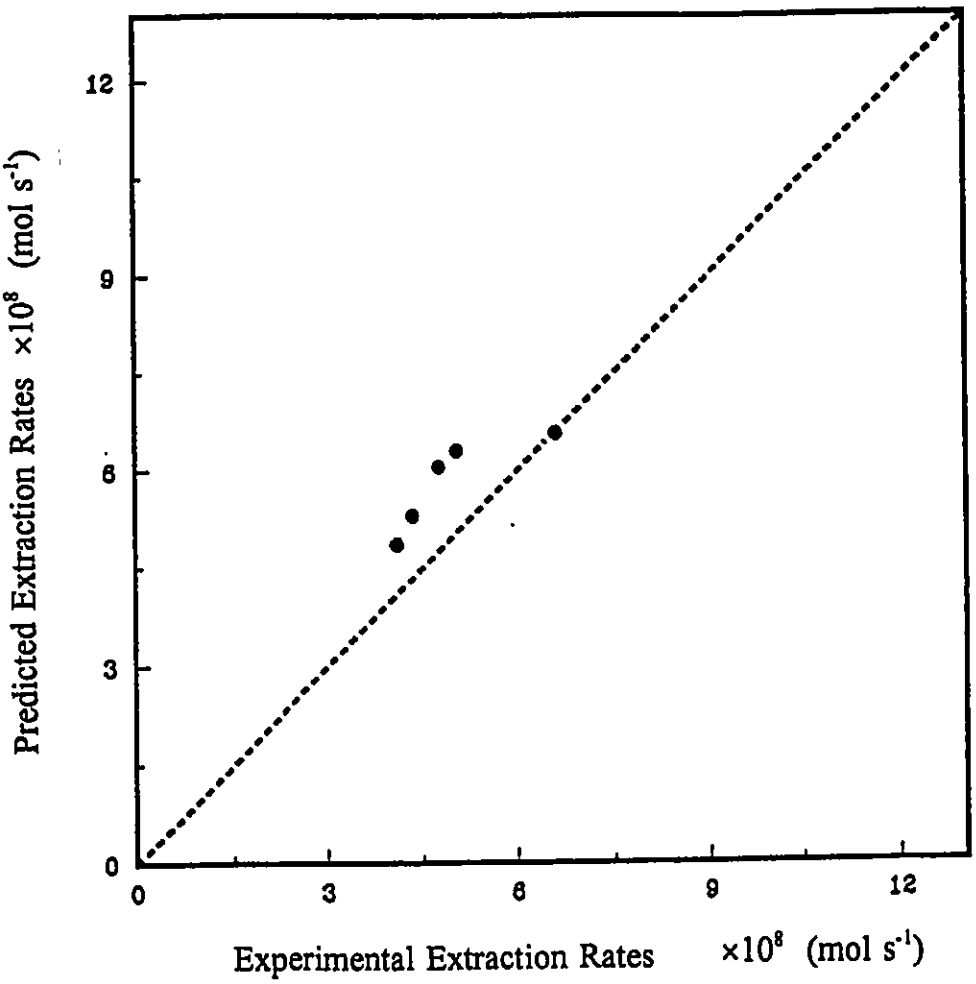

Figure 5-7: Comparison of experimental and predicted extraction rates at different organic phase rotation speeds.
Experimental Conditions: T = 25 °C; A = 7.775×10^{-3} m^2; pH = 5.0; C_{Co2SO4} = 0.01 kmol m^{-3}; C_{Na2SO4} = 0.0 kmol m^{-3}; C_{H2A2}= 0.2695 kmol m^{-3}; C_{TBP}= 0.1832 kmol m^{-3} and n_{aq} = 2.5 s^{-1}; and n_{org}= 2.7 s^{-1}.

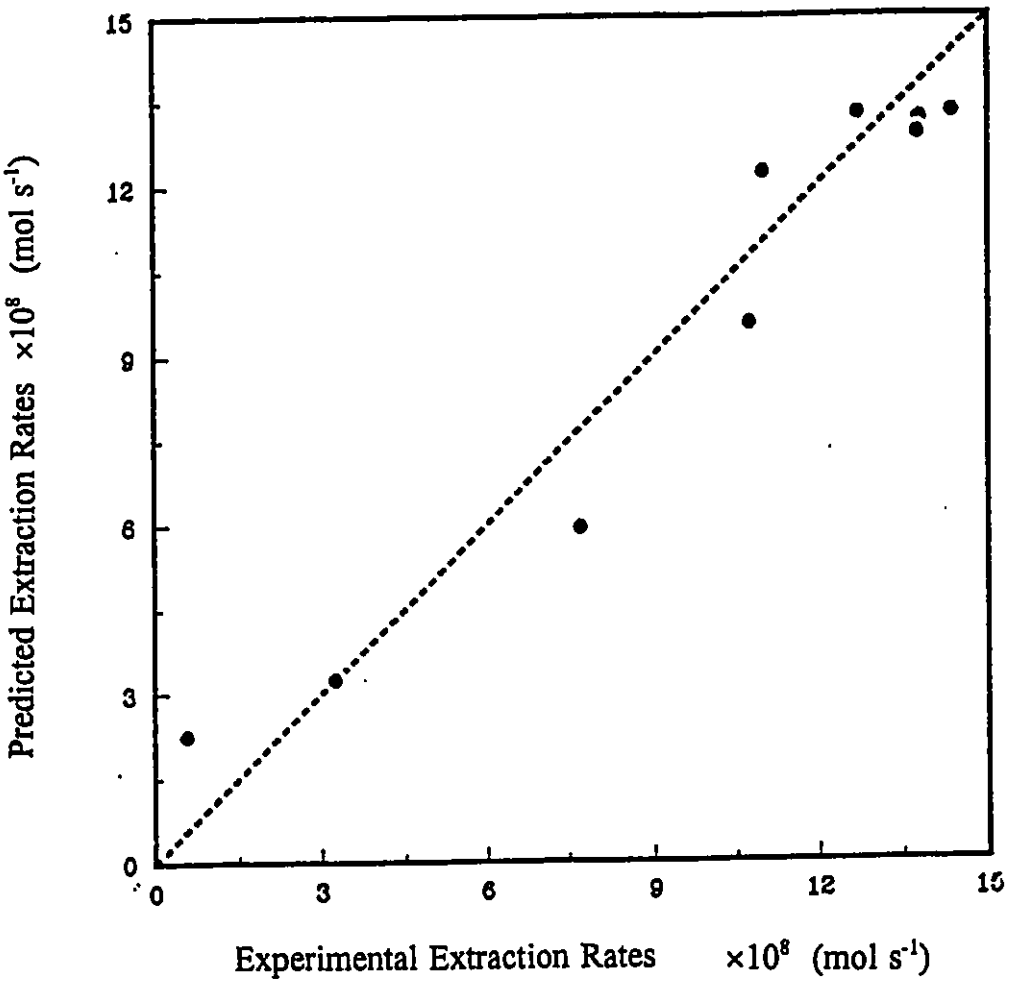

Figure 5-8: Comparison of experimental and predicted extraction rates at different pH values.
Experimental Conditions: T = 25 °C; A = 7.775×10^{-3} m^2;
C_{Co2SO4} = 0.01 kmol m^{-3}; C_{Na2SO4} = 0.0 kmol m^{-3};
C_{H2A2}= 0.2695 kmol m^{-3}; C_{TBP}= 0.1832 kmol m^{-3}; n_{aq} = 2.5 s^{-1}; and
n_{org}= 2.7 s^{-1}.

CHAPTER 6

Conclusions

1. The Lewis cell modified by using auto-titration and "gravity leg" techniques was proved to be very useful in studying cobalt extraction into HDTMMP.
2. The driving force equation should be expressed using activities rather than concentrations.
3. Extraction resistance for the $CoSO_4$-HDTMPP was investigated. The phase diffusion resistance is dependent on the hydrodynamic conditions in each phase. The interfacial resistance is dependent on the interfacial chemical reaction rate and interfacial area.
4. For the $CoSO_4$-HDTMPP system, the apparent activation energy was 39.4 kJ mol^{-1}.
5. The kinetics of cobalt extraction with HDTMPP can be explained by means of a mixed diffusion-chemical reaction controlling mechanism:

(i) the cobalt ion diffusion from the aqueous bulk phase to the interface;

Step 1 $$Co^{2+} \rightarrow Co_i^{2+}$$

(ii) the reaction of the second order chelation at the interface;

Step 2 $$CoA_{ad}^{+} + \overline{HA}_i = CoA_{2ad} + H_i^{+}$$

and (iii) the organic cobalt complex diffusion from the interface to the organic bulk phase.

Step 3 $$\overline{CoA}_{2i} \rightarrow \overline{CoA}_2$$

The controlling step could be expected to change when the experimental conditions are changed.

6. The proposed model for the extraction process was found as follows:

$$J = \frac{A \times a_{Co} \times a_{H_2A_2}}{3.69 \times 10^6 Re_{aq}^{-1/2} + 4.89 \times 10^5 Re_{org}^{-1/2} + 1.52 \times 10^9 a_H}$$

The predicted values were in agreement with the experimental data over most of the range of variables investigated.

References

Albery, J.W. and P.R. Fick, Proceedings of Hydrometallurgy'81, IMM, F5, 1-5, Manchester (1981).

Andersson, C.,, S. Andersson, J.O. Liljenzin, H. Reinhardt and J. Rydberg, Acta Chem. Scand., **23**, 2781 - 2790 (1969).

Berthelot, M. and J. Jungfleisch, J. Ann. Chem. Phys., **26**, 396 - 406 (1872).

Blumberg, R., Liquid-liquid Extraction, Chapter 1, p.1, Academic Press, London (1988).

Chen, C., M.S. Thesis of Chinese Academy of Sciences, Beijing (1986).

Cianetti, C, and P.R. Danesi, Solvent Ext. and Ion Exch., **1**, 9 - 24 (1983).

Coleman, C.F. and J.W. Roddy, Solvent Ext. Rev., 1, 63 - 70 (1971).

Coulson, J.M. and T.F. Richardson, Chemical Engineering, Chapter 13, p.443 Pergamon Press, Oxford (1990).

Cyanamid, Solvent Extraction Reagent, p.1, American Cyanamid Company, New York (1990).

Danesi, P.R., and R.Chiavizia, CRC Crit. Rev. Anal. Chem., **10**, 1 - 15 (1980).

Danesi, P.R., Solvent Ext. and Ion Exch. **2**, 29 40 (1984).

Dreisinger, P.B. and W. C. Cooper, Solvent Ext. and Ion Exch., **4**, 317 - 328 (1986).

Fu, X., Physical Chemistry, Chapter 8, p.241, People's Education Press, Beijing (1979).

Fu, X. and J.A. Golding, Solvent Ext. and Ion Exch., **6**, 889 - 1002 (1988).

Fu, X., Z. Hu, Y. Lui, and J.A. Golding, Solvent Ext. and Ion Exch., **8**, 573 - 590 (1990).

Golding, J.A., and C.B. Barclay, Can. J. Chem. Eng., **66**, 970 - 989 (1988).

Hughes, M.A., and V. Rod, Hydrometallurgy, **12**, 267 - 285 (1984).

Kamen, A.A., Thèse est présentér à l'école Nationale, Supérieure des Mines de Paris (1983).

Komasawa, I., J. Chem. Eng. Japan., **13**, 209 - 220 (1980).

Komasawa, I., T.Otake and I. Hattori, J. Chem. Eng., Japan, **16**, 384 - 398 (1983).

Komasawa, I., T.Otake and Y.Hagaki, J. Inorg. Nucl. Chem., **43**, 3351 - 3361 (1981).

Lewis, J.B., Chem. Eng. Sci., **3**, 248 - 259 (1954).

Lewis, J.B., Chem. Eng. Sci., **3**, 260 - 274 (1954).

Li, J., Ph.D thesis of TsingHua University, Beijing (1988).

Li, Y. and Li, Z, Rare Metal (Chinese), 4, 35 -47 (1985).

Li, Y., J. Phy. and Chem., **95**, 1-12 (1985).

Li, Y.G., Thermodynamics of Metal Solvent Extraction (Chinese), Chapter 1, p.1, TsingHua University Press, Beijing (1988).

Li, Z., Chem. Met. (Chinese), **3**, 47 - 60 (1987).

Lo, T.C., M.H. Baird and C. Hanson, Handbook of Solvent Extraction, Chapter 4, p.441, John Wiley & Sons, New York (1983).

Perron, L.,, Cobalt, Canadian Minerals Yearbook, (to be published) (1994).

Pitzer, K.S., J. Phys. and Chem., **77**, 268 - 280 (1973).

Pratt, H.R.C., Handbook of Solvent Extraction, Chapter 3, p.320, John Wiley & Sons, New York (1983).

Ritcey, G.M., A.W., Ashbrook and B.H., Lucas, CIM Bull., **68**, 111 - 123 (1975).

Ritcey, G.M. and A.W.Ashbrook, Chapter 1, Solvent Extraction, Part I, p.194, John Wiley & Sons, New York (1984).

Reinhardt, H., and J.H.A. Rydbery, Handbook of Solvent Extraction, Chapter 3, p.207, John Wiley & Sons, New York (1983).

Shen, J. and Gao Z., Appl. Chem. (Chinese), **4**, 9 - 18, (1984).

Shen, J., H.Gao, Z.Gao and S.Sun, J. Shandong Univ. (Chinese), **2**, 76 - 90 (1985).

Wang, X., Analysis of Chemistry, Chapter 5, p.480 Press of People's Education, China (1987).

Whitman, W.G., Chem. Met. Eng., **29**, 147 - 161 (1923).

Yan, C., M.E. Thesis of TsingHua University, Beijing (1989).

Yang, L., T. Michel and W. Nitsch, Solvent Ext. and Ion Exch., **11**, 119 - 133 (1993).

Zhu T., J. Chem. Eng. and Ind. (Chinese), **44**, 343 - 359 (1993).

Zhuo, Y. and Z. Li, J. Chem. Eng. and Ind. (Chinese), **1**, 10 -23 (1986).

Appendix 1

Experimental Data

The original experimental kinetic data for the extraction of $CoSO_4$-HDTMPP are given in the following tables. J is the extraction rate; mol s^{-1}. b_L is the slope of the linear relationship between the absorbance and time.

Table A-1: Kinetic experiment: Effect of aqueous phase cobalt concentrations.
Experimental conditions: T = 25 °C; A = 7.775×10^{-3} m^2;
$C_{Na_2SO_4}$ = 0 kmol m^{-3}; pH = 5.0; $C_{H_2A_2}$ = 0.2695 kmol m^{-3};
C_{TBP} = 0.1832 kmol m^{-3}; Re_{aq} = 2102.5; and Re_{org} = 110.5.

C_{CoSO_4}	0.0125	0.025	0.05	0.10	0.20	0.30	0.50
t s	kmol m^{-3}	kmol m^{-3}	kmol m^{-3}	kmol m^{-3}	kmol m^{-3}	kmol m^{-3}	kmol m^{-3}
000	0.000	0.000	0.000	0.000	0.000	0.000	0.000
500	0.007	0.007	0.013	0.015	0.018	0.029	0.019
1000	0.011	0.016	0.024	0.027	0.032	0.038	0.039
1500	0.016	0.025	0.036	0.041	0.046	0.055	0.058
2000	0.024	0.034	0.048	0.054	0.061	0.066	0.076
2500	0.028	0.042	0.061	0.067	0.076	0.086	0.094
3000	0.034	0.050	0.072	0.081	0.091	0.100	0.111
3500	0.040	0.058	0.084	0.094	0.104	0.118	
4000	0.046	0.065	0.092	0.108			
4500	0.051		0.109	0.118			
5000	0.060						
5500	0.064						
$b_L\times10^5$	1.14	1.64	2.36	2.70	2.91	3.17	3.63
J $\times10^8$	4.65	6.68	9.60	11.00	11.9	12.9	14.8

Table A-2: Kinetic experiment: Effect of aqueous phase Na_2SO_4 concentrations.
Experimental conditions: T = 25 ^{0}C; A = 7.775×10^{-3} m^2;
C_{CoSO_4} = 0.10 kmol m^{-3}; pH = 5.0; $C_{H_2A_2}$ = 0.2695 kmol m^{-3};
C_{TBP} = 0.1832 kmol m^{-3}; Re_{aq} = 2102.5; and Re_{org} = 110.5

$C_{Na_2SO_4}$	0.01	0.02	0.05	0.10	0.20	0.50
t s	kmol m^{-3}	kmol m^{-3}	kmol m^{-3}	kmol m^{-3}	kmol m^{-3}	kmol m^{-3}
000	0.00	0.000	0.000	0.000	0.000	0.000
500	0.005	0.010	0.006	0.012	0.008	0.007
1000	0.020	0.026	0.018	0.024	0.021	0.014
1500	0.036	0.039	0.030	0.038	0.032	0.021
2000	0.048	0.055	0.042	0.055	0.043	0.028
2500	0.062		0.056	0.064	0.056	0.035
3000	0.072		0.068	0.078		0.043
3500	0.090	0.066	0.081	0.090		
4000	0.104	0.083				
$b_L \times10^5$	2.84	2.98	2.75	2.62	2.33	1.42
$J \times10^8$	11.6	12.13	11.18	10.65	9.46	5.77

Table A-3: Kinetic experiment: Effect of interfacial area.
Experimental conditions: T = 25 ^{0}C; C_{CoSO_4}=0.10 kmol m^{-3}; $C_{Na_2SO_4}$ = 0 kmol m^{-3}; pH = 5.0; $C_{H_2A_2}$ = 0.2695 kmol m^{-3}; C_{TBP} = 0.1832 kmol m^{-3}; Re_{aq} = 2102.5; and Re_{org} = 110.5

A m^2	1.153	2.749	3.358	4.340
000 s	0.000	0.000	0.000	0.010
500	0.003	0.003	0.006	0.020
1000	0.006	0.009	0.013	0.031
1500	0.008	0.014	0.021	0.031
2000	0.012	0.021	0.028	0.040
2500	0.015	0.026	0.034	0.046
3000	0.021	0.032	0.041	0.056
3500		0.039	0.049	0.063
$b_L \times 10^5$	0.642	1.21	1.41	1.44
$J \times 10^8$	2.611	4.91	5.73	5.86

Table A-4: Kinetic experiment: Effect of extractant concentrations.
Experimental conditions: $T = 25\ ^0C$; $A = 7.775\times10^{-3}\ m^2$;
$C_{CoSO_4} = 0.10$ kmol m^{-3}; $C_{Na_2SO_4} = 0$ kmol m^{-3}; pH = 5.0;
$C_{TBP} = 0.1832$ kmol m^{-3}; $Re_{aq} = 2102.5$; and $n_{org} = 2.7\ s^{-1}$

C_{H2A2}	0.135	0.0270	0.0674	0.135	0.202
t s	kmol m^{-3}	kmol m^{-3}	kmol m^{-3}	kmol m^{-3}	kmol m^{-3}
000	0.000	0.000	0.000	0.000	0.000
500	0.002	0.007	0.004	0.020	0.009
1000	0.004	0.024	0.013		0.035
1500	0.007	0.030	0.024		0.049
2000	0.011	0.039	0.033	0.042	0.073
2500	0.013	0.049	0.042	0.058	0.091
3000	0.019	0.058	0.052	0.073	0.109
3500		0.068	0.058	0.091	
4000			0.069		
4500			0.079	0.128	
5000				0.148	
$b_L \times10^5$	0.587	0.978	1.86	3.16	3.98
$J \times10^8$	2.39	3.98	7.59	12.9	16.2

Table A-5: Kinetic experiment: Effect of TBP concentrations.
Experimental conditions: T = 25 ^{0}C; A = 7.775×10^{-3} m^2;
C_{CoSO_4} = 0.10 kmol m^{-3}; $C_{Na_2SO_4}$ = 0 kmol m^{-3}; pH = 5.0;
$C_{H_2A_2}$ = 0.2695 kmol m^{-3}; Re_{aq} = 2102.5; and Re_{org} = 110.5.

C_{TBP}	0.0183	0.0366	0.0733	0.183	0.366
T s	kmol m^{-3}	kmol m^{-3}	kmol m^{-3}	kmol m^{-3}	kmol m^{-3}
000	0.000	0.000	0.000	0.000	0.000
500	0.008	0.005	0.005	0.007	0.006
1000	0.016	0.017	0.017	0.015	0.019
1500	0.024	0.032	0.028	0.024	0.030
2000	0.034	0.039	0.038	0.028	0.041
2500	0.042	0.048	0.048	0.040	0.051
3000		0.058	0.056	0.049	0.064
3500	0.061	0.069	0.068	0.057	0.072
4000	0.070	0.080	0.080	0.065	
$b_L \times 10^5$	1.57	1.77	2.09	1.67	2.12
$J \times 10^8$	6.21	7.20	8.51	6.81	8.62

Table A-6(1): Kinetic experiment: Effect of pH.
Experimental conditions: T = 25 ^{0}C; A = 7.775×10^{-3} m^2;
C_{CoSO_4} = 0.10 kmol m^{-3}; $C_{Na_2SO_4}$ = 0 kmol m^{-3}; pH = 5.0;
$C_{H_2A_2}$ = 0.2695 kmol m^{-3}; C_{TBP} = 0.1832 kmol m^{-3};
Re_{aq} = 2102.5; and Re_{org} = 110.5

pH	1.8	2.6	2.95	3.1	3.3	3.5
000 s	0.000	0.000	0.000	0.000	0.000	0.000
500	-0.003				0.007	0.003
1000		-0.005		-0.002		0.006
1500	-0.007	-0.006	-0.010			0.008
2000		-0.010		-0.003		
2500	-0.013		-0.016		0.009	0.019
3000		-0.014		-0.004		
3500	-0.016		-0.019		0.012	
4000		-0.020				
4500			-0.026	-0.007	0.014	0.037
5000						
5500		-0.027				0.044
$b_L \times10^5$	-0.477	-0.543	-0.509	-0.0436	0.147	0.793
$J \times10^8$	-1.94	-2.21	-2.072	-0.584	0.57	3.227

Table A-6(2): Kinetic experiment: Effect of pH.
Experimental conditions: T = 25 ^{0}C; A = 7.775×10^{-3} m^2;
C_{CoSO_4} = 0.10 kmol m^{-3}; $C_{Na_2SO_4}$ = 0 kmol m^{-3}; pH = 5.0;
$C_{H_2A_2}$ = 0.2695 kmol m^{-3}; C_{TBP} = 0.1832 kmol m^{-3};
Re_{aq} = 2102.5; and Re_{org} = 110.5.

pH	3.9	4.4	5.5	6.0	6.5	7.0
000 s	0.000	0.000	0.000	0.000	0.000	0.000
500	0.009		0.021	0.024	0.015	0.020
1000	0.021	0.030	0.039	0.034	0.030	0.036
1500	0.029		0.050	0.046	0.045	0.058
2000	0.039	0.055	0.071	0.061		
2500	0.046					
3000	0.056	0.086				
3500	0.065					
4000	0.076	0.111				
4500	0.088	0.126				
$b_L \times 10^5$	1.89	2.64	3.38	3.39	3.12	3.53
$J \times 10^8$	7.70	10.7	13.8	13.79	12.7	14.4

Table A-7: Kinetic experiment: Effect of aqueous phase stirrer speed.
Experimental conditions: $T = 25\ ^{0}C$; $A = 7.775\times10^{-3}\ m^2$;
$C_{CoSO_4} = 0.050$ kmol m^{-3}; $C_{Na_2SO_4} = 0$ kmol m^{-3}; pH = 5.0;
$C_{H_2A_2} = 0.2695$ kmol m^{-3}; $C_{TBP} = 0.1832$ kmol m^{-3}; and $Re_{org} = 110.5$.

$N\ s^{-1}$	0.5	0.76	0.92	1.56	2.55	4.15
Re_{aq}	420	640	773	1312	2102	3490
000 s	0.000	0.000	0.000	0.000	0.000	0.000
500	0.005	0.006	0.006	0.008	0.010	0.015
1000	0.011	0.012	0.012	0.016	0.021	0.029
1500	0.016	0.017	0.020	0.023	0.031	0.044
2000	0.020	0.023	0.026	0.030	0.042	0.057
2500	0.026	0.029	0.033	0.038	0.052	0.073
3000	0.030	0.034	0.039	0.046	0.062	0.088
3500	0.036	0.040	0.046	0.054	0.072	0.102
4000	0.040	0.046	0.052	0.062	0.083	
4500	0.046	0.052	0.058	0.069	0.093	0.131
5000	0.050	0.057	0.065	0.076	0.104	0.144
5500	0.057	0.063	0.071			
$b_L \times10^5$	1.03	1.15	1.30	1.53	2.08	2.86
$J \times10^8$	4.21	4.67	5.30	6.23	8.45	11.6

Table A-8: Kinetic experiment: Effect of organic phase stirrer speed.
Experimental conditions: T = 25 ^{0}C; A = 7.775×10^{-3} m^2;
C_{CoSO_4} = 0.050 kmol m^{-3}; $C_{Na_2SO_4}$ = 0 kmol m^{-3}; pH = 5.0;
$C_{H_2A_2}$ = 0.2695 kmol m^{-3}; C_{TBP} = 0.1832 kmol m^{-3}; and Re_{aq} = 2102.5.

N s^{-1}	0.81	1.24	2.70	3.60	5.0
Re_{org}	33.1	50.7	110.5	147	204
000	0.000	0.000	0.000	0.000	0.000
500	0.004	0.007	0.005	0.006	0.011
1000	0.008	0.015	0.012	0.012	0.020
1500	0.012	0.019	0.018	0.018	0.029
2000	0.017	0.024	0.023	0.025	0.037
2500	0.020	0.029	0.029	0.031	0.045
3000	0.023	0.034	0.035	0.037	0.052
3500	0.027	0.039	0.041	0.043	0.061
4000	0.032	0.041	0.047	0.050	0.071
4500	0.036	0.049	0.053	0.055	0.078
5000	0.039	0.054	0.058	0.062	0.086
5500	0.045	0.059	0.064	0.068	0.095
$b_L \times10^5$	1.01	1.06	1.17	1.24	1.62
J $\times10^8$	4.10	4.33	4.75	5.04	6.00

Table A-9: Kinetic experiment: Effect of temperature.
Experimental conditions: $A = 7.775\times10^{-3}$ m^2; C_{CoSO_4}=0.050 kmol m^{-3}; $C_{Na_2SO_4}$ = 0 kmol m^{-3}; pH = 5.0; $C_{H_2A_2}$= 0.2695 kmol m^{-3}; C_{TBP} = 0.1832 kmol m^{-3}; Re_{aq} = 2102.5; and Re_{org} = 110.5.

T °C	15.2	21.3	35.3	43.0	48.0	57.0
000 s	0.000	0.000	0.000	0.000	0.000	0.000
500	0.008	0.010		0.030	0.041	0.076
1000	0.011		0.027	0.061	0.082	0.108
1500		0.025		0.086	0.119	0.166
2000	0.036		0.073	0.123	0.146	0.255
2500		0.041		0.140	0.181	0.379
3000	0.045		0.135	0.166	0.221	0.579
3500		0.058		0.193	0.249	
4000	0.057		0.142			
4500		0.076	0.164			
5000	0.068		0.178			
5500		0.093	0.197			
6000	0.079	0.100	0.216			
$b_L \times10^5$	1.11	1.69	4.00	5.57	7.14	11.33
$J \times10^8$	4.51	6.88	16.28	22.67	29.06	46.11

Appendix 2

Analysis of Organic Phase Cobalt Concentration

Ultraviolet spectrophotometry technology has been used to detect the organic phase cobalt concentration. The method is based upon the application of the Beer-Lambert Law:

$$A = \log\ (I_0 / I) = EdC$$

where,

A = absorbance;

I_0 = intensity of light entering the sample;

I = intensity of light leaving the sample solution;

d = path length, cm or mm;

E = molar absorbance or molar extraction coefficient, $cm^2\ mol^{-1}$; and

C = concentration of the solution in the sample solution, kmol m^{-3}.

The cobalt-HDTMPP-kerosene solution is blue. The perfect straight line is shown as the relationship between the organic phase cobalt concentration and its absorbance, when the concentration is lower than 0.05 kmol m^{-3}, seen as a standard curve, Figure A-1.

Under the conditions of the kinetic experiments, the organic phase cobalt concentrations were very low because of the slow extraction rate. Normally the organic phase cobalt concentrations were lower than 1×10^{-3} kmol m^{-3} during the experiments. The cobalt concentration could be measured directly by the spectrophotometer. At 549 nm, there is a maximum absorbance for the cobalt organic compound.

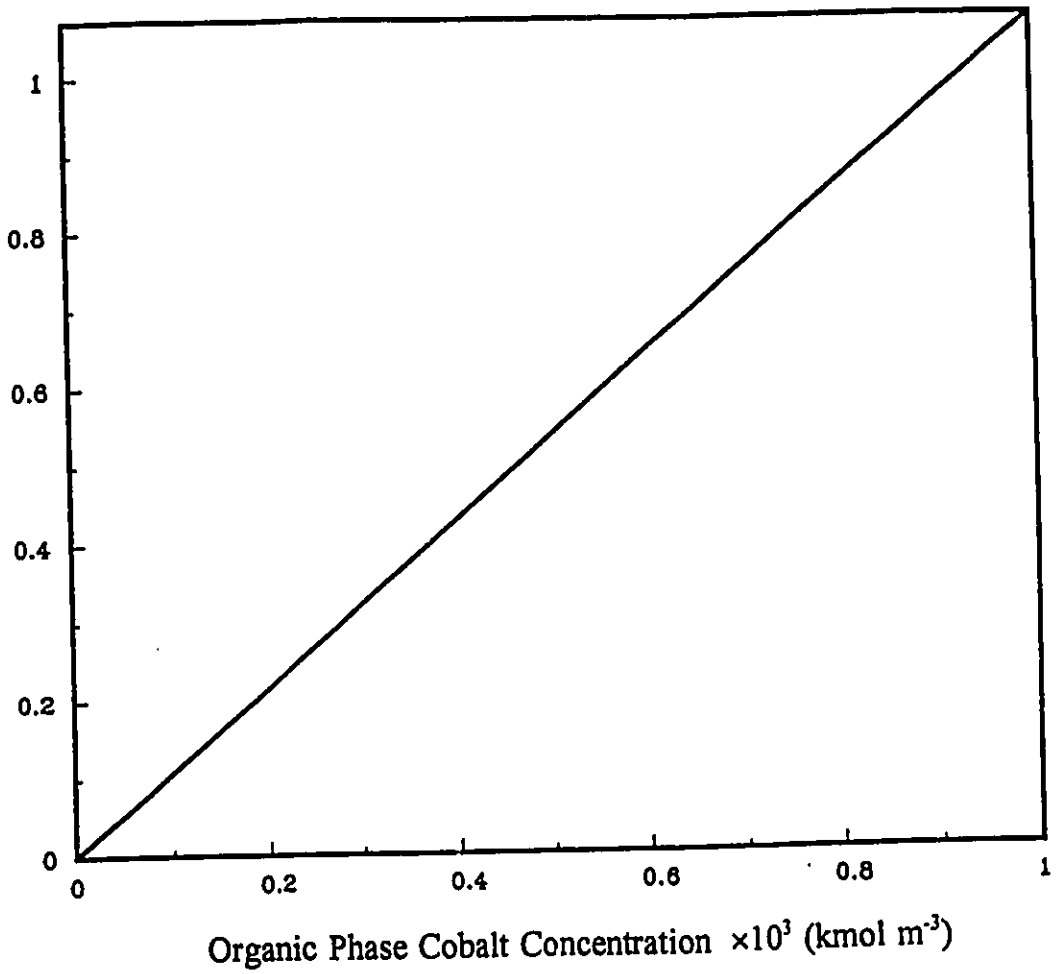

Figure A-1: Calibration curve of organic phase cobalt concentration.

Appendix 3

Analysis of Aqueous Phase Cobalt Concentration

The EDTA titration method is used to determine the aqueous phase cobalt concentration.

1. Prepare 0.01M EDTA standard solution by dissolving about 1.99 of the A.C.S-grade di-sodium salt ($Na_2H_2Y.2H_2O$, formula weight 327) in 500 ml of distilled water.

2. Prepare the pH =10 ammonia buffer solution by diluting 32 g of ammonium chloride and 285 ml of concentration ammonium hydroxide to 500 ml with distilled water. Store in a polyethylene bottle.

3. Determine the aqueous phase cobalt concentration by pipetting exactly 50 ml of the sample of the $CoSO_4$ solution into each of the three clean 250 ml flasks

and then add 1 ml of ammonia buffer and comagite indicator to the first sample and titrate with 0.01M EDTA at 60 ^{o}C from a 25 ml buret to a clear blue end point.